UNIVERSITY OF THESSALY

SCHOOL OF ENGINEERING

DEPARTMENT OF MECHANICAL ENGINEERING

INTEGRATED COMPUTATIONAL SIMULATION OF THE MECHANICS OF BREATHING

Diploma Thesis

By **Georgios Giamagas** and **Nikolaos Monokrousos**

Submitted for the partial fulfillment
of the requirements for the Degree of
Diploma in Mechanical Engineering

Volos, June 2018

Certified by the members of the Thesis Committee:

1st Member: Dr. Bontozoglou Vassilios
(Supervisor) Professor, Department of Mechanical Engineering
University of Thessaly

2nd Member: Dr. Andritsos Nikolaos
Professor, Department of Mechanical Engineering
University of Thessaly

3rd Member: Dr. Pelekasis Nikolaos
Professor, Department of Mechanical Engineering
University of Thessaly

Acknowledgments

At first, we would like to express our gratitude to Dr. Bontozoglou Vassilios for his valuable guidance throughout the production of this thesis. Dr. Bontozoglou devoted an important part of his time to support our efforts and maximize the credibility of our results. Therefore, we consider ourselves priviliged to have worked under his exemplary supervision.

In addition, we would like to thank the members of the thesis committee i.e. Dr. Andritsos Nikolaos and Dr. Pelekasis Nikolaos, for the time they spent to examine our thesis, provide supportive revisions and evaluate our performance.

Last but not least, we are grateful to our parents for their moral and financial support, during the whole period of our academic studies.

Abstract

The thesis examines theoretically and computationally the problem of airflow during a full breathing cycle, i.e. inspiration and expiration. Airflow prediction in the human lungs is an intriguing, yet necessary task of medical research, as it is related to the main lung diagnostic tool, spirometry. Extensive research has already been done, mainly on the problem of forced expiration, motivated by the understanding of the effort-independent part of the spirometric test, which serves as an indicator of various pulmonary diseases.

The presently developed methodology is based on mathematical models of lung and chest elasticity, and of the temporal variation of the muscle force during inspiration and expiration. A combination of the above permits estimation of the alveolar pressure, which is the driving force for the motion of air, taking respectively negative and positive gauge values during inspiration and expiration. The flow of air is subject to viscous pressure drop along airways and to convective pressure drop at the bifurcations. These contributions are calculated by a quasi-steady assumption, i.e. using the steady-state equations with a time-varying driving force. The problem is complicated by the elasticity of the airways, which is taken into account by a literature model that estimates their diameters as function of the intramural pressure (the difference between the local pressure value inside the airway and the outer−pleural−pressure).

The results include predictions of the temporal variation of air flow rate and lung volume. By eliminating the explicit dependence on time, the standard spirometric form of flow rate versus volume is recovered. Initial estimates are made for rigid airways and are subsequently improved by taking into account elasticity in a mean sense. More specifically, airway diameter is considered spatially uniform but temporally varying. Finally, the complete problem of the response of an elastic tube to a varying pressure gradient is solved following a convenient integration procedure. This result remains to be incorporated in the full lung model and is expected to provide more accurate estimates.

Contents

List of Figures

List of Tables

CHAPTER 1. Introduction to Respiration

This chapter constitutes a presentation of the general principles of respiration. At first, the physics of gas exchange in the lungs are briefly discussed. Then, the anatomy of the human respiratory system is explained and existing models describing the geometry of the trancheobronchial tree are presented.

The goals of respiration are to provide oxygen to the tissues and to remove carbon dioxide. In order for these goals to be achieved, four main functional procedures take place during respiration:

1) pulmonary ventilation, the exchange of air through inspiration and expiration, between the atmosphere and the lung alveoli.
2) oxygen and carbon dioxide diffusion between the blood and the alveoli
3) transport of oxygen and carbon dioxide in the blood and the body fluids to and from the cells
4) regulation of ventilation and other aspects of respiration.

1.1 Physical Principles of Gas Exchange

Right after fresh air from the environment begins circulating to the lung alveoli, the diffusion of oxygen from the alveoli into the pulmonary blood and the diffusion of carbon dioxide in the opposite direction, take place. *Diffusion* is defined as the process in which molecules move randomly and intertwine their ways in both directions through the respiratory membrane.

However, when it comes to respiratory physiology, it is important to examine not only the basic mechanism of the diffusion, but also the *rate* at which it occurs. The source of energy that is provided so as diffusion to occur, is the kinetic motion of the molecules themselves, which strike each other and bounce their ways in new, random directions.

In respiratory physiology, one deals with mixtures of gases, since the air (atmospheric, humidified, alveolar or expired) is a mixture of gases, mainly of oxygen (O_2), nitogen (N_2), carbon dioxide (CO_2) and water vapor (H_2O). *Partial pressure* is the pressure caused by each of these gases alone and the rate of diffusion of each of these gases is directly proportional to it.

The air inside the lung alveoli differs by any means from the atmospheric air. The difference in the concentrations of gases in the two “types” of air is due to several reasons: during breathing, only

part of the alveolar air is replaced by the atmospheric one, while oxygen is constantly being absorbed from the alveolar air. In addition, there is a non-stop diffusion of carbon dioxide from the pulmonary blood into the alveoli and finally, the dry atmospheric air of the environment that enters the respiratory system is humidified, before it even reaches the alveoli. The table given below (Guyton, Hall, 1956) shows the partial pressures of respiratory gases as they enter and leave the lungs (at sea level: 1 atm), as well as the concentration (in the parenthesis) of each gas that comprises the particular kind of air of each column:

Partial Pressures of Respiratory Gases as They Enter and Leave the Lungs (at Sea Level)

	Atmospheric Air* (mm Hg)		Humidified Air (mm Hg)		Alveolar Air (mm Hg)		Expired Air (mm Hg)	
N_2	597.0	(78.62%)	563.4	(74.09%)	569.0	(74.9%)	566.0	(74.5%)
O_2	159.0	(20.84%)	149.3	(19.67%)	104.0	(13.6%)	120.0	(15.7%)
CO_2	0.3	(0.04%)	0.3	(0.04%)	40.0	(5.3%)	27.0	(3.6%)
H_2O	3.7	(0.50%)	47.0	(6.20%)	47.0	(6.2%)	47.0	(6.2%)
TOTAL	760.0	(100.0%)	760.0	(100.0%)	760.0	(100.0%)	760.0	(100.0%)

* On an average cool, clear day.

Table 1:Partial pressures of respiratory gases as they enter and leave the lungs (Guyton,Hall,1956)

Once oxygen has diffused from the alveoli into the pulmonary blood, it is transported - in combination with hemoglodin - to the tissue capillaries, where it is released for use by the tissue cells. In the cells, oxygen reacts with plenty of foodstuffs so as to form large quantities of carbon dioxide, which (carbon dioxide) returns back to the lungs.

1.2 The Ideal Gas Law

When examining pulmonary ventilation, we assume that the fluid (air) that flows through the airways, behaves as an ideal gas (Feher, 2016). The Ideal Gas Law describes the relation between pressure and volume in an ideal gas as:

$$PV = nRT$$

where P is the pressure (in atm, mmHg, Pa, or some other appropriate unit), V is the volume, n is the number of moles, R is the universal gas constant, and T is the temperature in Kelvin. The values of the universal gas constant R, depending on the units of the other parameters are given in the table below:

Values of the Universal Gas Constant R			
Values of R	**Units**	**Values of R**	**Units**
8.314472	$J \cdot K^{-1} \cdot mol^{-1}$	83.14472	$L \cdot mbar \cdot K^{-1} \cdot mol^{-1}$
0.082057	$L \cdot atm \cdot K^{-1} \cdot mol^{-1}$	8.314472×10^{-5}	$m^3 \cdot bar \cdot K^{-1} \cdot mol^{-1}$
8.205745×10^{-5}	$m^3 \cdot atm \cdot K^{-1} \cdot mol^{-1}$	10.73159	$ft^3 \cdot psi \cdot °R^{-1} \cdot lb\text{-}mol^{-1}$
8.314472	$L \cdot kPa \cdot K^{-1} \cdot mol^{-1}$	0.73024	$ft^3 \cdot atm \cdot °R^{-1} \cdot lb\text{-}mol^{-1}$
8.314472	$m^3 \cdot Pa \cdot K^{-1} \cdot mol^{-1}$	1.98588	$Btu \cdot °R^{-1} \cdot lb\text{-}mol^{-1}$
82.05745	$cm^3 \cdot atm \cdot K^{-1} \cdot mol^{-1}$	62.36367	$L \cdot torr \cdot K^{-1} \cdot mol^{-1}$

Table 2: Values of the Gas Constant R (https://chemengineering.wikispaces.com/Gas+constant)

The inverse relation between pressure and volume is the basic principle applied during pulmonary ventilation: an increase in the thoracic cavity volume surrounding the lungs, causes a decrease in the pressure of the gas in the lungs and air rushes in from the environment. Conversely, a decrease in the volume of the thoracic cavity, results an increase in the pressure of the gas in the lungs and therefore, air moves from the lungs back out into the environment.

An interesting case concerning lung behavior is when an amount of air is static inside the lung and no airflow takes place i.e. during breath hold. In order to understand the relation between the volume and the pressure of the air contained inside the lung, when the glottis is closed and no airflow takes place, Boyle's Law needs to be propounded. In 1662, Robert Boyle observed, during various and reliable experiments, the changes in the pressure (when the volume varies) and the volume (when the pressure varies) that take place, when the temperature of the system is being held constant.

Boyle concluded that when the temperature of the gas is kept constant, the volume of the gas is inversely proportional to its pressure. For example, and provided that the temperature of the system is being held constant, when the volume of the gas is increased, the pressure of the gas should decrease, whilst when the pressure of the gas is increased, the volume of the gas should decrease.

Boyle's statement can be expressed mathematically through the formula:

$$P V = K$$

where P is the pressure, V is the volume and K is the proportionality constant (https://chemistry.tutorvista.com/physical-chemistry/boyles-law.html).

Therefore, and under the assumption that temperature remains constant, if volume V_1 and pressure P_1 of a given mass of a gas are changed to V_2 and P_2 respectively, then:

$$P_1 V_1 = P_2 V_2 = K \quad \text{(at constant mass and temperature)}$$

A clear consequence of Boyle's law is the lung shrinkage during freediving, which is demonstrated in the figure below. Freedivers take a deep breath and hold the air into their lungs during the dive. Pressure steadily rises as they descend deeper gaining 1 atm per 10 meters. These results to a remarkable compression of the air in their lungs, according to Boyle's law.

A special feature of human physiology called blood shift, which is part of the dive reflex, is what prevents the lungs from collapsing in deep dives. Blood goes into the lungs and into the pulmonary capillaries in the alveoli walls. This causes the capillaries to expand and compress the intra-alveolar gases. Intra-alveolar gas pressure, overall lung gas pressure, and therefore overall pressure inside the chest all increase as a result. The pressure increase inside the chest opposes water pressure on the outside of the chest (Johnson, 2015).

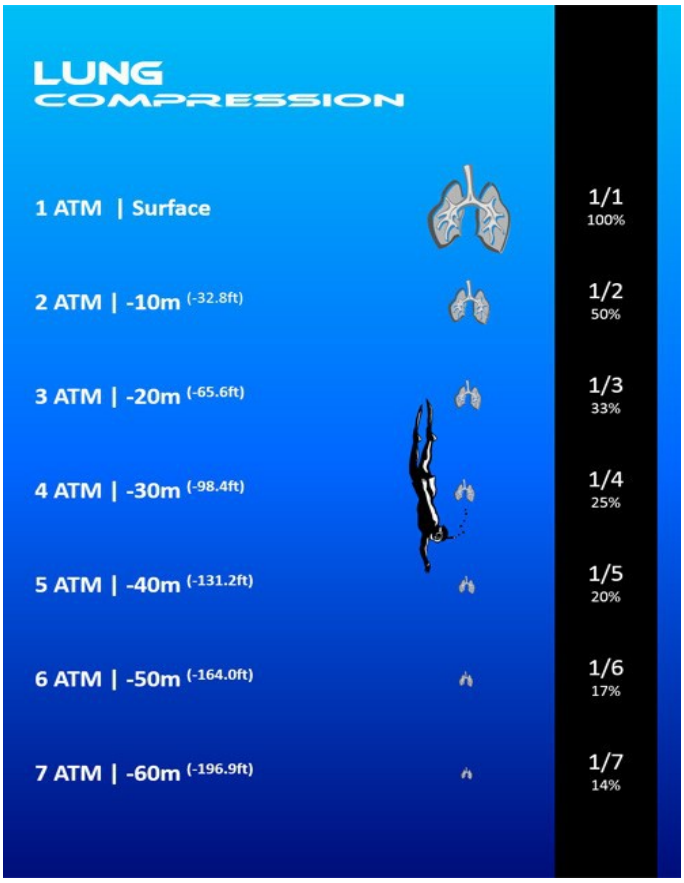

Figure 1.2.1: Pressure – lung volume behavior in depth

1.3 Geometry of the Human Respiratory System

The human respiratory system and the respiratory passageways are presented in Figure 1.3.1.

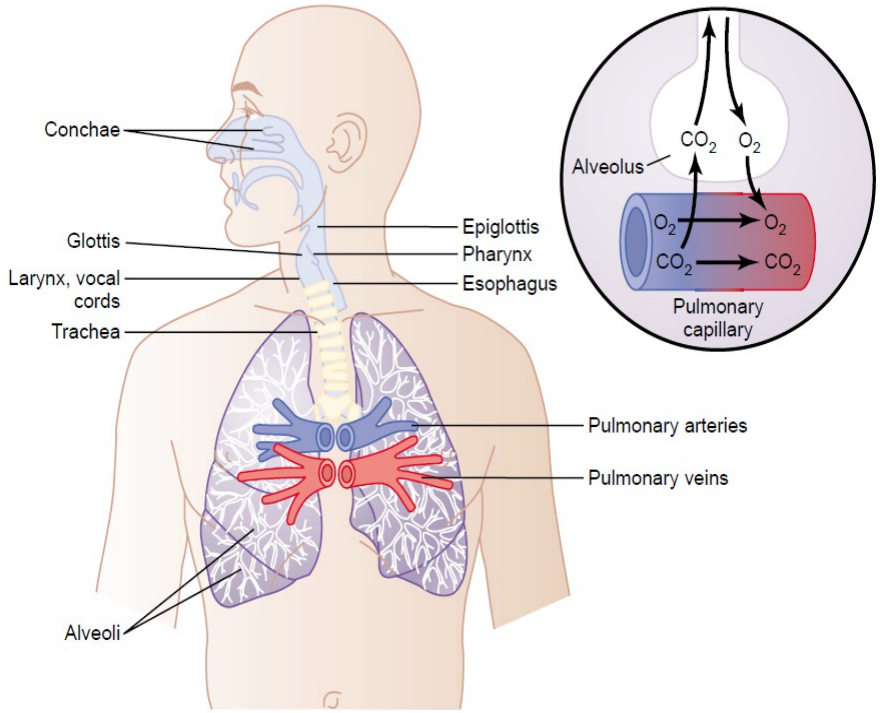

Figure 1.3.1: The respiratory system and the system passageways (Guyton, Hall, 1956)

The air flows to and from the lungs, passing through the trachea, bronchi and bronchioles. The respiratory system consists of the following parts:

Conchae: Conchae or nasal conchae (or nasal turbinates) are the two narrow, curled, spongy bones that protrude from the nasal cavity walls in the human nose. Nasal conchae are covered from a thick membrane out of mucus and are responsible for guiding the airflow through the passages of the nose, specifically during inhalation. In addition, they slow down the air that enters the nasal cavity, so it remains more time in it, in order to be dehumidified. Last but not least, the nasal conchae are responsible for the warm-up and the air filtration, since they regulate the air in a way where it goes through the mucus membrane and cilia (http://www.therespiratorysystem.com/nasal-conchae-nasal-turbinates/).

Pharynx: The pharynx is a musculo-membranous conduit that extends from the base of the skull to the lower level of the cricoid cartilage, where the esophagus starts. The pharynx consists of a group of muscles that function as valves, allowing the air and the food to flow through safely. It can be divided into three regions: nasopharynx, oropharynx and the laryngopharynx (Cheesman, Burdett, 2011)

Epiglottis: The epiglottis is a thin, leaf-shaped structure at the higher border of the larynx, or voice box. Most of the day, the epiglottis is relaxed at the edge of the pharynx, so that air is able to enter the pharynx, either from the nose or the mouth and head into the lungs. When we shallow food or drink, the epiglottis moves and performs its vital function, that is protecting the body from chocking on the material that would normally block the airway.
(http://www.innerbody.com/image_digeov/dige02-new2.html).

Glottis: The glottis is the space between the vocal cords that allows the passage of air in and out of the trachea, via the contractions of the diaphragm and other accessory respiratory muscles (Mehran, 2018).

Esophagus: The esophagus is the conduit that connects directly the pharynx and the stomach and it consists of cervical, thoracic and abdominal parts. It goes down into the thorax, where it lies successively in the upper and the back part of the central compartment of the thoracic cavity, before it enters the abdominal cavity. It is considered to be a muscular and cylindrical, with an average length for an adult individual subject of 25 – 30 cm (Mahadevan, 2017).

The trachea, bronchi, bronchioles and the alveoli will be described extensively below, where the human tracheobronchial tree is introduced and presented.

1.4 The Human Tracheobronchial Tree

A complete model of the branching pattern of the human bronchial tree remains obscure, although several different models have been described so far. The tracheobronchial tree derived by *Weibel* (Weibel, 1963) based upon careful anatomic measurements, has been widely used by health physicists to represent the overall tree geometry of an average adult human lung.

Weibel's model indicates one trachea, two main bronchi, four lobar bronchi, 16 segmental bronchi, etc. However, since bronchus length varies, pairs of daughter bronchi oftenly differ in size and trifurcations may occur, the mathematical relationship of the model is probably unlikely to be true in practice.

Work using three-dimensional (3-D) computed tomography to reconstruct the branching pattern of the airways has shown that, a regular dichotomy system does occur for at least the first six generations. From this point and beyond, the same study showed trifurcation of some bronchi and airways that terminated at generation 8.

Briefly, the human tracheobronchial tree consists of the following parts (Lumb, 2017):

Trachea (Generation 0): The adult trachea has an approximate diameter of 1.8 cm and length of 11 cm. Intrathoracic pressure changes are not applied to the part of the trachea in the neck, although that part is really vulnerable to pressures arising in the neck due, for example, to tumours or haematoma formation. In order to “block” the trachea, an external pressure of the order of 4 kPa (40 cmH2O) is actually sufficient. During a cough, for example, the trachea can be compressed by the raised intrathoracic pressure within the chest, as -according to Bernoulli's law-, the decreased diameter of the trachea increases the linear velocity of the gas that flow through it and therefore the efficiency of removal of secretions. A normal trachea during a rigid bronchoscopy can be seen in *Figure 1.4.1*:

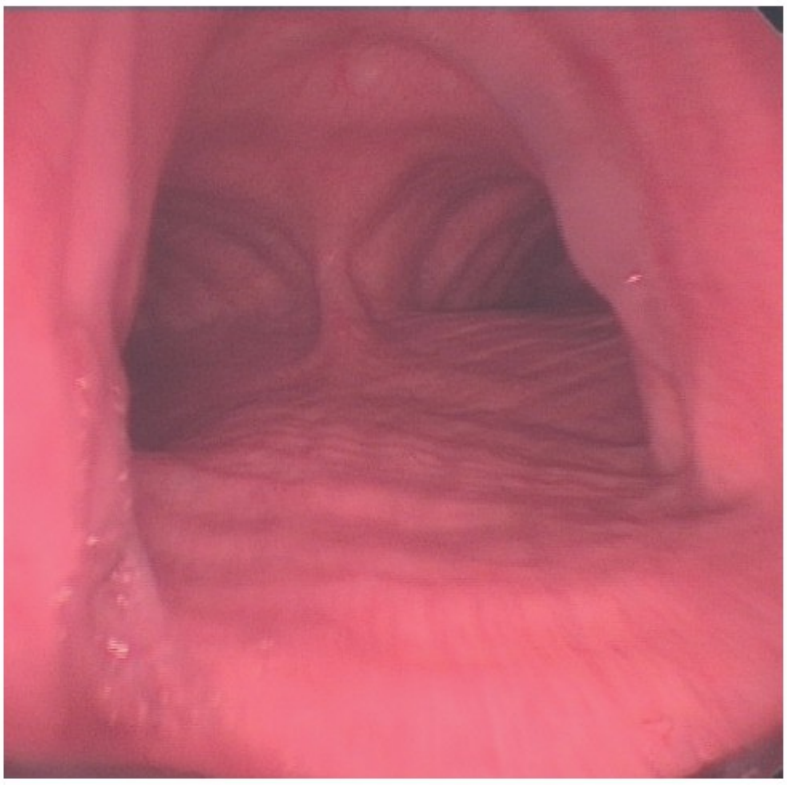

Figure 1.4.1: Normal trachea viewed during a rigid bronchoscopy (Lumb, 2017)

Main, Lobar and Segmental Bronchi (Generations 1 to 4): As we mentioned before, an assumption of Weibel's model is that the conducting airways are assumed to form an -approximately- symmetric bifurcating tree. In real life, the trachea bifurcates asymmetrically, and the right bronchus is wider and makes a smaller angle with the long axis of the trachea. Therefore, foreign bodies, such as air, dust, of fluids tend to enter the the right bronchus in preference to the left. Bronchi in this group (down to generation 4) are sufficiently regular to be individually named. At the third generation, the total cross-sectional area of the respiratory tract is minimal. These bronchi are subjected to the full effect of changes in intrathoracic pressure and will collapse when the intrathoracic pressure exceeds

the intramural pressure by ~5 kPa or 51 cmH2O) (the definitions of intrathoracic and intramular pressure are given in chapter 2.3). This occurs in the larger bronchi during a forced expiration, limiting peak expiratory flow rate.

Small Bronchi (Generations 5 to 11): The small bronchi extend through about seven generations, with their diameter progressively falling from 3.5 to 1 mm. In a normal subject, even during a forced expiration, the intraluminar pressure in the small bronchi rapidly rises to more than 80% of the alveolar pressure, which is more than the extramural (intrathoracic) pressure.

Bronchioles (Generations 12 to 14): At about the eleventh generation, where the internal diameter is ~1 mm, important changes take place. The total cross-sectional area of the airways increases until, in the terminal bronchioles, it is about 100 times the area at the level of the large bronchi. Therefore and under normal conditions, the flow resistance of these smaller airways (less than 2 mm diameter) is considered negligible.

Respiratory Bronchioles (Generations 15 to 18): Down to the smallest bronchioles, the airways are used entirely to conduct and humidify. Beyond this point, there is a gradual transition from conduction to gas exchange. In the four generations of respiratory bronchioles (15-18) there is a gradual increase in the number of alveoli in their walls. They have a well-defined muscle layer with bands which loop over the opening of the alveolar ducts and the mouths of the mural alveoli. There is no significant change in calibre of advancing generations of respiratory bronchioles (~0.4 mm diameter).

Alveolar Ducts (Generations 19 to 22): The difference between the terminal respiratory bronchiole and the alveolar ducts which arise from them, is that the the alveolar ducts have no walls other than the mouths of mural alveoli (approximately 20 in number). The alveolar septa comprise a series of rings forming the walls of the alveolar ducts and containing smooth muscle. Approximately 35% of the alveolar gas resides in the alveolar ducts and the alveoli that arise directly from them.

Alveolar Sacs (Generation 23): The last generation of the air passages differs from alveolar ducts solely because they are blind. It is estimated that about 17 alveoli arise from each alveolar sac and account for about half of the total number of alveoli.

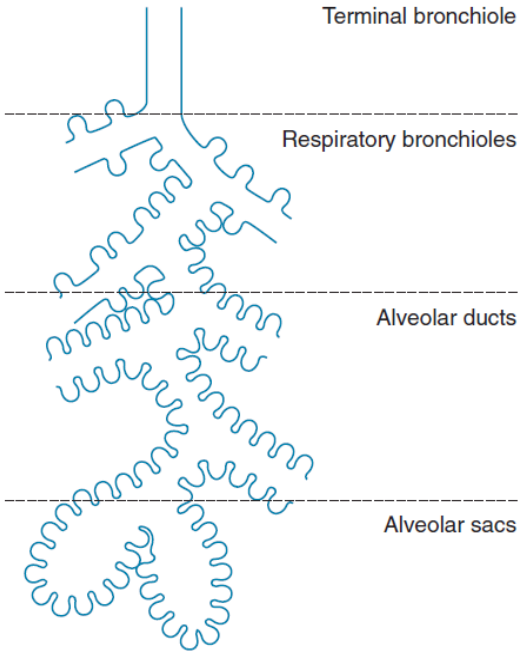

Figure 1.4.2: A single pulmonary acinus showing four generations between the terminal bronchiole and the alveolar sacs (Lumb, 2017)

The Alveoli: A pulmonary alveolus (plural: alveoli, from Latin alveolus, "little cavity") is a hollow cavity found in the lung parenchyma, and is the basic unit of the respiratory system. (https://en.wikipedia.org/wiki/Pulmonary_alveolus). The mean total number of alveoli has been estimated as 400 million, but ranges from about 270 to 790 million, depending on the height of the subject and the total lung volume. The size of the alveoli depends on lung volume, but due to gravity, they are normally larger in the upper part of the lung, except at maximal inflation, when the vertical gradient in size disappears. At functional residual capacity (*chapter 2.2*), the mean diameter of a single alveolus is 0.2 mm and the total surface area of the alveoli is ~130 m^2.

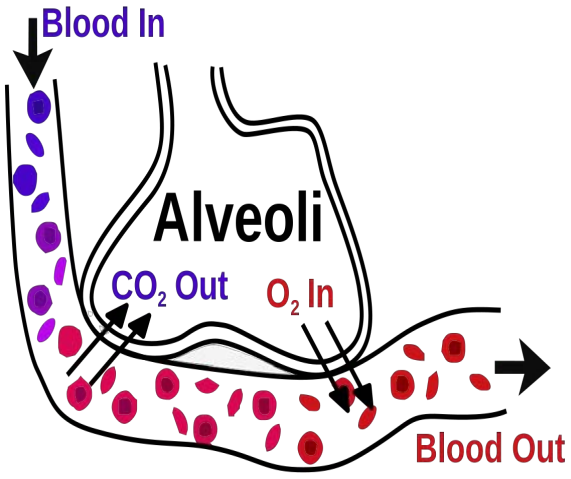

Figure 1.4.3: Function of an alveoli (https://en.wikipedia.org/wiki/Pulmonary_alveolus)

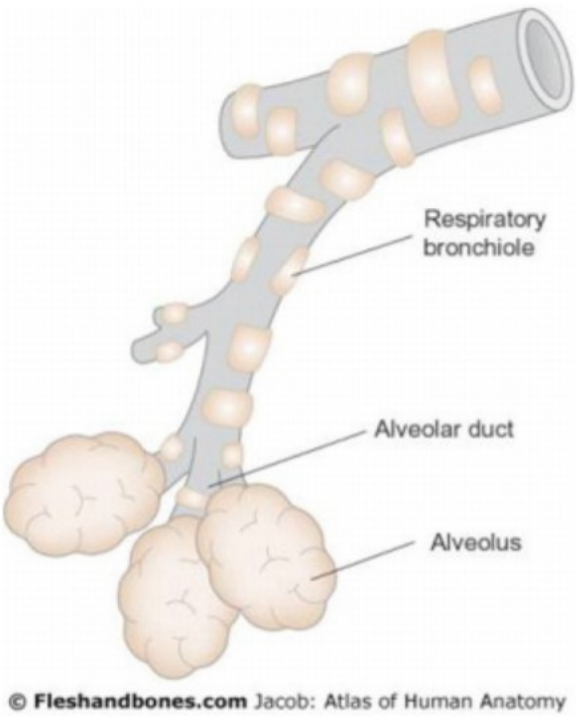

Figure 1.4.4: The bronchioles and alveoli. (Reprinted from Atlas of Human Anatomy, Jacob, Copyright 2001, with permission from Elsevier.)

1.5 Weibel's Model for the Human Tracheobronchial Tree Geometry

The tracheobronchial tree derived by *Weibel* (Weibel, 1963), as mentioned before, was based upon careful anatomic measurements and is being used widel to represent the overall tree geometry of an average adult human lung. Weibel's model numbered successive generations of air passages from the trachea (generation 0) down to alveolar sacs (generation 23) (Lumb, 2017). The conducting airways are assumed to form an -approximately- symmetric bifurcating tree, with g, the generation number, ranging from 0 at the trachea to 16 at the periphery (Lambert et al., 1982), or 23 at the last order of the terminal bronchioles. Also, as a rough approximation, one might assume that the number of passages in each generation is double that in the previous generation, and the number of air passages in each generation is approximately indicated by the number 2 raised to the power of the generation number. Therefore airflow q in the tube of generation g in the dichotomous bronchial tree, given the value of the flow in the mouth Q, is calculated according to the formula (Polak, 1998):

$$q(g)=Q\cdot 2^{(-g)}$$

Weibel's model measured the dimensions of lungs of the adult male, inflated to the expansion of 4.8 liters (or 4800 cm^3), that is the ¾ of the total lung capacity (TLC), as cited by *Weibel and Gomez* (Weibel, Gomez, 1962) and *Weibel* (Weibel, 1963). The table below, summarizes the linear dimensions of the airways, the volumes and the number of alveoli for each generation, which are modelled by empirical equations.

Dimensions of Weibel's Model

Generation	Number of branches	Diameter (cm)	Length (cm)	Volume (cm^3)	Number of alveoli (10^5)
0	1	1.800	12.000	30.500	0
1	2	1.220	4.760	11.250	0
2	4	0,830	1.900	3.970	0
3	8	0.560	0.760	1.520	0
4	16	0.450	1.270	3.460	0
5	32	0.350	1.070	3.300	0
6	64	0.280	0.900	3.53	0
7	128	0.230	0.760	3.85	0
8	256	0.186	0.640	4.45	0
9	512	0.154	0.540	5.17	0
10	1024	0.130	0.460	6.21	0
11	2048	0.109	0.390	7.56	0
12	4096	0.095	0.330	9.82	0
13	8192	0.082	0.270	12.45	0
14	16384	0.074	0.230	16.40	0
15	32768	0.066	0.200	21.70	0
16	65536	0.060	0.165	29.70	0
17	131072	0.054	0.141	41.80	6
18	262144	0.050	0.117	61.10	20
19	524288	0.047	0.099	93.20	60
20	1048576	0.045	0.083	139.50	210
21	2097152	0.043	0.070	224.30	415
22	4194304	0.041	0.059	350.00	840
23	8388608	0.041	0.050	591.00	1430

Table 3: Weibel's Model for FRC=0,75 TLC= 4.8 L (Soong, Nicolaides, Yu, Soong, 1979)

The dimensions given in *Table 3* are based upon a FRC at 3/4 TLC as computed previously, although it is normally expected that the value of FRC is about 1/2 TLC (3200 cm^3). As a consequence, the dimensions of the present model need to be corrected. In order to extract the correct dimensions of the lung's proportions, we assume -although inaccurately (Marshall, Holden, 1963)- that inside the airways and alveoli of the lung, uniform expansion and contraction take place. *Hughes et al.* (Hughes, Hoppin, Mead, 1972) and *Wilson et al.* (Wilson, Massarella, Pride, 1974) proved that the volumetric changes of the lung are proportional to the cube of linear dimensions, by determining the linear scale factor, s , as:

$$s=(3200/4784.6)^{(1/3)}$$

such that the linear dimensions and alveolar volume along with their standard deviations are corrected, to maintain the coefficients of variation previously stated. The correction factor that is being used, corresponds to a uniform linear contraction of 12.5%, quite close to the appropriate scaling correction for the non-homogeneous case that was suggested by *Marshall and Holden* (Marshall, Holden, 1963) and *Pedley et al*. (Pedley, Schroter, Sudlow, 1970). *Table 4* summarizes the results of the statistical procedure that was followed:

Linear airway dimensions, volume calculations and coefficients of variation (σ/μ) corresponding to a FRC of 3200 cm^3

Generation	Diameter (cm)		Length (cm)		Volume (cm^3)
	μ	σ/μ	μ	σ/μ	
0	1.574	0.10	10.494	0.10	20.423
1	1.067	0.125	4.163	0.15	7.443
2	0.726	0.15	1.662	0.25	2.750
3	0.490	0.175	0.665	0.30	1.002
4	0.394	0.20	1.111	0.35	2.161
5	0.306	0.23	0.936	0.425	2.203
6	0.245	0.275	0.787	0.50	2.372
7	0.201	0.325	0.665	0.575	2.703
8	0.163	0.35	0.560	0.65	2.977
9	0.135	0.42	0.472	0.70	3.444
10	0.114	0.50	0.402	0.75	4.182
11	0.095	0.575	0.341	0.80	4.985
12	0.083	0.66	0.289	0.81	6.408
13	0.072	0.675	0.236	0.775	7.812
14	0.065	0.60	0.201	0.725	10.839
15	0.058	0.50	0.175	0.65	14.995
16	0.052	0.40	0.144	0.50	20.448
17	0.047	0.30	0.123	0.40	28.308
18	0.044	0.22	0.102	0.30	40.277
19	0.041	0.15	0.087	0.225	60.227
20	0.039	0.13	0.073	0.175	92.575
21	0.038	0.10	0.061	0.15	142.579
22	0.036	0.10	0.052	0.11	218.510
23	0.036	0.098	0.044	0.10	370.355

Source	μ	σ/μ
Alveolus volume (cm^3)	7.022×10^{-6}	2.0×10^{-1}
Number of alveoli	2.981×10^{8}	7.0×10^{-2}
FRC (cm^3)	3.200×10^{3}	2.1×10^{-2}

Table 4: Linear airway dimensions, volume calculations and coefficients of variation (σ/μ) corresponding to FRC=3200 cm^3 (Soong, Nicolaides, Yu, Soong, 1979)

CHAPTER 2. Mechanics of Breathing

In the present chapter, the general concepts concerning the mechanics of breathing are introduced. Many different muscles are involved in the kinetics of the air through the lungs. At first, the function of these muscles is briefly discussed. After that, the different lung volume states as well the different pressures acting on the lungs are defined. Pressure volume behavior in relation to lung compliance and surface tension is explained and finally the basic resistances during airflow through the lungs are commented.

2.1 Introduction to the Muscles of Respiration

One of the most important muscles of respiration, is that of the *diaphragm.* The diaphragm consists of a thin, dome-shaped sheet of muscle, which is inserted into the lower ribs and it separates the thoracic cavity (contains the heart and the lungs) from the abdominal cavity (contains the liver, stomach and intestines). It is of a such a high importance, as it is supplied by phrenic nerves that originate high in the cervical region. In adults, the diaphragm has a total surface area of approximately 900 cm^2 (Gauthier, Verbanck, Estenne, et al., 1994).

When the diaphragm contracts, the abdominal contents move down and forward and the vertical dimension of the chest cavity is increased, while the rib margins are lifted and moved out, increasing the crosswise diameter of the thorax. The increase in the volume of the thoracic cavity, causes a decrease in the intrathoracic pressure so that, if the glottis is open, air flows from the environment to the human lungs. Controlling the motion of the diaphragm is an essential function of the human respiratory system, since we use our diaphragm to speak, eat, sing, etc.

The *external intercostal muscles* are the ones who connect adjacent ribs and they move with a slightly slope forward and downward. When these muscles contract, they pull the ribs forward and upward, causing an increase in both the lateral and the anteroposterior diameters of the thorax (West, 2012).

The *accessory muscles of inspiration* consist of the scalene muscles which lift up the first two ribs, and the sternomastoids, which raise the sternum. During exercise, these muscles contract strongly, though during quiet breathing they are quite inactive (West, 2012).

The most important muscles during expiration are those of the abdominal wall. When these muscles contract, the diaphragm is pushed upward, since the abdominal pressure is raised. During

coughing, vomiting and defecation, these muscles contract forcefully. Also, the *internal intercostal muscles* participate in the active expiration by pulling the ribs downward and inward, action exactly opposite to the one of the external intercostal muscles.

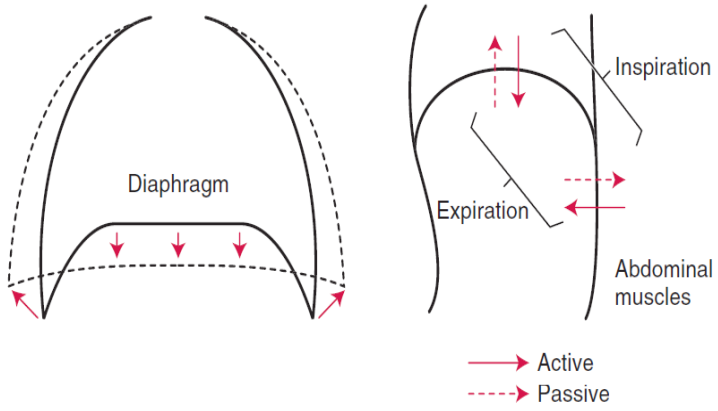

Figure 2.1.1: Diaphragm during inspiration and expiration (West, 2012).

2.2 Lung volumes and capacities

In order to study pulmonary ventilation, doctors and health physicists record the volume movement of the air into and out of the lungs, with a process called *spirometry*. A typical, basic spirometer can be seen in *Figure 2.2.1*.

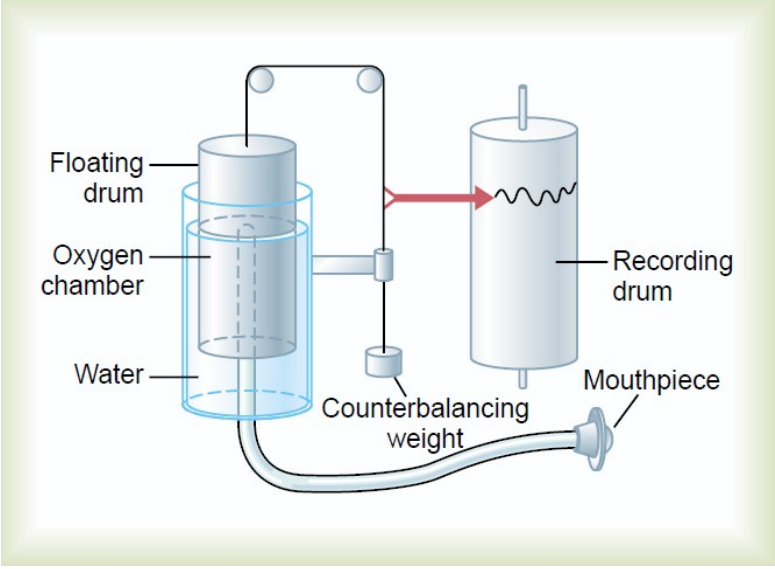

Figure 2.2.1: Spirometer (West, 2012)

The spirometer consists of a recording drum inverted over a chamber of water, counterbalanced by a weight. The mouth of the patient connects with the gas chamber through a tube, while inside the drum is a breathing gas, usually air or oxygen. When the patient breathes in and out of the chamber, the drum rises and falls, whilst a recording of the drum's motion is made on a moving sheet of paper.

For ease when describing the procedures that take place during pulmonary ventilation, the air in the lungs has been specifically categorized into four volumes and four capacities, as shown in the figure below:

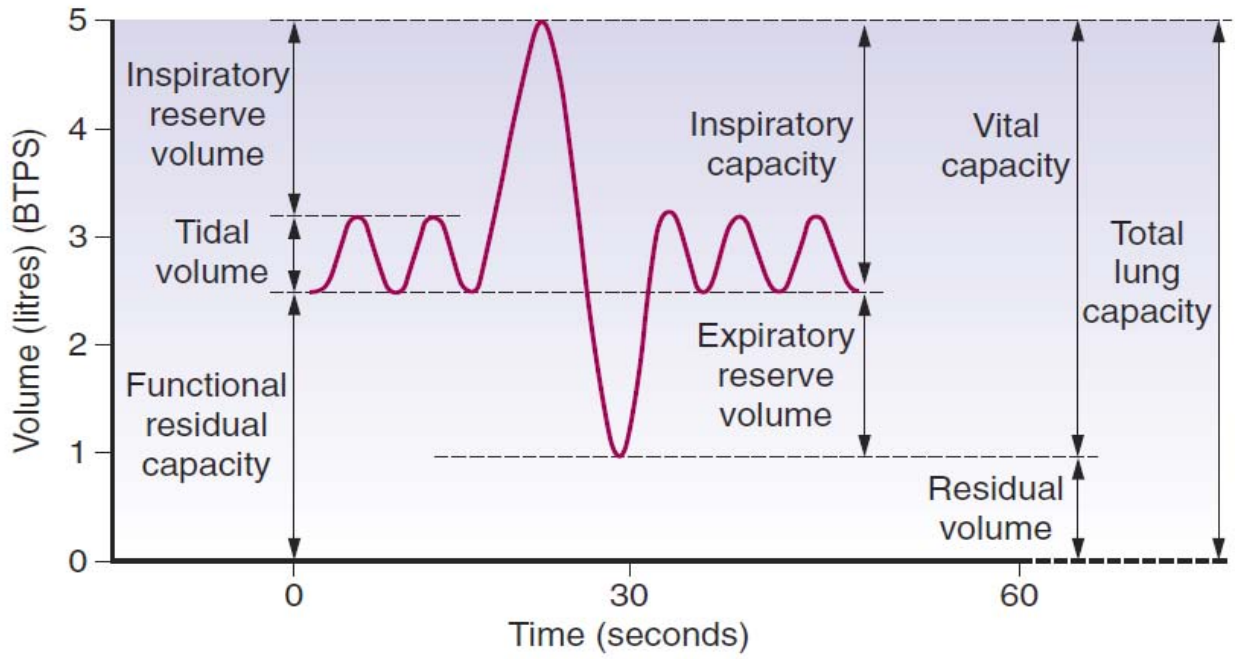

Figure 2.2.2: Static lung volumes of Dr. Nunn in 1990.The 'spirometer curve' indicates the lung volumes that can be measured by simple spirometry (Lumb, 2017)

Lung Volumes Definitions

Tidal volume (TV). The volume of air that flows through the airways during each normal inspiration and expiration (quiet breathing); it amounts to about 0.5 liters in the average young man.

Inspiratory reserve volume (IRV). The maximal volume of air that can be inhaled over and above the normal tidal volume; about 3 liters.

Expiratory reserve volume (ERV). The extra amount of air that can be exhaled by forceful expiration after the end of a normal tidal expiration; about 1.1 liters.

Residual volume (RV). The volume remaining after the forced expiration. It depends on the balance between the maximal expiratory force of the muscles and the elastic forces opposing the lung volume reduction; about 1.2 liters.

Note: when added together, the four pulmonary lung volumes equal the maximum volume to which the lungs can be expanded.

Lung Capacities Definitions

A ‘capacity’ usually refers to a measurement comprised of more than one ‘volume’, approach used when describing events in the pulmonary cycle. Extensively:

Inspiratory capacity (IC). The sum of Tidal volume (TV) and Inspiratory reserve volume (IRV); about 3.5 liters

Vital capacity (VC). The maximum amount of air a person can exhale from the lungs, after the filling and expiring the lungs to their maximum extent. (VC) equals the Inspiratory reserve volume (IRV) plus the Tidal volume (TV) plus the Expiratory reserve volume (ERV); about 4.6 liters.

Total lung capacity (TLC). The volume of gas in the lungs at the end of a maximal inspiration, that is the maximum volume to which the lungs can be expanded with the greatest possible inspiratory effort. (TLC) equals the sum of Vital capacity (VC) and Residual volume (RV); about 5.8 liters. It is achieved when the maximal force generated by the inspiratory muscles is, balanced by the forces opposing expansion. Expiratory muscles are also contracting strongly at the end of a maximal inspiration.

Functional residual capacity (FRC). This is the lung volume at the end of a normal expiration and it equals the sum of Expiratory reserve volume (ERV) and Residual volume (RV).

The Functional residual capacity (FRC), as well as all the other volumes and capacities, depend on many factors, such as: body size, sex, age, posture, ethnic group, obesity (Guyton,Hall,1956). All these factors must be taken into consideration when attempting to ascertain “normal” values for lung volumes in an individual subject. For example:

- for an individual Caucasian male aged between 25 to 65 years and in an upright posture, a predicted “normal” value for (FRC) is calculated as for:

$$(FRC) = (5.95\, x\, height) + (0.019\, x\, age) - (0.086\, x\, BMI) - 5.3$$

where: (FRC) in litres, (height) in meters, (age) in years , Body Mass Index (BMI) in kg/m^2.

- all pulmonary volumes and capacities are about 20 – 25% greater in men than in women, in large and athletic people than in small and asthenic one and in people who live at higher altitudes.

Among these pulmonary volumes and capacities, a few simple algebric exercises and interrelations can be applied:

$$(VC)=(IC)+(ERV)=[(TV)+(IRV)]+(ERV)$$

and

$$(TLC)=(VC)+(RV)=(FRC)+(IC)=[(IC)+(ERV)]+(RV)=[(IRV)+(TV)+(ERV)]+(RV)$$

2.3 Lung Pressures: Definitions and Relations

There is multitude of different pressures action on the lung during respiration. The calculation of these pressures is an essential part of our model. In the present chapter, a complete list of lung pressure definitons, as they will be used below, is provided.

Atmospheric or Barometric Pressure (Patm)

Atmospheric Pressure is taken as reference pressure, equal to zero centimeters of water at any point during the breathing cycle.

$$Patm=0\,(cmH_2O)$$

Alveolar Pressure (Palv)

Alveolar Pressure is the pressure inside the lung alveoli. When the lung is at rest with the glottis open and no air is flowing into or out of it, the pressures in all parts of the respiration tree, all the way down to the alveoli, are all equal to the atmospheric pressure.

$$\text{At rest:} \quad Palv=Patm=0\,(cmH_2O)$$

Driving Pressure (Pd)

The Driving Pressure is the thrusting force for breathing. It is defined as the difference between alveolar and atmospheric pressure and since atmospheric is always zero, as stated above, driving pressure equals alveolar pressure.

$$Pd = Palv - Patm = Palv - 0 = Palv$$

Expiration requires alveolar pressure to be higher than atmospheric, that is positive in sign:

$$Palv > Patm \;\Rightarrow\; Palv - Ptm > 0 \;\Rightarrow\; Palv > 0$$

Inspiration requires alveolar pressure to be lower than atmospheric, that is negative in sign:

$$Palv < Patm \;\Rightarrow\; Palv - Ptm < 0 \;\Rightarrow\; Palv < 0$$

Equilibrium between alveolar and atmospheric pressure means no airflow as stated above :

$$Palv = Patm \;\Rightarrow \text{No Airflow}$$

Pleural Pressure (Ppl)

Pleural or Intrapleural Pressure is the pressure of the fluid in the narrow space between the lung pleura and the chest wall pleura. Normally, the pressure within the pleural cavity is slightly less than the atmospheric pressure, in what is known as negative pressure. This subatmospheric pleural pressure tends to expand the lungs towards the chest wall. Pleural pressure is negative in sign for all inspirations and most expirations. However, during rapid expirations it becomes positive in sign (collapsing the lungs).

$$Ppl < 0 \;\Rightarrow \text{Rest, Inspiration or Tidal Expiration}$$
$$Ppl > 0 \;\Rightarrow \text{Rapid or Forced Expiration}$$

Airways' Lateral Pressure (Plt)

Airways' Lateral Pressure is the pressure inside the lung airways. It is uniform and equal to alveolar pressure while the lungs are at rest. During respiration lateral pressure is different from point to point along each airway, since there are dissipative pressure losses as the air moves from the airway's inlet to its outlet.

Transmural or Transpulmonary Pressure (Ptm)

We call transmural pressure the pressure difference between the two sides of the airways' walls, which means the difference between airways' lateral pressure and pleural pressure, which is uniform around the airways. During respiration, the airways' lateral pressure from point to point

along the bronchial tree is different from the alveolar, due to friction and convective pressure losses. While at rest, airways' lateral pressure is uniform along the bronchial tree and equal to alveolar pressure.

$$\text{Respiration:} \quad Ptm = Plt - Ppl \quad \text{(Non-Uniform)}$$
$$\text{At Rest:} \quad Ptm = Palv - Ppl \quad \text{(Uniform)}$$

Lung Static Recoil Pressure (ΔPL or PstL)

The lung static recoil pressure describes the elastic properties of the lung. It is defined, when the lungs are at rest, as the pressure difference between the alveolar pressure, which is uniform inside the lung airways and the pleural pressure, which is also uniform and surrounds the airways.

$$PstL = Palv - Ppl$$

Lung static recoil pressure is zero while the lungs are at their resting volume, which is the residual volume.

Chest Static Recoil Pressure (ΔPch or PstCH)

Similarly to the lungs, the elastic properties of the chest are described with its chest static recoil pressure. This recoil pressure is the result of the pressure difference between the intrapleural cavity and the atmosphere.

$$PstCH = Ppl - Patm$$

The chest's resting volume, where its static recoil pressure is equal to zero, is approximaly at 0.75% of the TLC.

Respiratory System Static Recoil Pressure (ΔPtotal or PstRS)

The static recoil pressure of the respiratory system is the sum of the static recoil pressures of the lung and chest.

$$PstRS = PstL + PstCH$$

Respiratory Muscle Pressure (Pmuscle or Pe)

Muscle Pressure is the pressure exerted by the muscles of the respiratory system during breathing. Expiratory muscles can exert considerably greater forces on the lungs, than inspiratory muscles. Analytical equations describing the variation of muscle pressure with time during breathing, are developed in *chapter 4*.

2.4 Pressure-Volume Curve

In humans, the expanding pressure around the lungs is due to the increase in the volume of the chest cage. It can be seen in the pressure-volume curve (Figure 2.4.1), that during inflation and deflation, the lung volumes curves follow a completely different path. The lung volume at any given pressure during deflation is greater than the one during inflation. This behavior of the system is known as *hysteresis* (Cheng, DeLong, Franz, Petsonk, Frazer, 1995). Both curves are non-linear and tend to become flatter at high expanding pressure. The horizontal axis demonstrates the transpulmonary pressure, numerically equal to the pressure around the lung, when the alveolar pressure is equal to atmospheric.

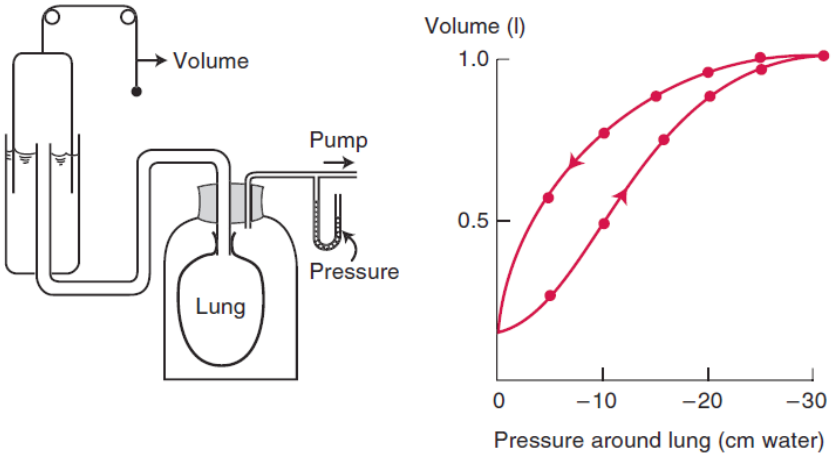

Figure 2.4.1: Measurement of the pressure-volume curve on an excised lung. The measurement of the lung volume is made by helding the lung at each pressure for a few seconds (West, 2012).

When no expanding pressure is applied on the lung, there is still some air left in it. In fact, even if the pressure around the lung exceeds the atmospheric one, some more air is lost due to the closure of the smaller airways, causing gas to trap inside the alveoli. This phenomenon, more oftenly occuring in higher lung volumes with increasing age and during some types of lung diseases (West, 2012), is called airway closure (see below).

Briefly, airway closure was firstly proved experimentaly by *Burger and Macklem* (Burger, Macklem, 1968) in 1968, who managed to describe the closure of smaller airways during expiration. It was *Hughes et al.* (Hughes, Rosenzweig, Kivitz, 1970) in 1970, who during animal studies, provided evidence of airway closure to the very small airways (≈0.4–0.6mm in diameter). The primary mechanical effect responsible for the airway closure is the surface tension developing at the interface between the liquid lining and the air inside the airway.

In healthy lungs, airway closure incurs exclusively in the small airways and especially, when the diameters have their lowest values, that is by the time expiration ends. Then, and according to the law of mass conservation, the liquid film is at its thickest (Heil, Hazel, Smith, 2008). At larger airways, airway closure happens, either due to certain pathological conditions (such as an increase in the volume of the fluid in pulmonary oedema) or is a consequence of a medical intervention in a patient (such as the replacement of the surfactant by a liquid plug in the larger airways) (Espinosa, Kamm, 1998). Finally, the probability of airway closure to happen is actually higher during sleep, obesity and general anaesthesia (Appelberg, Pavlenko, Bergman, Rothen, Hedenstierna, 2007).

2.5 Lung and Chest Compliance

Lung compliance is the measure of the distensibility of the lung, which is its ability to expand. There are two different kinds of compliance, the static and the dynamic lung compliance. Static compliance is the change in volume for any applied pressure, while dynamic compliance is the lung's compliance at any time, during actual movement of air.

Compliance is calculated according to the following equation:

$$Compliance = C = \frac{\Delta V}{\Delta P}$$

where is ΔV the change in volume, and ΔP is the change in pleural pressure.

Lungs with a low compliance are stiff (high elastic recoil), while lungs with high compliance are pliable (low elastic recoil).These are two cases often seen in fibrosis and emphysema respectively as demonstrated in the figure below.

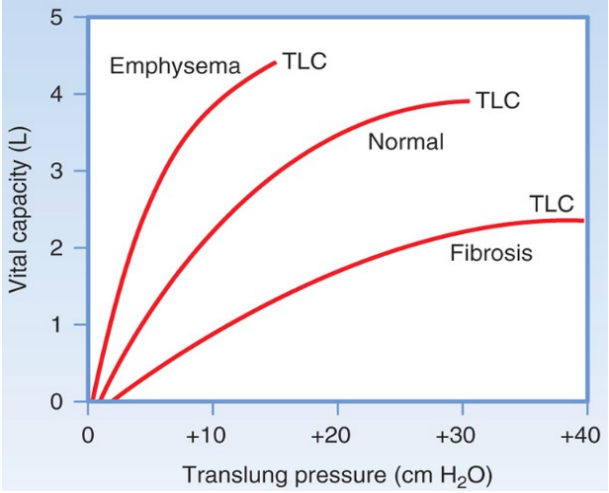

Figure 2.5.1: Pressure-Volume curves for three different lungs: normal, with fibrosis and with emphysema (Koeppen, Stanton, 2008)

Lung compliace is highest at moderate lung volumes; that is around (FRC) and much lower at either very low or very high lung volumes. This behavior is observed because of the difficulty with the initial lung inflation at low volumes and the limit of the chest wall expansion at high lung volumes.

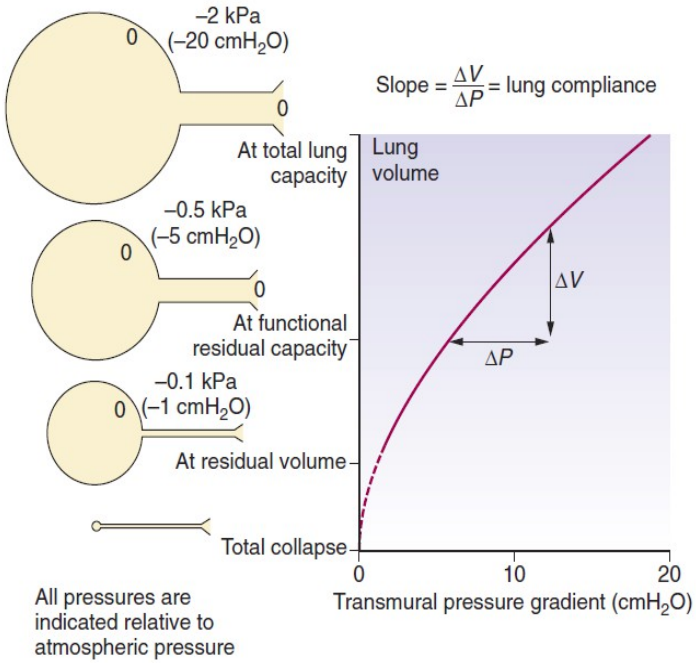

Figure 2.5.2: Variation of lung compliance along the volume-pressure curve (West, 2012).

The compliance of the lungs demonstrates lung hysteresis,as mentioned in *chapter 2.4* (Pressure-Volume Curve); that is, the compliance is different on inspiration and expiration for identical volumes. The total work of the breathing cycle is the area contained in the loop, which is demonstrated below.

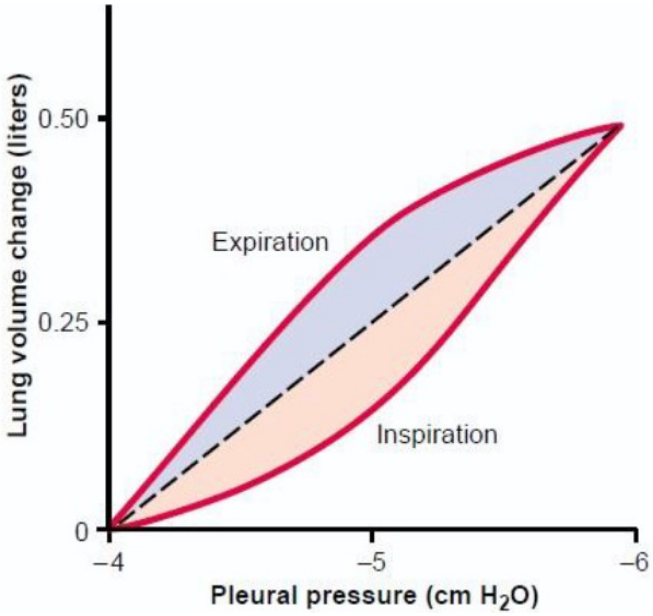

Figure 2.5.3: Lung compliance hysteresis between expiration and inspiration (Guyton, Hall, 1956)

At expanding pressures of -5 to -10 cm H_2O, the lung is either really distensible or very compliant, while the mean compliance of the human lung is approximately 100-200 ml/cm H_2O. Lung compliance depends on the size of the lung, as for larger lung volumes, higher compliance values are achieved.

Chest compliance or the compliance of the thoracic cage, is defined as the change in lung volume per unit change in the pressure gradient, between atmosphere and the intrapleural space. Although it is not usual to measure this quantity, its value range between 150-250 ml/cm H_2O, same units as the lung compliance (Lumb, 2017).

The compliance of lung and chest are considered to be in series, so as the total compliance of the respiratory system is analogous to electrical capacitance in an electrical circuit. Therefore:

$$\frac{1}{total\ compliance} = \frac{1}{lung\ compliance} + \frac{1}{chest\ compliance} \quad ,$$

or if instead of compliance, elasticity of the lung and chest are considered, the relationship changes into:

$$total\ elastance = lung\ elastance + chest\ elastance$$

Analytical equations describing the static recoil pressures of the lung, the chest and the respiratory system at any lung volume are developed in c*hapter 4*.

2.6 Surface Tension

An important factor that determines the pressure-volume behavior of the lung is the surface tension of the liquid film that covers the alveoli. Surface tension is the result of the attractive forces between adjacent molecules of the liquid, which are much stronger than those between the liquid and the gas (Feher, 2016). Thereby, the liquid surface area becomes as small as possible. One can observe this phenomenon by blowing a soap bubble at the end of a tube. Then, the surfaces of the bubble (inner surfaces of the alveoli) interfere with each other as much as possible, forming a sphere and generating a pressure that can be calculated using Laplace's Law. This attraction of the surfaces' molecules for each other within the sphere, opposes expansion and the alveoli's try to collapse. Eventually, surface tension opposes the forces expanding the lung during inspiration.

Laplace’s law for pressure within a bubble when there is air on both sides, creating two fluid air interfaces is described by the formula:

$$P = \frac{4T}{r}$$

where P is the pressure generated in the bubble, T is the surface tension and r is the radius of the bubble. In a liquid-lined spherical alveolus and when only one surface is involved, 2 replaces 4 in the numerator (West, 2012).

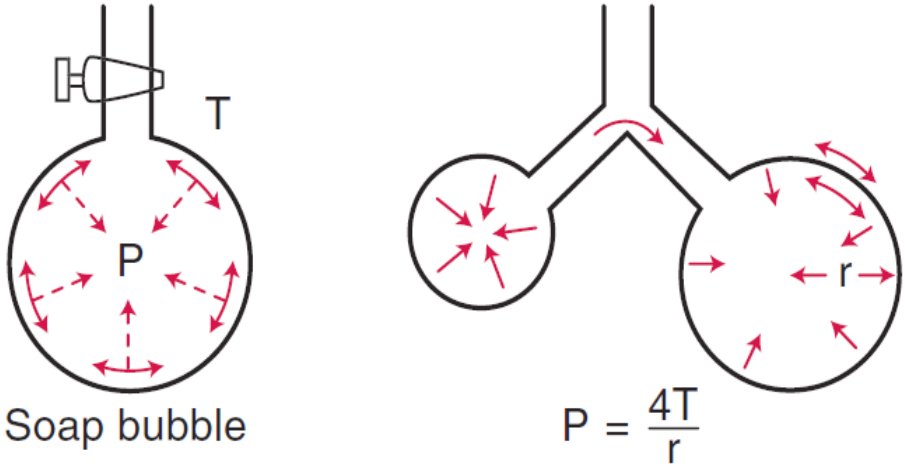

Figure 2.6.1: A soap bubble blown on the end of a tube and two different sized bubbles (West, 2012)

Note: since the smaller bubble generates a larger pressure ($\downarrow r \Rightarrow \uparrow P$) , it blows up the larger one.

In conclusion, the law predicts that a smaller bubble will have a higher pressure within it and that when two bubbles are connected, the smaller bubble will empty into the larger bubble since this is the downhill pressure gradient (Barrow, Pandit, 2017).

However, alveoli are not actually spherical and are lined by pulmonary surfactant that acts to reduce surface tension. This surfactant, produced by type 2 pneumocytes, is a complex mixture of several phospholipids, proteins, and ions and is a surface active agent in the water, to wit it reduces the surface tension of the water.

Briefly, the main functions of the pulmonary surfactant and the reasons that make its presence so important during pulmonary ventilation are that it:

- causes the hysteresis in the lung volume pressure curve
- stabilizes alveolar size
- reduces the work of breathing
- keeps alveoli dry.

2.7 Airway Resistance

Airway resistance is one of the most basic features of the mechanics of breathing. When air flows through a tube, either during inspiration or expiration, a difference of pressure arises between the two ends of the tube, which depends on the rate and the pattern of the flow (West, 2012). Airway resistance is defined as the ratio of driving pressure divided by flow through the airways and it specifies the pressure required so as a flow of air with velocity of 1L/s is achieved (Kaminsky). In order to measure airway resistance, one must know the net flow of air through the lung and the driving pressure for flow, which equals the difference between alveolar pressure and mouth pressure.

When the flow rate is low, the stream lines are parallel to the sides of the tube and the flow is considered to be *laminar*. Laminar flow prevails in larger airways (Barrow, Pandit, 2017), whilst the first observations and conclusions on this kind of flow were made by the French physician Jean Léonard Marie Poiseuille. If the airway is represented by a simple, straight, rigid, circular tube with laminar flow circulating through it, the volume flow rate is given by:

$$Q = \frac{\pi r^4 Pd}{8 \mu L}$$

where, π=3.14159, r is the radius of the tube, Pd is the driving pressure, μ is the viscocity of the gas and L is the length of the tube. Thus, driving pressure Pd is proportional to flow rate Q, or $P_d = K Q$. Since airway resistance R is the driving pressure divided by the flow rate, we conclude that:

$$R = \frac{8 \mu L}{\pi r^4}$$

Notice the importance of tube radius: the r^4 relationship demonstrates how sensitive airway resistance R is to the size of the tube, varying inversely proportional to the 4^{th} power of the radius. For example, if the radius is halved, resistance increases 16 times, when doubling the length L of the tube only doubles the resistance.

Turbulent flow differs a lot from laminar flow. For instance, driving pressure Pd is not directly proportional to flow rate Q, but -approximately- to its square, that is: $Pd = K Q^2$. As it was mentioned before, in turbulent flow the viscocity of the gas is less important then its density, which when increased, causes an increase in the pressure drop for the flow given.

Although convenient, the above calculation of the airway resistance R is considered to be an approximation only, since the airways are not rigid and both laminar and turbulent flow can occur during the flow of the air through them. In addition to the non-linear and non-rigid behavior of the airflow and the airways respectively, the airways generate a complex network of both series and parallel pathways. Moving from the central to the peripheral lung, the total cross sectional surface of the airways increases rapidly and the net airway resistance R drops ultimately. From the 5th to the 8th generation airway resistance rises out due to the small number of narrow airways, but after this region, the existance of more airways per generation but with considerably smaller diameters, result in an increase of the cross sectional area and an overall decrease of the airway resistance. A decrease in successive airway generations appears in both the velocity of the gas and airways diameter, from a maximum value in the trachea to approximately zero at the start of the pulmonary accinus (generation 15). In large diameter airways the length of the individual airway is smaller than the entrance length. As a result of these physical factors, laminar flow can be originally established after approximately the 11th airway generation (Lumb, 2017). The total airway resistance of the respiratory system is a sum of each's airway resistance, due to the parallel arrangement of the airways, that is approximately 2 cm H_2O/L/s, with 25% originating in the chest wall and 75% within the lung (Kaminsky).

2.8 Tissue Resistance

In 1955, *L. E. Mount* related a part of the mechanic work of breathing to the resistance caused by the deformation of the tissues (Mount, 1955) and afterwards, *D' Angelo et al.* (D'Angelo, Calderini, Torri, 1989) described how the part of the respiratory resistance due to the viscoelastic behavior of the tissue, could be measured. One can sufficiently understand the importance of the tissue resistance by the fact that in healthy, anaesthetised subjects, tissue resistance is almost half the size of the total respiratory system resistance (D'Angelo, Calderini, Torri, 1989), while it seems to remain unaffected by end - expiratory volume or tidal volume.

It is both the lung and the chest wall tissues that comprise tissue resistance, but the most important contribution is that of the chest wall (D'Angelo, Tavola, Milic-Emili, 2000), although the significance of tissue resistance of the chest wall, and especially when it comes to lung diseases, is often underestimated.

An accepted value of the lung tissue resistance is referenced as 500 Pa*s/L. (Polak, 1998)

2.9 Respiratory System Resistance

As mentioned before, in order to calculate resistance, one has to determine the simultaneous measurement of both gas flow and the driving pressure gradient. When it comes to respiration, it is often hard to measure the difference of pressure between the mouth and the alveoli, while there are many different methods for measuring the values of the parts that comprise the respiratory system resistance (Lumb, 2017). Although the values of the total respiratory system resistance vary due to the large changes in the lung volumes and other methodological differences, some typical values of the total respiratory system resistance for a healthy male subject are given in the table below:

Components of Respiratory System Resistance

	Mouth and Pharynx	Larynx and Large Airways	Small Airways <3-mm Diameter	Alveoli and Lung Tissue	Chest Wall	Total
Contribution (kPa. l^{-1}.s)	0.05	0.05	0.02	0.02	0.12	0.26
Airway resistance	Body plethysmograph interrupter technique					0.12
Pulmonary resistance	Pressure flow technique					0.14
Respiratory system resistance	Oscillating air flow technique End-inspiratory interruption					0.26

Table 5: Components of Respiratory System Resistance. (blue boxes show whitch components contribute to each form of the resistance, while the text inside these boxes states the methology used to measure them) (Cotes, Chinn, Miller, 2006)

CHAPTER 3. Fundamentals of Fluid Mechanics

In this chapter, the main concepts of fluid mechanics concerning airflow through pipes are presented. Initially, general concepts such as laminar and turbulent flow, Newtonian behavior, flow development in a pipe and compressibility are briefly discussed. Afterwards, the mathematical analysis of Hagen-Poiseuille describing laminar flow in a pipe and the Darcy-Weisbach, pressure drop-airflow relation are cited. Finaly, Bernoulli's principle is also presented, since Bernoulli effects are present along the bronchial tree, something which will become clear in a following chapter.

3.1 Fundamental Characteristics of Fluid Flow in the Airways

Generally speaking, in order to describe completely fluid motion, three spatial dimensions -independent from each other- and time are required. When a flow is not time-dependent, it is called *steady*. In contrast, when a flow depends on the time variable, it is called *unsteady* (Kundu, Cohen, Dowling, 2012). The flow of the air through the human airways in the problem this thesis is analysing, is considered to be quasi-steady.

In order to simplify, visualise and realise better the airflow to and from the human lungs, the motion of the fluid will be examined in less then the three dimensions which would be required to fully describe it, one dimension in particular. *One-dimensional flow* is the flow which can be characterised by one independent, spatial dimension, lined up with either the flow direction or the cross-stream direction (such as the radial distance R of a tube), see *Figure 3.1.1*.

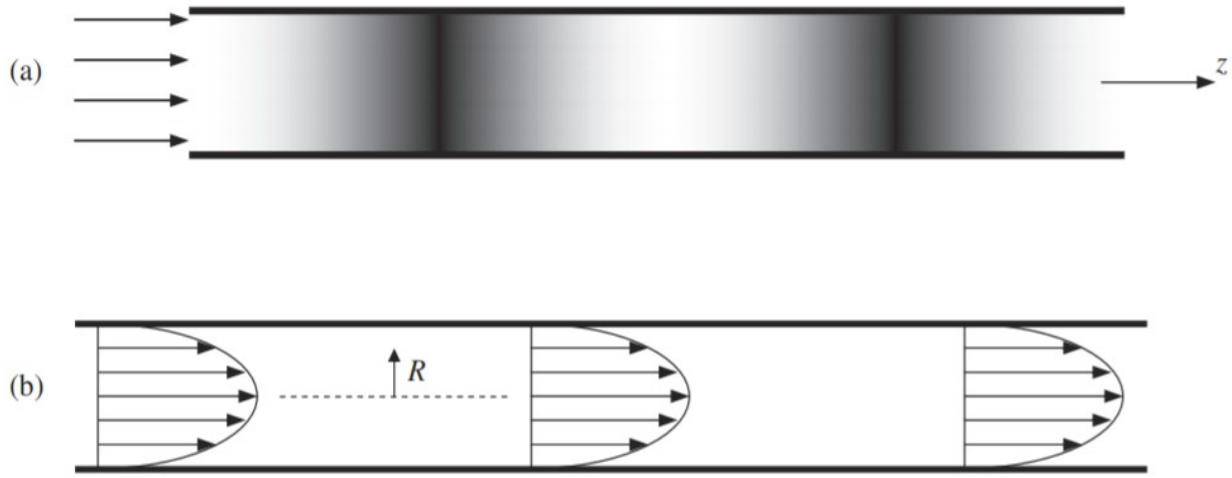

Figure 3.1.1: (a) one-dimensional flow in which the density of the gas varies in the stream-wise z direction only. (b) one-dimensional flow in which the velocity of the gas varied in the cross-stream R direction only (Kundu, Cohen, Dowling, 2012).

3.1.1 Laminar and Turbulent Flow

The viscous flow of a fluid inside a cylindrical pipe such as the airflow inside a lung airway can appear in three different types, which are laminar, transitional and turbulent flow. The three types of flow are distinguished, according to the way in which the fluid's particles move. More specifically:

Laminar flow is the viscous flow regime in which the fluid's particles move smoothly in layers. In every such layer, the distribution of velocity of the fluid is uniform along the transverse (to the fluid's flow direction) cross section of the layer. Therefore, in laminar flow there is no velocity component in the transverse to the fluid's flow direction. During a fully-developed laminar flow, the gas in the center of the tube moves approximately twice as fast as the average velocity (West, 2012). This way, when a spike of gas moves rapidly down the axis of the tube, changing the velocity of the gas across the diameter of the tube, the velocity profile of the gas is created. This means that in laminar flow, there is no macroscopic mixing between neighboring layers, but only microscopic due to the thermal movement of the molecules (Παπαϊωάννου, 2002).

Turbulent flow is the viscous flow regime in which the fluid particles' motion is characterised by chaotic changes in pressure and flow velocity. In turbulent flow vortices, eddies and wakes make the flow unpredictable. Turbulent flow is not characterised by the the high axial flow velocity like the laminar one and the viscocity of the gas in not as important as the density of the gas, which when increased, the pressure drop for the given flow is also increased.

Transitional flow is a mixture of laminar and turbulent flow regimes. For example, a flow through a pipe can be turbulent near the center and laminar near the edges of the pipe.

Reynolds number determines, to a large extent, whether a flow will be laminar or turbulent and is given by the formula:

$$Re = \frac{d\,u\,\rho}{\mu} \quad ,$$

where d is the diameter of the tube, u the average velocity of the gas, ρ the density and μ the viscocity of the gas. In a smooth, straight tube, turbulence appears when Reynolds number exceeds approximately the value of 2000 (West, 2012). Higher Reynolds' number values indicate that inertial forces dominate over the viscous one. Also, notice that for higher velocity of the gas and larger radius (and diameter) of the tube, turbulence is most likely to occur, while lower density gases produce less turbulence.

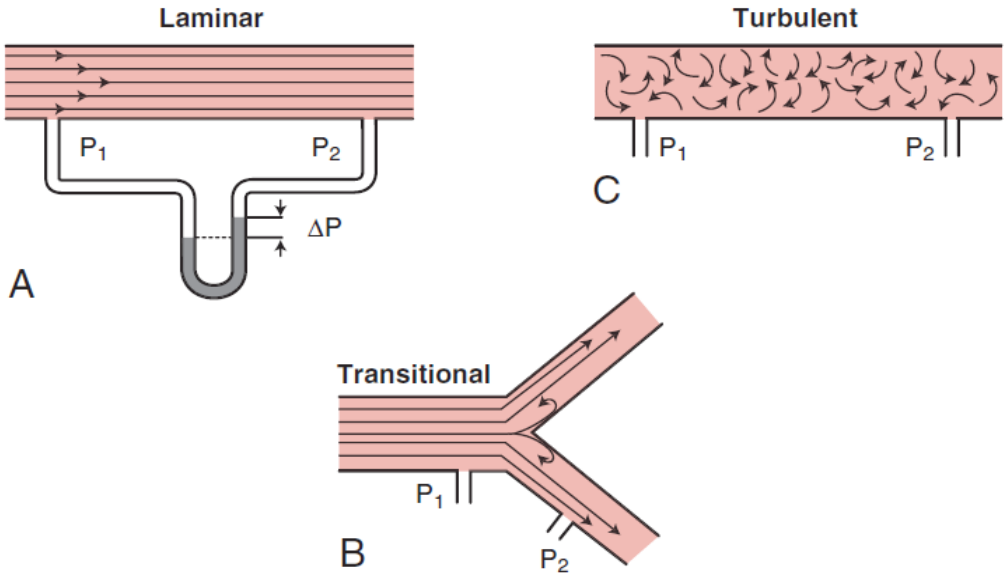

Figure 3.1.1.1: A) Laminar flow B) Transitional flow with eddy formation at branches C) Turbulent flow. Airway resistance R is (P1 – P2)/Q (West, 2012)

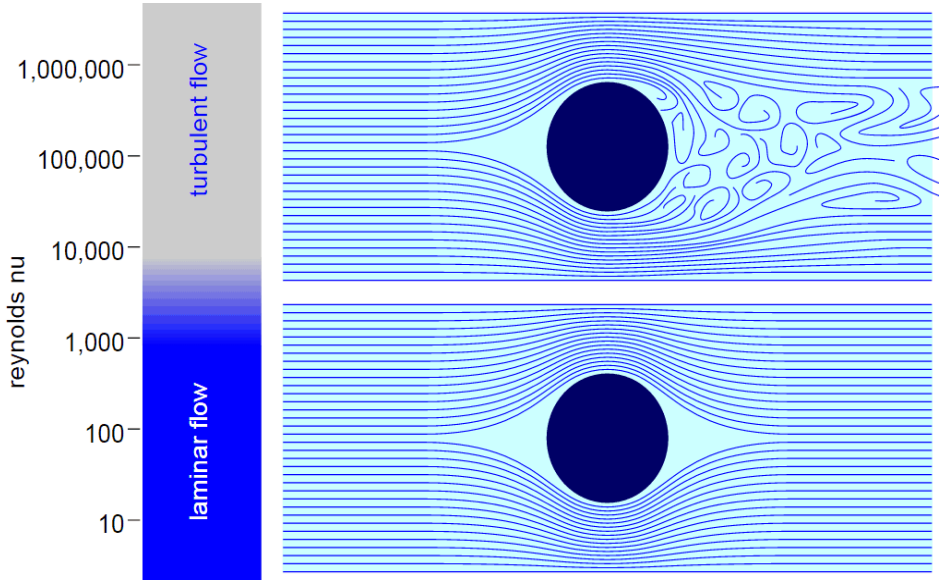

Figure 3.1.1.2: Laminar and turbulent flows at the wake of a cylinder.

3.1.2 Newtonian – Non Newtonian Fluids

Newtonian fluids are the fluids in which the viscous stresses at every point are linearly proportional to the local strain rate. Newtonian fluids obey to Newton's law of viscosity, which states that the ratio of the viscous shear stress developed in a point of the flow field to the respective angular strain rate, is equal to the dynamic viscosity of the fluid (Παπαϊωάννου, 2002):

$$\frac{viscous\ shear\ stress}{angular\ strain\ rate} = dynamic\ viscocity$$

or if τ_{yx} is the viscous shear stress, μ is the dynamic viscosity and γ_{yx} the anngular strain rate, then:

$$\tau_{yx} = \mu \gamma_{yx} \quad (1)$$

with: $\gamma_{yx} = \frac{\partial u_x}{\partial y} + \frac{\partial u_y}{\partial x}$,

which for one-dimension x-flow is written: $\gamma_{yx} = \frac{\partial u_x}{\partial y}$,so Eq. (1) becomes: $\tau_{yx} = \mu \frac{\partial u_x}{\partial y}$.

This equation is known as Newton's law of viscosity and is applied only for laminar, one-dimensional Newtonian fluid flows. In general, Newtonian behavior appears in gases flows and in most common liquid flows. Air and water are considered Newtonian fluids. Therefore, the assumption of Newtonian fluid flow in the lung airways is completely justified. The main characteristic of a Newtonian fluids is that viscosity is for them a real property, whose value depends on the molecular nature and the state (pressure and temperature) in which the fluid is.

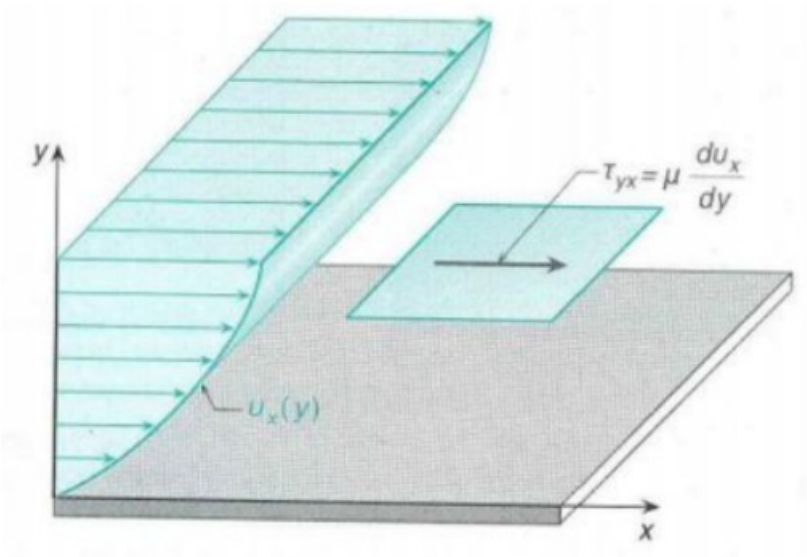

Figure 3.1.2.1: Laminar, one-dimensional Newtonian fluid flow over a plate. (Παπαϊωάννου, 2002)

Non–Newtonian fluids are the fluids in which the dependance of the shear stress to the strain rate is not linear. The slope of the flow curve is not only dependant to the pressure and the temperature

of the fluid but also to the angular strain rate. In these fluids, viscosity has no meaning and it is not a real property of the fluid. It has meaning only when it is connected to a certain shear stress rate.

Non-Newtonian behavior is not generally present in lung fluid flows. However, the bulk rheology of mucus is characterized by a non-Newtonian viscosity that is nonlinear with shear rate, posing strong resistance to deformation at low shear rates and weak resistance at high shear rates. The viscoelasticity of mucus is characterized by a log-linear shear thinning of viscosity (Lai, Wang, Wirtz, Hanes, 2009).

3.1.3 Developing – Fully Developed Flow - Entrance Length in a Pipe

In the entrance region the flow is called *hydrodynamically developing flow*, since the velocity profile in this region is still developing. *Hydrodynamically fully developed flow* is called the flow in the region beyond the entrance length, where the flow has fully developed. A flow can be hydrodynamically fully developed when its normalized temperature profile remains uniform and this kind of flow has the same characteristics as a fully developed flow, which is neither heated nor cooled, inside the tube. During laminar flow in the fully developed region, the velocity profile is *parabolic* and during turbulent flow somewhat flatter, due to the swirly motion of the particles and more vigorous mixing in the radial direction (Çengel, Cimbala, 2006).

The uniformity of the velocity profile during laminar flow, when the flow has surpassed the entrance length, is a phenomenon which can be expressed mathematically by the condition:

$$\frac{\partial u(r,x)}{\partial x}=0 \quad \Rightarrow \quad u=u(r)$$

where x if the direction of the flow along the tube.

Hydrodynamic entrance length is the region where the fluid develops a velocity profile and a non-uniform flow, due to viscous forces from the interior wall of the tube. The distance a flow travels after entering the tube and before it becomes fully developed, is called *entrance length* (https://en.wikipedia.org/wiki/Entrance_length) and that is when the parameters that characterise the flow no longer depend on the change of the distance in the tube. The velocity of the fluid at the entrance of the tube is uniform and after a while, its particles that are in touch with the interior surface of the tube, are restrained due to the no-slip condition.

The velocity profile of the fluid is developed, since the viscous forces of the wall prevent the motion of the layer in touch with the wall and its adjacent layers and slow these layers down gradually. In order for the conservation of mass law to be applied, the velocity of the central layers of the fluid increases to counterbalance the velocity of the sideway layers of the fluid. Thus, a velocity gradient across the cross section of the pipe is created (Figure 3.1.3.1).

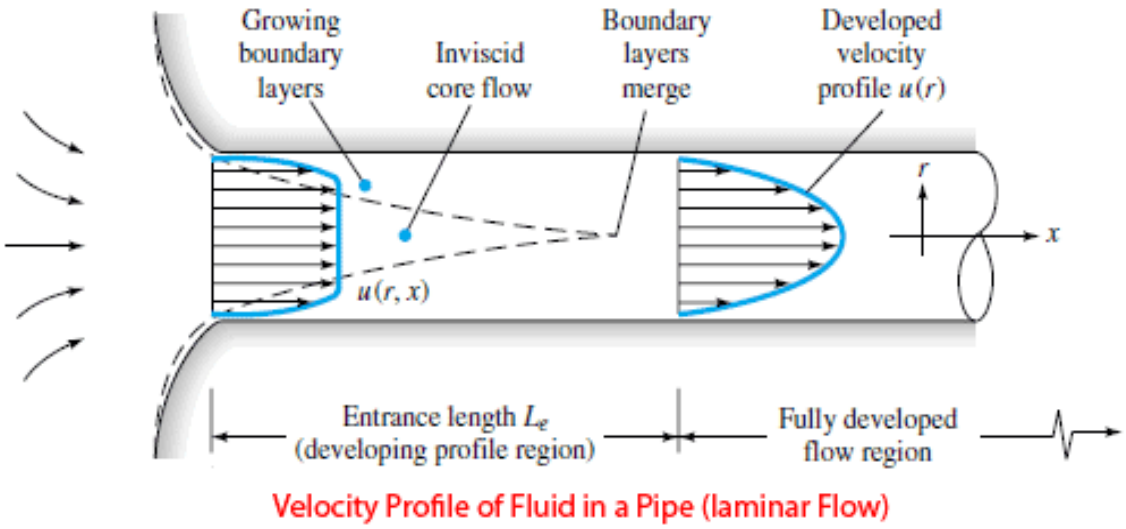

Figure 3.1.3.1: Velocity profile of fluid in a pipe during laminar flow (Sinaga)

The entrance length can be numerically expressed with the dimensionless Entrance Length Number as: $El = \frac{l_e}{d}$ (https://www.engineeringtoolbox.com/entrance-length-flow-d_615.html), where El is the Entrance Length Number, l_e is the length to fully developed velocity profile (length unit) and d is the diameter of the tube (length unit).

@ Laminar Flow: $El_{laminar} = 0.06\,Re$

@ Turbulent Flow: $El_{turbulent} = 4.4\,Re^{1.6}$,where Re is the Reynolds number.

3.1.4 Compressible – Incompressible Flow

The most important difference between compressible and incompressible flow is that, in compressible flow the physical properties of the fluid depend on the area enclosing it, the frictional forces applied from the interior wall of the tube and possible heat transfer. The importance of

compressibility can be assessed by introducing the Mach number M, defined as the ratio of the fluid velocity to the speed of sound:

$$M = \frac{u}{c}$$

Using the Mach number, compressible flow can be categorised (Kundu, Cohen, Dowling, 2012) as:

Incompressible flow: $M = 0$. During the motion of the fluid, the density of the fluid does not depend on the pressure in the flow field and remains constant.

Subsonic flow: $0 < M < 1$. During the motion of the fluid, no shock waves appear in the flow. In engineering problems, for subsonic flows with Mach number less than 0.3, the flow is treated as incompressible.

More specifically, for most of the biological applications, flow will be subsonic (Rubenstein, Yin, Frame, 2015): that means the Mach number will be less than 1, while in the airways the mass conservation law is applied, since a decrease in the cross sectional area of the airway causes an increase in the velocity of the fluid.

In this thesis, the flow of the air through the airways is considered to be incompressible. Up to date and for most of the research that has been done on airflow, flow has been considered to be incompressible, since the air in the nose enters with a low velocity. However, since the density and viscocity of the air both depend on the temperature of the environment surrounding it, for big temperature differences between the nasal cavity and the environment, the incompressibility assumption might be inaccurate.
(https://www.tandfonline.com/doi/full/10.1080/10255842.2017.1307343?scroll=top&needAccess=true&).

3.2 Hagen–Poiseuille Flow

Airflow is mostly laminar inside most generations' lung airways. The velocity distribution and pressure drop for laminar flow inside a cylindrical lung airway can be calculated according to the Hagen-Poiseuille mathematical analysis (Παπανίκας, 2010), which will be cited in the present chapter. For a cylindrical pipe of radius R, tilted by an angle a, the flow is parallel and axisymmetric. The shear stress depends only on the radius r of the pipe.

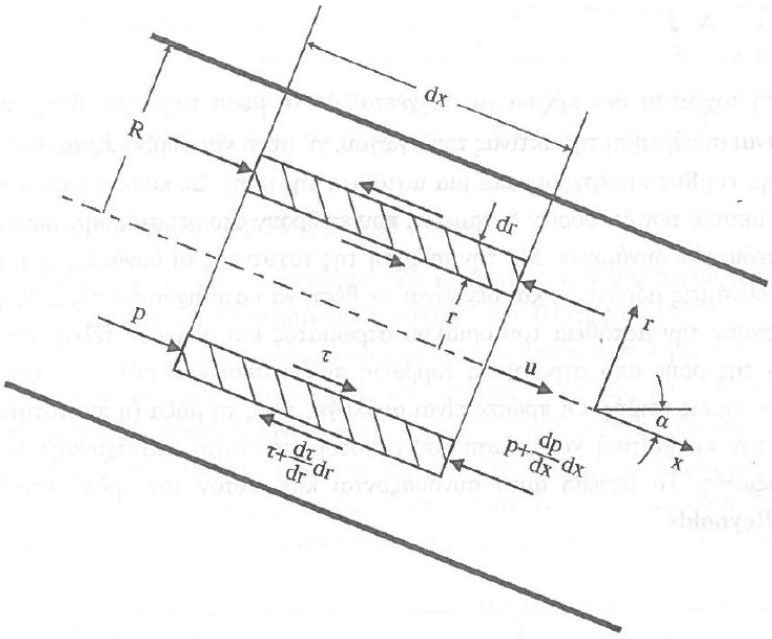

Figure 3.2.1: Laminar flow in a cylindrical tube (Παπανίκας, 2010)

According to the balance of forces in a cylindrical element of the fluid of length dx and radius r:

$$r\pi dr\times(P-P+\frac{dP}{dx}dx)+2\pi\text{rdrdx}\rho\text{gsina}-(\tau\times2\pi\text{rdx}-(\tau+\frac{d\tau}{dr}dr)\times2\pi(r+dr)dx)=0$$

or

$$-r\frac{dP}{dx}+r\rho gsina-(d\frac{(\tau r)}{dr}+\frac{d\tau}{dr}dr)=0$$

the term $\frac{d\tau}{dr}dr$ is of second order and can be neglected, thus:

$$\frac{-dP}{dx}+\rho gsina-\frac{1}{r}\frac{d(\tau r)}{dr}=0 \quad\Rightarrow\quad \frac{-dP}{dx}r\,dr+\rho gsina\,r\,dr-d(\tau*r)=0$$

Integrating the last equation along the radious of the pipe, we get: $\tau=\frac{r}{2}(\frac{-dP}{dx}+\rho gsina)$

and for a pipe or a section of a pipe with length l between two cross-sections 1 and 2, the pressure drop due to friction is: $\Delta P=P_1-P_2$

Integrating along the pipe's length (l) between x_1 and x_2 (x_2-x_1 =l):

$$\tau_l=-\frac{r}{2}\int_{x_1}^{x_2}dP+\frac{r}{2}lgsina \quad\Rightarrow\quad \tau=\frac{r}{2}(\frac{P_1-P_2}{l}+\rho gsina)$$

This means that the shear stress is linearly dependant on the pipe's radius.

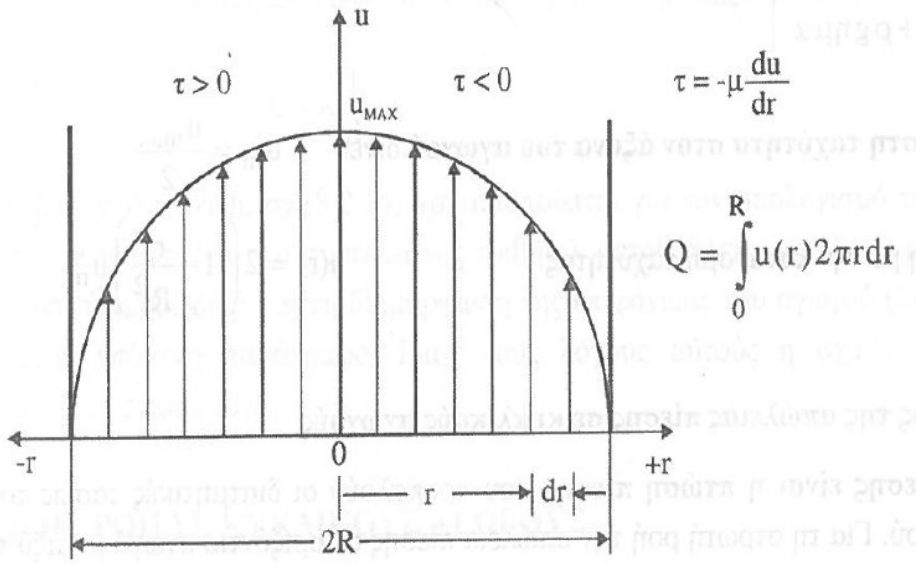

Figure 3.2.2: Volumetric flow rate and shear sterss' sign in a tube (Παπανίκας, 2010)

Introducing the friction law for a Newtonian fluid (Newton's law of viscosity):

$\tau = -\mu \frac{d u_x}{d y}$,we can determine the velocity distribution as followed:

$$-\mu \frac{du}{dr} = \frac{r}{2}\left(\frac{P_1 - P_2}{l} + \rho g \, sina\right)$$

Integrating the above equation along the pipe's radius between its axis and its wall, we get the velocity distribution:

$$u(r) = \frac{r^2}{4\mu}\left(\frac{P_1 - P_2}{l} + \rho g sina\right) + C$$

Applying the no slip condition at the pipe's wall, we have @ r=R: u=0 (m/s). so:

$$u(r) = \frac{R^2}{4\mu}\left(\frac{P_1 - P_2}{l} + \rho g sina\right)\left(1 - \frac{r^2}{R^2}\right)$$

The relation between velocity and the pipe's radius is parabolic, this means that velocity is maximum at the pipe's axis:

$$@\ \text{r=0}: \quad u = u_{max} = \frac{R^2}{4\mu}\left(\frac{P_1 - P_2}{l} + \rho g sina\right)$$

Finally, the flow rate can be calculated as followed:

$$Q = \int_0^R u(r)2\pi r dr \quad \Rightarrow \quad Q = \frac{\pi R^4}{8\mu}\left(\frac{P_1 - P_2}{l} + \rho g sina\right)$$

This means that in laminar flow inside a pipe, the flow rate (Q) is proportional to the fourth power of the radius and proportional to the pressure drop due to friction.

3.3 Darcy-Weisbach Equation

The pressure loss due to friction at the pipe's walls can be related to the average velocity according to the phenomenological Darcy-Weisbach equation. For laminar flow in a cylindrical, horizontal (a=0) pipe , the average fluid velocity is (Παπανίκας, 2010):

$$u_m = \frac{Q}{A} = \frac{R^2}{8\mu}\frac{P_1 - P_2}{l} \quad ,$$

so the pressure drop between two cross-sections 1 and 2 is:

$$\Delta P_\tau = P_1 - P_2 = 8\mu \frac{l}{R^2} u_m$$

This means that for laminar flow the pressure drop is proportional to the average velocity.

The above equation can be written again in terms of the pipe's diameter d and the dynamic pressure $q = \rho u^2 / 2$ as followed:

$$\Delta P_\tau = \frac{64}{Re}\frac{l}{d}\rho\frac{u_m^2}{2}$$

where the Reynolds number has been used: $Re = \frac{d u_m}{v} = \frac{d \rho u_m}{\mu}$

The dimensionsless term $f_D = \frac{64}{Re}$ is the friction factor of the pipe and is directly proportional to the shear stress τ_o at the pipe's walls:

$$\tau_o = -\mu\left(\frac{du}{dr}\right)_{r=R} = -\mu\left(\frac{-4r}{R^2}u_m\right)_{r=R} = \frac{4\mu}{R}u_m$$

and

$$f_D = \frac{64}{Re} = \frac{32\mu}{\rho u_m R} = 8\frac{\tau_o}{\rho u_m^2}$$

So the general form of the Darcy-Weisbach equation is:

$$\Delta P_\tau = f_D \frac{l}{d}\rho\frac{u_m^2}{2}$$

The friction factor is not a constant. It depends on the characteristics of the pipe and the fluid, as well as on the velocity of the fluid. It has been measured for various flow regimes and it can be calculated using empirical relations or be read from published charts. These charts are the Moody diagrams (Figure 3.3.1).

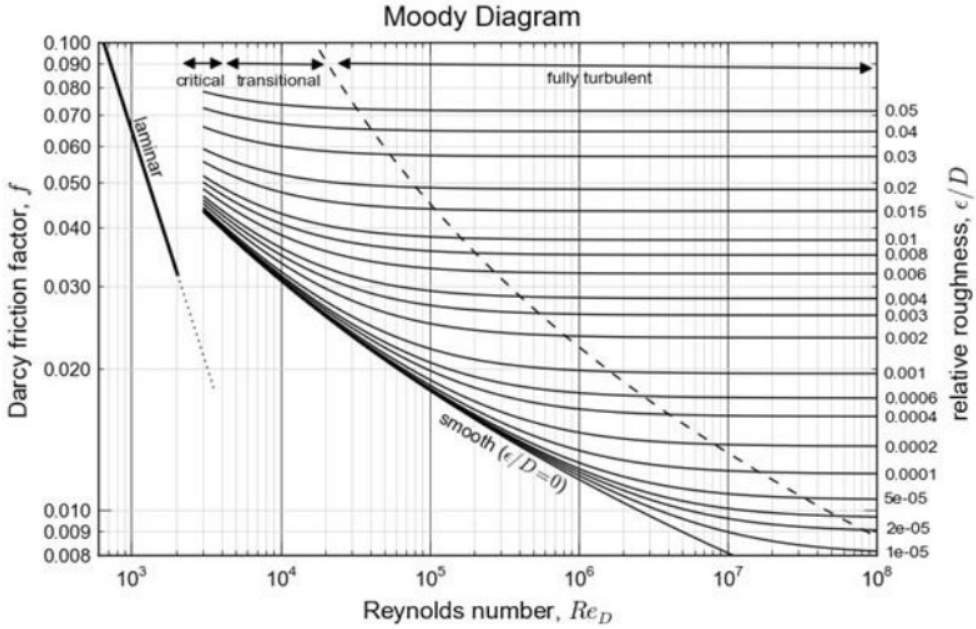

Figure 3.3.1: Moody diagram, graphically predicting the friction factor f_D according to the Reynolds number for various values of the relative roughness (ε/D) of the pipe. (https://en.wikipedia.org/wiki/Moody_chart)

3.4 Bernoulli's Principle

The Bernoulli's Principle in fluid dynamics states that the decrease in pressure or in the potential energy of the fluid follows a simultaneously increase in the speed of the fluid. At low Mach numbers, the density of a fluid parcel can be considered to be constant, regardless of pressure variations in the flow and therefore, the fluid can be considered to be incompressible. These flows are called incompressible flows. The flow is also considered quasi steady, without losses due to friction at the point of branching. During a forced vital capacity, considering the flow to be incompressible and quasi steady is completely justifiable (Lambert, Wilson, Hyatt, Rodarte, 1982) and as a result, the fluid satisfies all the restrictions governing the use of Bernoulli's equation, delivering one of its' most common forms (valid at any arbitrary point along a streamline):

$$\frac{u^2}{2}+g\,z+\frac{P}{\rho}=constant \quad \Rightarrow \quad \frac{1}{2}\rho\,u^2+\rho\,g\,z+P=constant$$

where the difference between the two points (z_1, z_2) in the airways of the lung during respiration is considered to be negligible. Therefore:

$$\frac{1}{2}\rho\,u^2+P=constant \quad \text{(Bernoulli's Equation)}$$

Bernoulli effect in the junctions between generations

According to the idealized lung geometry of *Weibel* (Weibel, 1963) which is used as the anatomical basis of our model, the generation number (g) ranges from 0 at the trachea to 23 at the most peripheral bronchioli (Hammersley, Olson, 1992), forming a symmetrically bifurcating tree of airways within the lungs. Assuming that the neutral cross-sectional areas are constant, there is a difference between the cross-sectional area of a mother tube (generation g) and the total cross-sectional area of the tubes in the next generation (generation g+1).

This difference leads to additional convective pressure losses or gains (during expiration and inspiration respectively) at the junctions between generations, which can be calculated according to the Bernoulli equation (equation of the conservation of the mechanical energy). Also, we assume that the transition from one generation to the next takes place over such a short distance, that dissipation is negligible (Polak, 1998)

Generally, with the exception of the three first generations, the total cross-sectional area of the tubes of each generation increases as we move to higher generations: $A(g+1)>A(g)$. We also assume that the cross-sectional area remains the same along the length of each airway.

The exact equations for the calculation of convective pressure variations between the junctions are cited in a special chapter of our mathematical model analysis.

CHAPTER 4: Mathematical Model Analysis

This chapter contains the set of equations describing the process of breathing. At first, equations concerning the elastic properties of the respiratory system are developed. Then, the driving pressure is determined in relation to muscle pressure, elastic forces and lung tissue resistance. Dissipative, convective and mouth pressure drops are calculated analytically and are equated with driving pressure, yielding the basic non-linear equation describing the airflow. Moreover, the formulas for the calculation of the airways cross-sectional area variation with transmural pressure, as developed by *Lambert et al.* (Lambert, Wilson, Hyatt, Rodarte, 1982) are cited, as well as the mechanism behind the emerging phenomenon of flow limitation is described. Finally, and as an extra, an accurate model which does not neglect airways' diameter variation along their length, as it was developed by *Filoche and Florens* (Filoche, Florens, 2011), is presented.

4.1 Quantitative Description of the Elastic Properties of the Lung

As mentioned before the distensibilities of the lung, the chest and the respiratory system as a total are described with compliance. The higher its compliance is, the easier it is for the lung or the chest to expand under the same applied pressure. Static compliance constitutes the slope of the lung volume-static recoil pressure curve. The exact relations between the different static recoil pressures and the lung volume are developed in the following chapter.

Lung Static Recoil Pressure

The lung static recoil pressure describes the elastic properties of the lung. It is defined, with the lungs being at rest, as the pressure difference between the alveolar pressure, which is uniform inside the lung airways and the pleural pressure, which is also uniform and surrounds the airways.

$$P_{stL} = P_{alv} - P_{pl}$$

There is an analytical relation for the calculation of the static recoil pressure of the lung P_{stL} at any lung volume V_L. The recoil pressure becomes maximal as lung volume tends to total lung capacity (TLC), since the elastic forces of the lung tend to collapse it to its residual volume (RV), where the recoil pressure is equal to zero. More specifically, static recoil pressure of the lung is a logarithmic function of lung volume (Polak, 1998):

$$P_{stL}(V_L) = \frac{V_m - V_0}{C_{L0}} \ln\left(\frac{V_m - V_0}{V_m - V_L}\right) \quad (1)$$

where, V_m and V_0 are the maximal and minimal lung volumes and C_{L0} is the lung compliance at zero recoil pressure. Using the same parameters as *A.G. Polak* (Polak, 1998), we have:

V_m=1.06·TLC= 7.5 (L), V_0=0.2·TLC= 1.4 (L), while the lung compliance at zero static recoil pressure (C_{L0}= 5.7 L/kPa or 559 mL/cmH_2O), was computed according to equation (1) for P_{stL}=3 (kPa) and V_L= 95%·V_m.

Chest Static Recoil Pressure

Similarly to the lungs, the elastic properties of the chest are described with its chest static recoil pressure. This recoil pressure is the result of the pressure difference between the intrapleural cavity and the atmosphere.

$$P_{stCH} = P_{pl} - P_{atm}$$

The function connecting the static recoil pressure of the chest (P_{stCH}) , with the lung volume (V_L) is also logarithmic. Chest static recoil pressure is also maximal at total lung capacity (TLC), but it becomes negative in sign, as lung volume tends to its residual volume (RV), meaning that below a certain lung volume the elastic forces of the chest tend to expand it. At residual volume, the chest static recoil pressure has its maximal negative value.

$$P_{stCH} = P_{max} - \left(\frac{V_m - V_0}{C_{CH}}\right) \ln\left(\frac{V_m - V_0}{V_L - V_0}\right) \quad (2)$$

where again V_m and V_0 are the maximal and the minimal lung volumes, P_{max} is the maximal chest static recoil pressure and C_{CH} is the compliance of the chest.

The parameters P_{max} and C_{CH} can be determined by solving the system of equations, which is produced from Eq. (2) for V_L =0.75·V_m and V_L=FRC. We consider that the static recoil pressure of the chest is equal to zero (P_{stCH}=0) and thus the chest is at its resting volume at approximately 0.75·V_m, while at functional residual capacity (FRC) the elastic forces of the lung and the chest are at equilibrium P_{stCH}=-P_{stL}.

$$@\ \ V_L = 0.75\mathrm{V}_m\ \ :\ \ P_{max} = \frac{V_m - V_0}{C_{CH}} \ln\left(\frac{V_m - V_0}{0.75\mathrm{V}_m - V_0}\right) \quad (2a)$$

$$@\ \ V_L = FRC\ \ :\ \ P_{stCH} = -\frac{V_m - V_0}{C_{L0}} \ln\left(\frac{V_m - V_0}{V_m - FRC}\right)$$

or

$$P_{max} - \frac{V_m - V_0}{C_{CHln}}\left(\frac{V_m - V_0}{FRC - V_0}\right) = -\frac{V_m - V_0}{C_{L0}} \ln\left(\frac{V_m - V_0}{V_m - FRC}\right) \quad (2b)$$

Substituting (2a) to (2b), we eventually get to a direct relation between the compliance of the chest C_{CH} and the compliance of the lung C_{L0}:

$$C_{CH} = -C_{L0} \frac{\ln\left(\frac{FRC - V_0}{0.75\mathrm{V}_m - V_0}\right)}{\ln\left(\frac{V_m - V_0}{V_m - FRC}\right)} \quad (3)$$

For FRC=2.6 (L) the compliance of the chest, according to Eq. (3), is C_{CH}=29.4 (L/kPa) or 2883 (mL/cmH_2O), and according to Eq. (2a) the maximal chest static recoil pressure is P_{max}=75.3684 (Pa) .

Note: the two values for lung and chest compliance determined above are not to be confused with the respective compliances found in medical bibliography. Lung compliance in our analysis represents the slope of the volume-recoil pressure curve of the lung at (RV), where the static recoil pressure is zero, while chest compliance is the slope of the chest curve at $0.75 \cdot \mathrm{V}_m$. Compliances found in medical bibliography constitute mean values of the curve's slope around (FRC) and are experimentally determined on unconsious patients, under mechanically supported breathing.

Respiratory System's Static Recoil Pressure

Setting the respiratory system together, we can determine its recoil presssure (P_{stRS}) as the algebraic sum of the static recoil pressure of the lung and of the chest. The respiratory system is at rest, when the elastic forces of the lung and the chest are oposite in direction and equal in magnitude. This happens at functional residual capacity (FRC) where P_{stRS}=0.

$$P_{stRS} = P_{stL} + P_{stCH} \quad (4)$$

Lung Volume- Recoil Pressure Graph

The elastic behavior of the respiratory system is demonstrated in a volume-recoil pressure diagram, with lung volume ranging from residual volume (RV) to total lung capacity (TLC). The equilibrium of elastic forces between the lung and the chest is achieved at functional residual capacity (FRC), where the recoil pressure of the respiratory system is zero.

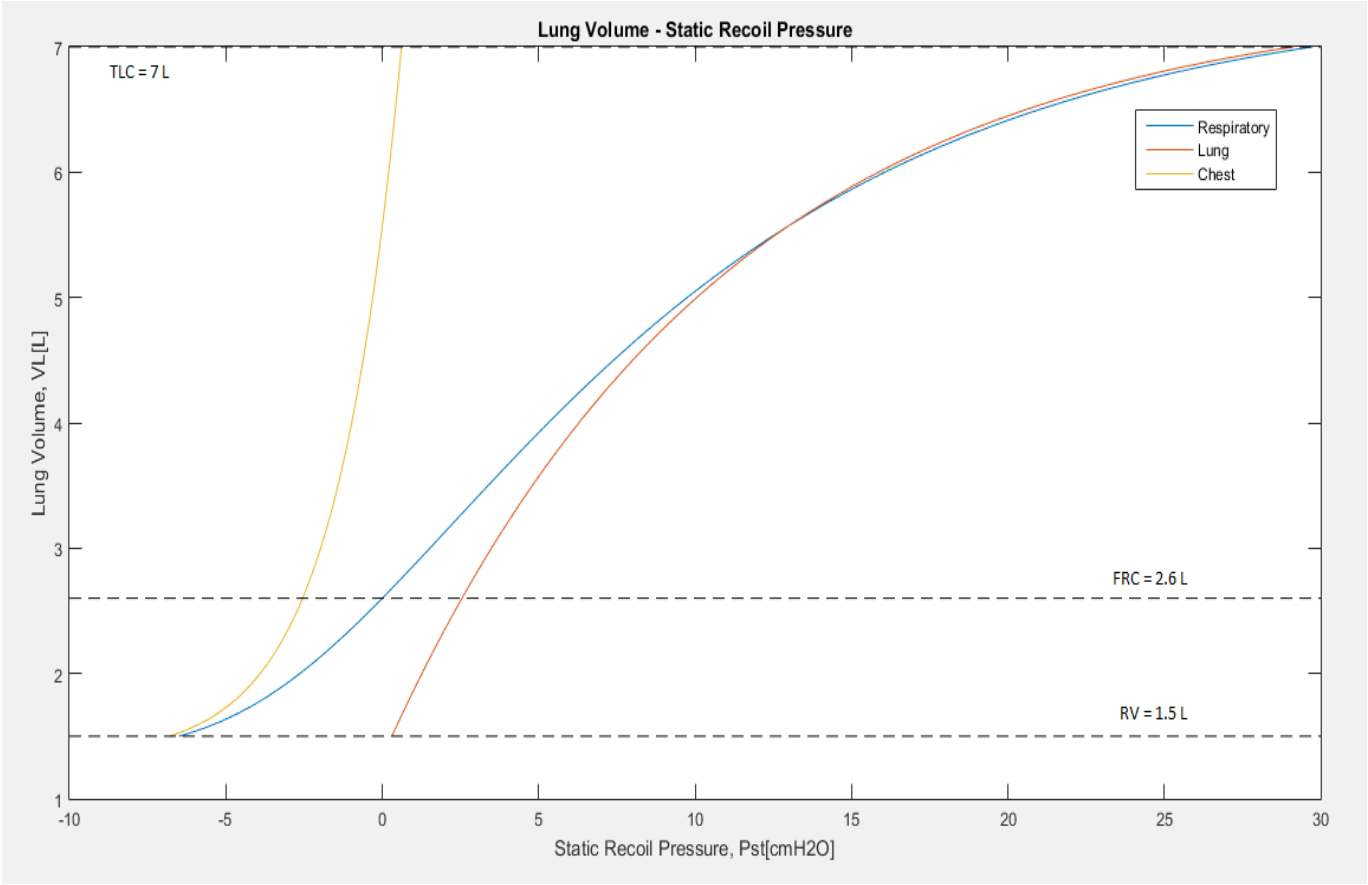

Figure 4.1.1 The three different lung volume- static recoil pressure curves.

Note: The piece of code used for the production of the above graph is contained in the main algorithm of the forced expiration calculation, which is cited in A*ppendix A*.

4.2 Quantitative Description of Driving Pressure

The driving pressure for breathing as described in a previous chapter, is defined as the difference between the alveolar and the atmospheric pressure. Since atmospheric pressure is considered as reference pressure and thus is equal to zero at any lung volume during breathing, driving pressure is actually equal to alveolar pressure. During forced expiration, the driving or alveolar pressure is greater than atmospheric pressure, meaning positive in sign and thus, air is forced to leave the lung

alveoli and move towards the mouth. The opposite is true during inspiration, when alveolar pressure is lower than atmospheric, resulting to the suction of atmospheric air into the lungs. Driving pressure is directly related to both respiratory muscle and elastic forces. In the following analysis a mathematical model, which allows the exact calculation of the driving pressure at any lung volume, is introduced.

Expiratory muscle pressure

According to *A.G. Polak* (Polak, 1998), who was based on the data of *Agostoni and Fenn (*Agostoni, Fenn, 1960), we can assume an exponential increase in muscle power during expiration. The pressure exerted by expiratory muscles is:

$$P_e(V)=\frac{P_m}{VC}\left(1-e^{-t/\tau}\right)(VC-V) \quad (1)$$

where V is the volume of the expired air, Pm is the maximal pressure that can be produced by expiratory muscles, (VC) is the vital capacity and τ is the time constant.

The variation of the expiratory muscle pressure during a forced expiration maneuver can be demonstrated assuming an exponential relation between the expired air volume (V) and time (t). This assumption is in agreement with experimental data collected during spirometric tests. Such a relation found in the work of *J. Jordanoglou et al.* (Jordanoglou et al., 1979) is:

$$V = FVC \times e^{\left(\frac{-t}{t_{eff}}\right)} \quad (2)$$

where (FVC) is the forced vital capacity and t_{eff} is the effective time of forced expiration, which coincides with the relation's time constant. Effective time is linearly depended on age and it can be determined according to the equation:

$$t_{eff}=0.1573+0.0141\,Age \quad (\ t_{eff}\ \text{in s and Age in years}\ )$$

Substituting Eq. (2) to Eq. (1), we get a direct muscle pressure-expired air volume relation, which is plotted over a full forced vital capacity FVC= 5.5 (L) volume change.

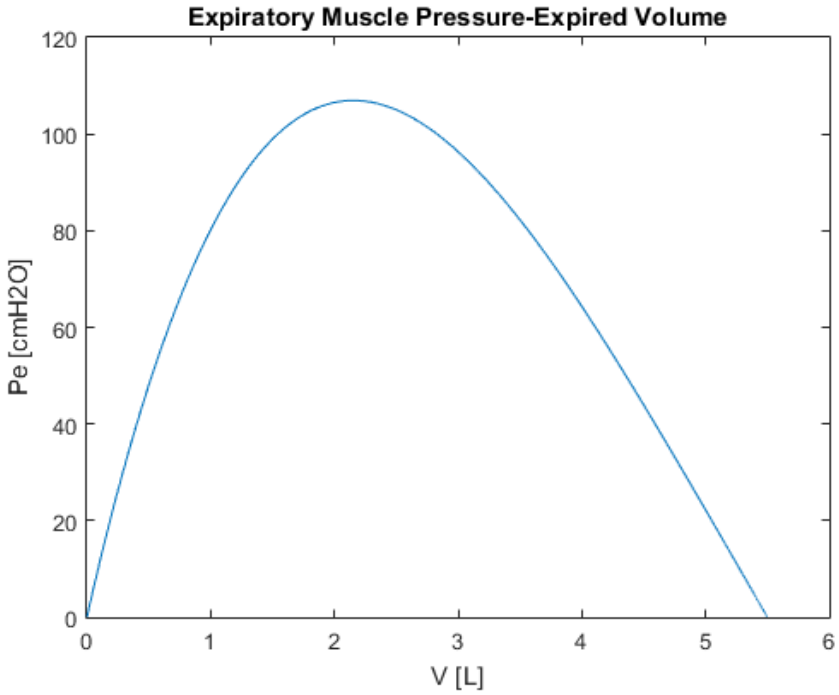

Figure 4.2.1 Expiratory muscle pressure-expired volume curve for a 25 year old man with P_m=24kPa or 245 cmH_2O and τ=0.2s.

Driving pressure

Following the analysis of *A.G. Polak* (Polak, 1998) the expiratory muscle pressure (P_e) is spent on two components: the driving pressure (P_d) and the pressure losses caused by respiratory tissue resistance (R_T) during airflow (Q) and thus:

$$P_e = P_d + R_T Q \quad (3)$$

Substituting Eq. (1) to Eq (3) we get the formula for the driving pressure:

$$P_d(V) = P_m\left(1 - e^{(-t/\tau)}\right)\left(1 - \frac{V}{VC}\right) - R_T Q \quad (4)$$

Modification

The above analysis is probably neglecting the elastic forces of the respiratory system, which should also be a component of muscle pressure. Therefore, a modified model which includes these forces in the calculation, was developed. A third component, which is the respiratory system static recoil pressure (P_{stRS}), described in a previous chapter, is added in Eq. (3):

$$P_e + P_{stRS} = P_d + R_T Q \quad (3')$$

Eq. (1) describing the muscle pressure is also altered, in order to agree with the new model as follows:

$$P_e(V) = -P_{stRS}(TLC) + (1 - e^{-t/\tau})\left(P_m \frac{VC - V}{VC} + P_{stRS}(TLC) - P_{stRS}(RV)\right) \quad (1')$$

where P_{stRS}(TLC) is the respiratory system's static recoil pressure at the beginning of expiration and P_{stRS}(RV) is the respiratory system's static recoil pressure at the end of it.

Thus the driving pressure is calculated as:

$$P_d(V) = -P_{stRS}(TLC) + (1 - e^{-t/\tau})\left(P_m \frac{VC - V}{VC} + P_{stRS}(TLC) - P_{stRS}(RV)\right) + P_{stRS}(V_L) - R_T Q \quad (4')$$

The relation between instant lung and expired air volumes is:

$$V_L = VC + RV - V \quad (5)$$

Inspiratory muscle and driving pressures

The same exponential variation was assumed for the inspiratory muscle pressure:

$$P_e(V) = \frac{P_m}{VC}(1 - e^{-t/\tau})(VC - V) \quad (6)$$

where now P_m is the maximal inspiratory muscle pressure, which is considerably lower than the respective pressure of expiration and V is the volume of the inspired air.

Again the driving pressure can be calculated as:

$$P_d(V) = P_m(1 - e^{(-t/\tau)})(1 - \frac{V}{VC}) - R_T Q \quad (7)$$

While the modification to include elasticity is:

$$P_e(V) = -P_{stRS}(RV) - (1 - e^{-t/\tau})\left(P_m \frac{VC - V}{VC} + P_{stRS}(TLC) - P_{stRS}(RV)\right) \quad (6')$$

and

$$P_d(V) = -P_{stRS}(RV) - (1 - e^{-t/\tau})\left(P_m \frac{VC - V}{VC} + P_{stRS}(TLC) - P_{stRS}(RV)\right) + P_{stRS}(V_L) - R_T Q \quad (7')$$

4.3 Dissipative Pressure Loss in an Airway of g Generation

In the analysis that follows, lung airways of each generation are considered as compliant tubes, which maintain a constant diameter along their length. This approximation is not completely accurate, since the transmural pressure during airflow through the airway varies across its length, leading to a variation of its diameter as we move from its inlet to its outlet (see chapter 4.8 An accurate model for the flexible tube). Airflow through each generation's pipe is considered to be laminar and thus the pressure drop due to friction can be calculated according to the Hagen-Poiseuille analysis, which was extensively cited in a previous chapter. Corrections for both entrance and turbulent phenomena are also introduced.

The pressure drop due to friction (ΔP_f) for laminar flow through a g generation pipe of the bronchial tree, with length L(g) and diameter D(g), can be calculated according to the Darcy-Weisbach equation, as described in a previous chapter:

$$\Delta P_f(g) = f_D \frac{L(g)\rho v^2(g)}{2\mathrm{D}(g)} \quad (1)$$

where v(g) is the mean air velocity in the pipe and f_D is the friction factor, which for laminar flow is $f_D = 64/\mathrm{Re}$. $\mathrm{Re} = \rho v(g) D(g)/\mu$ is the mean Reynolds number in the pipe.

Substituting to Eq. (1) we get:

$$\Delta P_f(g) = \frac{64\mu \mathrm{L}(g) v(g)}{2\mathrm{D}^2(g)} \quad (2)$$

The mean air velocity in the pipe can be written as: $v(g) = q(g)/A_c(g)$, with q(g) being the volumetric airflow through the pipe and $A_c(g) = \pi D^2(g)/4$ the pipe's crossectional area. Substituting to Eq. (2) we get the final expression for the dissipative pressure loss through a pipe:

$$\Delta P_f(g) = \frac{128\mu L(g) q(g)}{\pi D^4(g)} \quad (3)$$

However, according to the experimental work of *Reynolds* (Reynolds, 1982), entrance and inertial phenomena should be taken under consideration and thus Eq. (3) becomes:

$$\Delta P_f(g) = \frac{128\mu L(g) q(g)}{\pi D^4(g)} (a + bRe)$$

or

$$\Delta P_f(g) = a \frac{128\mu L(g) q(g)}{\pi D^4(g)} + b \frac{512\rho L(g) q^2(g)}{\pi^2 D^5(g)} \quad (4)$$

The two phenomenological constants a and b in the above equation account for entrance and inertial phenomena. According to *Filoche and Florens* (Filoche, Florens, 2011), constant a, which should be equal to 1 for an infinite straight pipe, accounts for the fact that the Poiseuille profile needs some time to set up in the branches of the network, as seen in a previous chapter. Constant b accounts for losses when inertial forces are present i.e. at higher velocities (turbulent flow).

As mentioned before, airflow q(g) in the airway of generation g is connected to the volumetric airflow Q in the mouth according to the following formula:

$$q(g) = Q 2^{-g}$$

This means that airflow is considered to seperate equally from a mother tube to the two daughters of the next generation at every junction along the bronchial tree.

Thus Eq. (4) becomes:

$$\Delta P_f(g) = a \frac{128\mu L(g) Q}{\pi D^4(g)} \frac{1}{2^g} + b \frac{512\rho L(g) Q^2}{\pi^2 D^5(g)} \frac{1}{2^{2g}} \quad (5)$$

So according to Eq. (5) dissipative pressure loss through generation g is a second order function of airflow Q.

4.4 Convective Pressure Variations between Generations

Convective pressure variations are also present during the airflow along the bronchial tree. These variations are a result of the acceleration or deceleration of the flow, which takes place at the junctions between generations, where the cross-sectional area decreases or increases respectively. Their calculation is based on the Bernoulli analysis, which was presented in a previous chapter.

Convective pressure recovery during inspiration

During inspiration, the air flows from the trachea (generation g=0) to the peripheral bronchioli (generation g=23) through the airways, due to the difference in pressure between those two points. Downstream end (L) of g generation's airway and upstream end (0) of (g+1) generation's airway are both presented in the figure below:

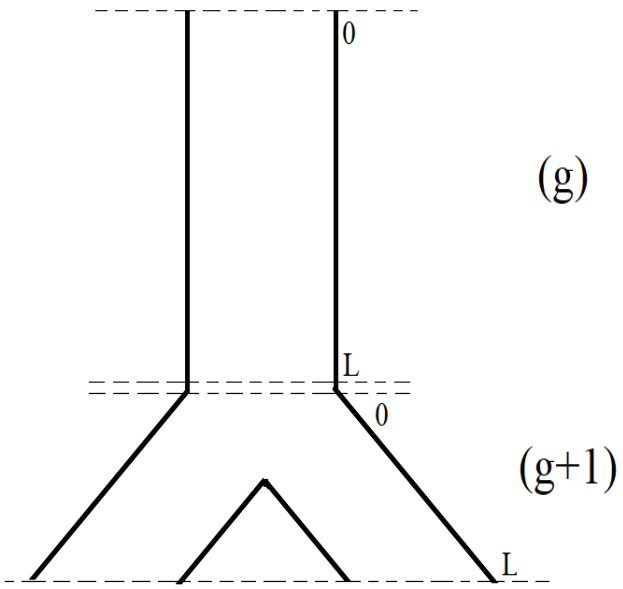

Figure 4.4.1 Generation sorting during inspiration

According to the Bernoulli Equation ,the relation between the pressure at the downstream end of g generation $P_L(g)$, and the pressure at the upstream end of (g+1) generation $P_0(g+1)$ can be extracted as followed:

$$\frac{1}{2}\rho u^2 + P = constant \Rightarrow P_L(g) + \frac{1}{2}\rho U_L^2(g) = P_0(g+1) + \frac{1}{2}\rho U_0^2(g+1) \Rightarrow$$

$$P_L(g) - P_0(g+1) = \frac{1}{2}\rho [U_0^2(g+1) - U_L^2(g)] \Rightarrow$$

where: $U=\frac{Q}{A}$ and Q: volumetric airflow in the mouth.

A_0: total cross-sectional area at the beginning of the bronchus

A_L: total cross-sectional area at the end of the bronchus

$q(g)=Q2^{(-g)}$: airflow q in the tube of generation g in the dichotomous bronchial tree

$$\Rightarrow P_L(g)-P_0(g+1)=\frac{1}{2}\rho[\frac{q^2(g+1)}{A_0^2(g+1)}-\frac{q^2(g)}{A_L^2(g)}]=\frac{1}{2}\rho[\frac{Q^2 2^{-2g}2^{-2}}{A_0^2(g+1)}-\frac{Q^2 2^{-2g}}{A_L^2(g)}]\Rightarrow$$

$$\Rightarrow P_L(g)-P_0(g+1)=\frac{1}{2}\rho Q^2 2^{-2g}[\frac{1}{4A_0^2(g+1)}-\frac{1}{A_L^2(g)}]\Rightarrow$$

$$\Rightarrow P_L(g)-P_0(g+1)=\frac{1}{2}\rho q^2(g)[\frac{1}{4A_0^2(g+1)}-\frac{1}{A_L^2(g)}]\Rightarrow$$

$$\Rightarrow \Delta P_c(g)=\frac{1}{2}\rho q^2(g)[\frac{1}{4A_0^2(g+1)}-\frac{1}{A_L^2(g)}] \text{ , or } \Delta P_c(g)=\rho\frac{Q^2}{2^{2g+1}}[\frac{1}{4A_0^2(g+1)}-\frac{1}{A_L^2(g)}]$$

In general, with the exception of the three first generations, the total crossectional area of the airways at each generation is increasing as we move to higher generations, since, despite the decrease in airways' size, there is a dramatic increase in their number.

Thus: $A_0(g+1)>A_L(g)$ and $\Delta P_c(g)<0$,which means that:

$$P_0(g+1)>P_L(g)$$

The above relation represents a pressure gain $\Delta P_c(g)$ that arises from convection in the junctions between airways as we move from the trachea to the alveoli. As mentioned before, the dissipative pressure loss due to branching is neglected.

Convective pressure loss during expiration

During expiration, the air flows from the peripheral bronchioli (generation g=23) to the trachea (generation g=0) through the airways, due to the difference in pressure among those two points. Downstream end (L) of g generation's airway and upstream end (0) of (g+1) generation's airways are both presented in the figure below:

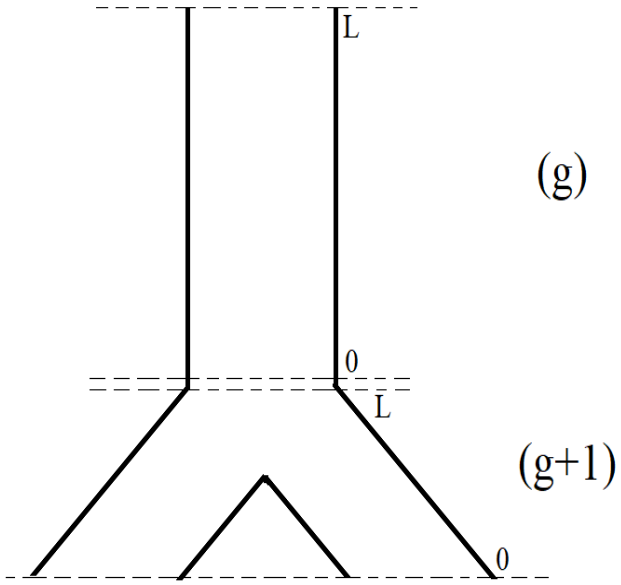

Figure 4.4.2 Generation sorting during expiration

Again according to the Bernoulli Equation, the relation between the pressure at the downstream end of (g+1) generation $P_L(g+1)$, and the pressure at the upstream end of g generation $P_0(g)$ is as follows:

$$P_0(g)-P_L(g+1)=\frac{1}{2}\rho q^2(g)[\frac{1}{4A_L^2(g+1)}-\frac{1}{A_0^2(g)}]\Rightarrow$$

$$\Rightarrow \Delta P_c(g)=\frac{1}{2}\rho q^2(g)[\frac{1}{4A_L^2(g+1)}-\frac{1}{A_0^2(g)}], \text{ or } \quad \Delta P_c(g)=\rho\frac{Q^2}{2^{2g+1}}[\frac{1}{4A_L^2(g+1)}-\frac{1}{A_0^2(g)}]$$

Since $A_0(g)<A_L(g+1)$ and $\Delta P_c(g)<0$, which means that:

$$P_0(g)<P_L(g+1)$$

The above relation represents an additional pressure drop $\Delta P_c(g)$ that arises from convection in the junctions between airways as we move from the alveoli to the trachea during expiration.

4.5 Basic Equation Modeling

In the present chapter the basic equation, which allows the calculation of the airflow at any lung volume during a forced expiration maneuver, is introduced. The equation is derived after equating the driving pressure for expiration with the total pressure losses along the bronchial tree. At first, the pressure losses due to dissipation and convection along the bronchial tree are calculated as the sum

of the respective individual losses of each generation, which were calculated in *chapters 4.3 and 4.4*. Then a prediction for the pressure drop in the mouth is added and total pressure losses are equalized with the driving pressure, which was calculated in *chapter 4.2,* yielding the final equation.

Total pressure loss due to friction

The equation for the calculation of the dissipative pressure loss was produced in *chapter 4.3.* Summing the pressure losses for every generation from the trachea (g=0) to the most peripheral bronchioli (g=23), we get the total dissipative losses along the bronchial tree:

$$\Delta P_f = \sum_0^{23} \Delta P_f(g) = \sum_0^{23} \frac{128\mu L(g)}{\pi D^4(g)} \frac{a}{2^g} Q + \sum_0^{23} \frac{512\rho L(g)}{\pi^2 D^5(g)} \frac{b}{2^{2g}} Q^2$$

or

$$\Delta P_f = Q \times \sum_0^{23} \frac{128\mu L(g)}{\pi D^4(g)} \frac{a}{2^g} + Q^2 \times \sum_0^{23} \frac{512\rho L(g)}{\pi^2 D^5(g)} \frac{b}{2^{2g}} \quad (1)$$

Total convective pressure losses

Similarly, summing all convective pressure drops, which were calculated for each junction in *chapter 1*, from the first junction between the trachea and the first bronchus to the last junction before the alveoli, the total convective pressure losses are:

$$\Delta P_c = \sum_0^{22} \Delta P_c(g) = \sum_0^{22} \frac{\rho}{2^{2g+1}} \left(\frac{1}{4 A_L^2(g+1)} - \frac{1}{A_0^2(g)} \right) Q^2$$

or

$$\Delta P_c = Q^2 \times \sum_0^{22} \frac{\rho}{2^{2g+1}} \left(\frac{1}{4 A_L^2(g+1)} - \frac{1}{A_0^2(g)} \right) \quad (2)$$

Mouth pressure drop

Another term describing an extra pressure drop inside the mouth during forced expiration is introduced. This pressure drop is described by the experimentally derived formula of *Jaeger and Matthys (*Jaeger, Matthys, 1968) and *Wheatley et al.* (Wheatley, Amis, Engel, 1991) as follows:

$$\Delta P_m = Q^r R_u \quad (3)$$

where R_U is a flow resistance coefficient and r is an exponent of value between 1.5 and 2.0. Q is the volumetric flow in the mouth.

Total pressure losses

Summing all three pressure drop components, calculated above we finally get the total pressure drop along the bronchial tree during forced expiration:

$$\Delta P_{total} = \Delta P_f + \Delta P_c + \Delta P_m \quad (3)$$

Note: The same equation is considered to apply for inspiration.

Basic equation modeling

The basic equation, which allows us to determine the airflow variation during respiration, is produced by equating the total pressure losses with the driving pressure of the breathing process:

$$P_d = \Delta P_{total} \quad (4)$$

with $P_d = P_e + P_{stRS} - R_T Q$ and $\Delta P_{total} = \Delta P_f + \Delta P_c + \Delta P_m$, Eq. (4) becomes:

$$P_e + P_{stRS} - R_T Q = \Delta P_f + \Delta P_c + \Delta P_m \quad \text{or} \quad P_e = \Delta P_f + \Delta P_c + \Delta P_m + R_T Q - P_{stRS} \quad (5)$$

Substituting the pressure loss relations calculated above in Eq. (5) we finally get:

$$P_e = Q \times \sum_0^{16} \frac{128\mu L(g)}{\pi D^4(g)} \frac{a}{2^g} + Q^2 \times [\sum_0^{16} \frac{512\rho L(g)}{\pi^2 D^5(g)} \frac{b}{2^{2g}} + \sum_0^{15} \frac{\rho}{2^{2g+1}} (\frac{1}{4A_L^2(g+1)} - \frac{1}{A_0^2(g)})] + Q^r \times R_u + R_T \times Q - P_{stRS}$$

where only the pressure losses of the first seventeen generations were included to the calcualtion. Pressure losses of higher generations are neglected, an approximation which is valid, considering the limited airflow occuring there, as a result of the huge number of short parallel connected airways.

This equation is a non- linear equation, which can be solved using a Newton- Raphson scheme, in order to determine the value of airflow (Q) at each time step.

Once this airflow is calculated we can determine the pressure drop along each airway of the tree, as well as a mean value of the pressure inside the airway as :

$$P_{av}(g)=\frac{P_{in}(g)+P_{out}(g)}{2}$$

This allows the calculation of a mean value for the transmural pressure of each airway, as the pressure difference between the average internal pressure and the uniform pleural pressure :

$$P_{tm}(g)=P_{av}(g)-P_{pl}$$

while the pleural pressure can be determined according to the lung static recoil pressure definition as :

$$P_{pl}=P_{alv}-P_{stL}$$

The determination of the transmural pressure is an important part of the calculation, since it allows us to take under consideration the airway diameters variability during the process, as it is extensively analyzed below.

4.6 Transmural Pressure-Airway Crossectional Area Variation

Lung airways in our model are considered to be compliant tubes. This means that, in contrast to stiff tubes, they are sensitive in variations of the transmural pressure. Airway diameters and, as a result, cross-sectional areas are different for each generation's airways, for different values of the transmural pressure. More specifically, the tubes tend to increase their cross-sectional areas as the transmural pressure, which was defined as the pressure difference between internal or lateral and pleural pressure, increases. The opposite is true when the transmural pressure decreases, which is the case of forced expiration. At this case, tubes tend to collapse.

The airway mechanics were described by *Lambert et al.* (Lambert, Wilson, Hyatt, Rodarte, 1982), who developed an analytical formula for the calculation of the first sixteen generations' airways cross-sectional areas in relation to the transmural pressure.

The *Lambert et al.* area-pressure curves

The airway mechanics are described by the value of the maximal cross-sectional area of an airway (Am) and the curves of normalized airway area, α=A/Am, as a function of transmural pressure (Ptm), for all generations. The normalized curves are represented by two rectangular hyperbolae, matched at zero pressure. The value of the fractional airway cross-sectional area (α) is given by (Lambert, Wilson, Hyatt, Rodarte, 1982):

$$\text{when Ptm} < 0: \quad \alpha = \alpha_0 \left(1 - Ptm / P_1\right)^{-n_1}$$

and

$$\text{when Ptm} >= 0: \quad \alpha = 1 - (1 - \alpha_0)\left(1 - Ptm / P_2\right)^{-n_2}$$

where:

- α_0 is the value of α at Ptm=0
- $P_1 = \alpha_0 n_1 / \alpha_0'$ and $P_2 = -n_2(1-\alpha_0)/\alpha_0'$, both equations for the vertical asymptotes produced by the slopes of the curves, dα/dPtm, who were also matched at Ptm=0 to yield a single value of the slope at that point, α_0'.

The curvature changes sign and is therefore discontinuous at Ptm=0. The values for the six parameters (α_0, α_0', n_1, n_2, Am, L) must be chosen for each value of z (number of generation), in order to specify the mechanical behavior of the bronchial tree *(Table 6)*.

z (generation)	# of branches(=2^z)	α0	α0'	n1	n2	Am (cm^2)	L(cm)
0	1	0,882	0,011	0,50	10,00	2,37	12,00
1	2	0,882	0,011	0,50	10,00	2,37	4,76
2	4	0,686	0,051	0,60	10,00	2,80	1,90
3	8	0,546	0,080	0,60	10,00	3,50	0,76
4	16	0,450	0,100	0,70	10,00	4,50	1,27
5	32	0,370	0,125	0,80	10,00	5,30	1,07
6	64	0,310	0,142	0,90	10,00	6,50	0,90
7	128	0,255	0,159	1,00	10,00	8,00	0,76
8	256	0,213	0,174	1,00	10,00	10,20	0,64
9	512	0,184	0,184	1,00	10,00	12,70	0,54
10	1024	0,153	0,194	1,00	10,00	15,94	0,47
11	2048	0,125	0,206	1,00	9,00	20,70	0,39
12	4096	0,100	0,218	1,00	8,00	28,80	0,33
13	8192	0,075	0,226	1,00	8,00	44,50	0,27
14	16384	0,057	0,233	1,00	8,00	69,40	0,23
15	32768	0,045	0,239	1,00	7,00	113,00	0,20
16	65536	0,039	0,243	1,00	7,00	180,00	0,17

Table 6. Model Parameters of bronchial mechanical properties. (Note: The trachea is assumed to have the same pressure-area behavior as the main-stem bronchi, z=1)

Using a Matlab code, which is presented in *Appendix D,* we were able to produce the complete set of model α=A/Am versus Ptm curves. Plotting the fractional airway cross-sectional area (α) against the transmural pressure (Ptm) for each generation from the trachea (z=0) to the 16th generation we got the following figure:

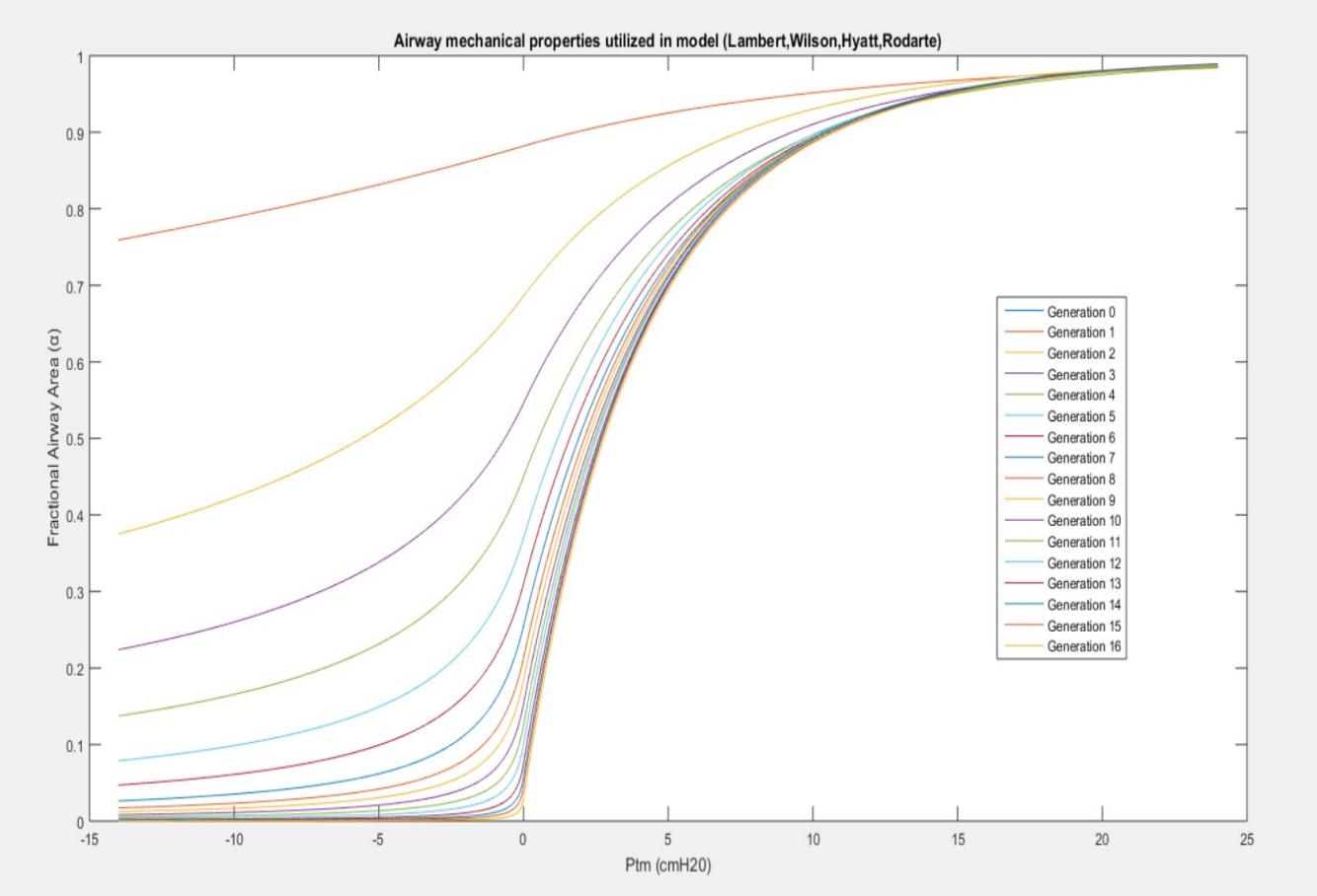

Figure 4.6.1. Fractional airway cross-sectional area (a) against transmural pressure (P) for each generation from trachea (generation 0) through sixteenth generation.

These results are very important, since they allow us to include the diameters' variation in the overall calculation. The airway diameters of each time step during forced expiration are calculated for the transmural pressures, which were computed in the previous step.

4.7 The Flow Limitation Mechanism

Flow limitation is a basic characteristic of forced expiration and a direct result of the compliant behavior of the airways, as described above. More specifically, the rapid decrease of transmural pressure due to the increase of pleural pressure and the pressure drop inside the airway tends to collapse the tube's walls. At some point the most compliant tubes of the bronchial tree narrow that much, as to limit the flow through them. This phenomenon is omnipresent and independent of the subject's effort to expire. Effort-independence is visible in maximum expiratory flow curves (MEFV) for different subjects, as it will be demonstrated below.

According to *Lambert et al* (Lambert, Wilson, Hyatt, Rodarte, 1982), the mechanism for flow limitation is the wave speed mechanism. This means that flow cannot exceed the value at which the speed at some point of the bronchial tree becomes equal to the wave speed. The latter happens at high and midlung volumes. More specifically, according to *Hyatt* (Hyatt, 1961) the effort-independent area is between 30%-60% VC (Vital Capacity). This can be explained considering that the lung muscles are incapable of producing sufficient pressure to reach the wave speed both at very high and very low lung volumes.

The wave speed mechanism as described by *Lambert et al.*:

Lateral pressure (P) at any point inside an airway:

$$P = P_A - 1/2\,\rho U^2 - \int_0^x f\,dx \quad (1)$$

where U is the local flow speed, ρ is the fluid density, f is the dissipative pressure loss per unit distance, and x is the coordinate along the airway axis.

Differantiating Eq. (1) we get:

$$\frac{dP}{dx} = -f/(1 - \frac{U^2}{c^2}) \quad (2)$$

The wave speed (c) is related to airway compliance (dA/dP) according to the following formula:

$$c^2 = A/(\rho \frac{dA}{dP})$$

The pressure gradient dP/dx becomes very large as the flow speed (U) approaches the wave speed (c). According to *Dawson and Elliott* (Dawson, Elliott, 1977) flow cannot exceed the value at which $U^2/c^2 = 1$ at any point in the bronchial tree.

Our model neglects the variation of the transmural pressure along the length of each airway (dP/dx) and thus is unable to predict the exact site of flow limitation. However, the exact analysis for the flow through a flexible pipe based on *Filoche and Florens* (Filoche, Florens, 2011) is extensively cited below.

4.8 An Accurate Model for Flexible Tubes

In order to describe sufficiently the flow in the complex network of human airways, we introduce a mathematical model of coupled equations, one for each of the flexible tubes as developed by *Filoche and Florens* (Filoche, Florens, 2011). Initially, one dimensional flow along each tube of the airway structure is assumed, where the interaction between the fluid and the interior walls of the tubes will be modeled, using state laws associating the local airway diameter and the transmural pressure applied around it. After calculating the average Reynolds number along the tube, given the diameters at the entrance and the exit of the airway, the one-dimensional differential equation describing the airflow in each tube will be exactly integrated.

In this particular mathematical model that we introduce, the assumptions that were made are:

- steady and incompressible flow in the collapsible tube
- one-dimensional flow along most of the length of each tube of the network
- a hydrodynamic diameter of the tube D(x) summarizes all the information required for the examined cross section
- *transmural pressure* P_{tm} is defined as the difference between the local pressure P(x) at the examined cross section and the local pressure P_{out} outside the tube:

  $$P_{transmural} = P_{tm} = P(x) - P_{out} \quad ,$$

  if P_{tm} is positive, that is the local pressure P(x) is greater than the pressure outside the tube P_{out} , the airway opens.

  if P_{tm} is negative, the airway tends to close (Filoche, Florens, 2011).
- $P_{out} = P_{pl}$, is the pressure outside the tube, else called pleural pressure and is considered to be uniform, so as: $\frac{dP_{pl}}{dx} = 0$ (1)

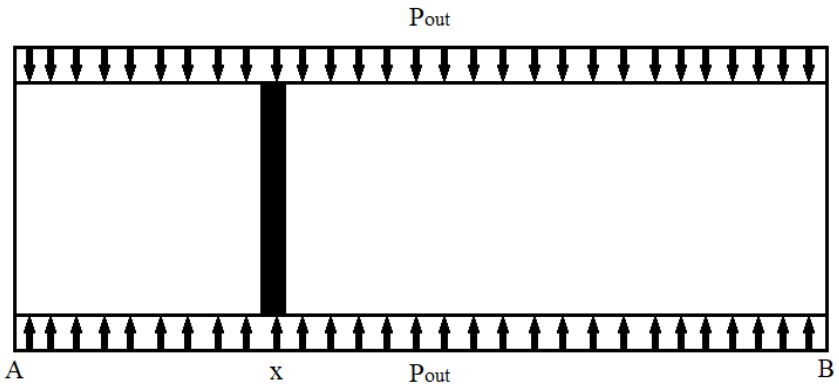

Figure 4.8.1: A random cross section of the tube at location x along its length, with pressure P_{out} applied outside of it.

Using the Bernoulli equation between the airway entrance A (corresponding to the coordinate x=0) and a random cross section of the airway at location x along its length, the following formula is obtained:

$$P_A+\frac{1}{2}\rho u_A^2=P(x)+\frac{1}{2}\rho u^2(x)+\int_A^x f(x)\,dx \quad \Rightarrow \quad P(x)=P_A+\frac{1}{2}\rho u_A^2-\frac{1}{2}\rho u^2(x)-\int_A^x f(x)\,dx \quad (2),$$

and by differentiating (2) with respect to the coordinate x:

$$\frac{dP(x)}{dx}=-\rho u(x)\frac{du(x)}{dx}-f(x) \quad (3),$$

where P_A and u_A are the pressure and the velocity of the flow at the entrance of the airway respectively, P(x) and u(x) are the pressure and the velocity of the flow at the random cross section of the airway, ρ is the density of the fluid. The function f(x) indicates the energy loss per unit of distance and comprehends viscous pressure losses per unit of distance and some times a constant gravity term defined as (-ρgcosθ) and equal to zero, when the direction of the gravity is vertical to the axis of the airway (θ = 90° ⇒cosθ = 0). Lastly, for the circular cross sectional are of the airway and for a volumetric flow rate Q, fluid velocity u can be expressed as:

$$Q=u(x)A(x) \;\Rightarrow\; Q=u(x)\left(\pi\frac{D^2(x)}{4}\right) \;\Rightarrow\; u(x)=\frac{Q}{\pi\frac{D^2(x)}{4}} \;\Rightarrow\; u(x)=\frac{4\mathrm{Q}}{\pi D^2(x)} \quad (4)$$

By derivating (4) with respect to the coordinate x:

$$\frac{du(x)}{dx}=\frac{4\mathrm{Q}}{\pi}\left(\frac{-2\mathrm{D}(x)}{D^4(x)}\right)\frac{dD(x)}{dx}=\frac{-8\mathrm{QD}(x)}{\pi D^4(x)}\frac{dD(x)}{dx}=\frac{-8\mathrm{Q}}{\pi D^3(x)}\frac{dD(x)}{dx}=\left(\frac{-2}{D(x)}\right)\left(\frac{4\mathrm{Q}}{\pi D^2(x)}\right)\frac{dD(x)}{dx} \quad ,$$

where according to (4) and by using the chain rule:

$$\frac{du(x)}{dx}=\left(\frac{-2\mathrm{u}(x)}{D(x)}\right)\frac{dD(x)}{dx} \quad \Rightarrow \quad \frac{du(x)}{dx}=\left(\frac{-2\mathrm{u}(x)}{D(x)}\right)\frac{dD(x)}{dP_{tm}}\frac{dP_{tm}}{dx} \quad (5).$$

For the transmural pressure which has been defined as $P_{tm}=P(x)-P_{pl}$:

$\frac{dP_{tm}}{dx}=\frac{d}{dx}(P(x)-P_{pl})=\frac{dP(x)}{dx}-\frac{dP_{pl}}{dx}$, where due to the fact that $\frac{dP_{pl}}{dx}=0$:

$$\frac{dP_{tm}}{dx}=\frac{dP(x)}{dx} \quad (6).$$

By combining (3), (5) and (6) :

$$\frac{dP_{tm}}{dx}=\frac{dP(x)}{dx}=-\rho u(x)\frac{du(x)}{dx}-f(x) \Rightarrow \frac{dP_{tm}}{dx}=-\rho u(x)[\frac{-2u(x)}{D(x)}\frac{dD(x)}{dP_{tm}}\frac{dP_{tm}}{dx}]-f(x) \Rightarrow$$

$$\Rightarrow \frac{dP_{tm}}{dx}=\frac{2\rho u^2(x)}{D(x)}\frac{dD(x)}{dP_{tm}}\frac{dP_{tm}}{dx}-f(x) \Rightarrow \frac{dP_{tm}}{dx}[1-\frac{2\rho u^2(x)}{D(x)}\frac{dD(x)}{dP_{tm}}]=-f(x) \quad (7),$$

where: $\frac{1}{c^2(x)}=\frac{2\rho}{D(x)}\frac{dP_{tm}}{dx}$ and c(x) is defined as the local wave speed.

Consequently the pressure gradient of the transmural pressure is:

$$\frac{dP_{tm}}{dx}[1-\frac{u^2(x)}{c^2(x)}]=-f(x) \Rightarrow \frac{dP_{tm}}{dx}=\frac{-f(x)}{1-\frac{u^2(x)}{c^2(x)}} \quad (8).$$

The denominator of equation (8) is the one that indicates wheter the phenomenon of flow limitation appears during the flow of the fluid in the airways, as analysed in the previous chapters.

For the total energy loss per unit of distance f(x) in a bronchus of a generation, the above relation was used (Reynolds, 1982):

$$f(x)=\Delta P_{pg}(a+bRe(x)) \quad ,$$

where a and b are assumed to be dimensionless constants, independent of generation and bronchial dimensions, Re(x) is the local Reynolds number, ΔP_{pg} is the Poiseuille viscous pressure loss over the bronchial length in generation g and μ is the fluid viscocity. Local Reynolds number and the Poiseuille viscous pressure loss are defined respectively as:

$$Re(x)=\frac{\rho u(x) D(x)}{\mu} \quad \text{and} \quad \Delta P_{pg}=\frac{128\mu Q}{\pi D^4(x)} \quad .$$

Therefore:

$$f(x)=\frac{128\mu Q}{\pi D^4(x)}[a+bRe(x)] \quad (9)$$

The first term of the equation refers to the viscous pressure losses for a Poiseuille flow, where a=1 for an infinite pipe, since the velocity profile of a Poiseulle flow needs some time to develop in the branches of the network. The second term of the equation refers to the existance of inertial effects during the flow in the airway, for example in higher velocities. *Reynolds*, through his analysis (Reynolds, 1982), proposed the values a=1.5 and b=0.0035, which are also the values used in the set of code developed in this thesis. These values indicate that even at very low Reynolds numbers, the pressure loss is greater than the pressure loss for a fully-developed laminar (Poiseuille) flow in a uniform tube, where a=1.

Briefly, differential equation (8) , one for each airway of the branches network, will be used in order to mathematically describe the flow distribution in the network. Biological networks such as the lung airway system examined in this thesis, tend to have several thousands of branches, making the calculation of the flow in the network almost impossible. On account of this difficulty, some sort of symmetry in the system is usually assumed, like an identicalness between a large number of branches, assumption used for example from *Barbini P. et al.* (Barbini, Bringhenti, Cevenini, Gnudi, 2005) or *Isabey D.* (Isabey, 1982).

The mathematical model proposed here transforms the differential equation (8) for each airway into a non-linear scalar equation by integrating it. This way, the unknowns of the problem will be the airflow through each of the airways and the transmural pressures at both ends of them, allowing us to compute the flow distribution in the entire network. The transformation process mentioned above is described mathematically, initiating by equation (8), as:

$$f(x)=\frac{128\mu Q}{\pi D^4(x)}[a+bRe(x)] \Rightarrow D^4(x)f(x)=\frac{128\mu Q}{\pi}[a+bRe(x)] \Rightarrow$$

$$\Rightarrow \int_A^B D^4(x)f(x)dx=\int_A^B\left(\frac{128\mu Q}{\pi}[a+bRe(x)]\right)=\frac{128\mu Q}{\pi}\left[aL+bL\frac{1}{L}\int_A^B Re(x)dx\right] \Rightarrow$$

$$\Rightarrow \int_A^B D^4(x)f(x)dx=\frac{128\mu QL}{\pi}[a+bRe_m(x)] \quad (10),$$

where L is the length of the airway and Re_m is the average quantity of Reynolds number along the airway,which can be estimated with good accuracy by using the average diameter of the airway as:

$$Re_m = \frac{4\rho Q}{\mu\pi\left(\frac{D_A + D_B}{2}\right)}$$

A and B are used to describe the both ends of the airway examined. The flexible airway and the unknowns involved in the integration can be seen in the figure below:

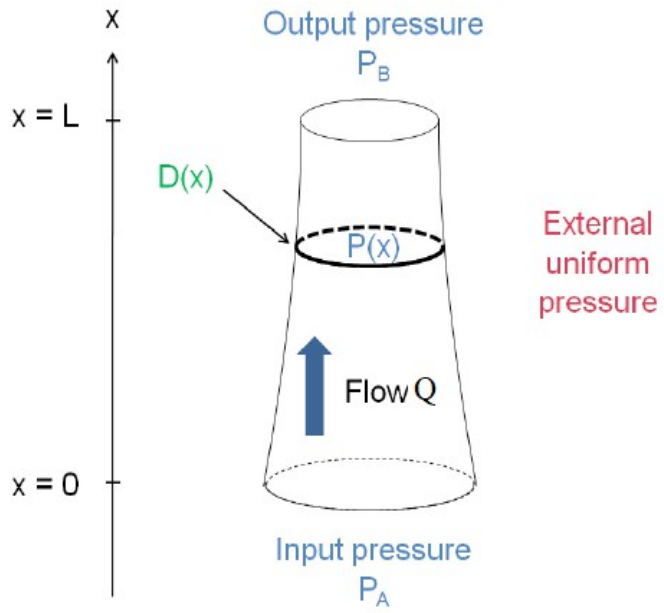

Figure 4.8.2: One elementary flexible airway of the lung airway system (Filoche, Florens, 2011)

In the figure, L is the length of the airway, P_A and P_B are the inner pressures at the both ends of the airway, Q is the volumetric flow rate and D(x) is the local diameter, while the external uniform pressure has been assumed to be uniform (equation (1)).

Using (8):

$$\frac{dP_{tm}}{dx} = \frac{-f(x)}{1-\frac{u^2(x)}{c^2(x)}} \Rightarrow \left(1-\frac{u^2(x)}{c^2(x)}\right)\frac{dP_{tm}}{dx} = -f(x) \Rightarrow \left(1-\frac{u^2(x)}{c^2(x)}\right)\frac{dP_{tm}}{dx}D^4(x) = -f(x)D^4(x) \Rightarrow$$

$$\Rightarrow \int_A^B \left(1-\frac{u^2(x)}{c^2(x)}\right)D^4(x)\frac{dP_{tm}}{dx}dx = -\int_A^B D^4(x)f(x)dx \quad \text{, where due to (10):}$$

$$\int_A^B \left(1-\frac{u^2(x)}{c^2(x)}\right) D^4(x)\, dP_{tm} = \frac{-128\mu QL}{\pi}\left[a+bRe_m(x)\right] \quad (11).$$

The left hand side of equation (11) is exactly integrated as:

$$\int_A^B \left(1-\frac{u^2(x)}{c^2(x)}\right) D^4(x)\, dP_{tm} = h(P_{tmB}) - h(P_{tmA}) - \frac{32\rho Q^2}{\pi^2}\ln\left(\frac{D_B}{D_A}\right) \quad (12),$$

where function $h(P_{tmi})$ for i =A or B, is defines as the primitive function of the fourth power of the state law of the flexible pipe and can be obtained by *Lambert et al.* (Lambert, Wilson, Hyatt, Rodarte. 1982), based on the whole analysis of the compliance of the airways and the variability of their diameters, when fluid flows through them.

As a result, the final formula is obtained as:

$$h(P_{tmB}) - h(P_{tmA}) - \frac{32\rho Q^2}{\pi^2}\ln\left(\frac{D_B}{D_A}\right) + \frac{128\mu QL}{\pi}\left[a+bRe_m(x)\right] = 0 \quad (13),$$

which allows us to compute the flow through the lung airway system with adequate accuracy.

CHAPTER 5: Results- Discussion

Based on the mathematical model presented above, we've been able to construct various algorithms, which provide results concerning the different variables of the problem (airflow,time, expired air volume and lung volume). The three main Matlab algorithms of forced expiration, inspiration and single tube airflow, along with the funtions they contain, can be found in Appendices A, B and C respectively. Results occuring for forced expiration, for both steady and variable airways' diameters are demonstrated. In addition, inspiratory airflow curves as well as joint figures of the two processes are created. Finally, the airflow-pressure drop behavior in a single compliant tube, based on the analysis of *Filoche and Florens* (see chapter 4.8) is presented. Results are compared to those of other models and spirometric tests and suggestions for future research topics are made.

5.1 Steady Diameters

A first attempt to approach the problem of forced expiration was made, assuming that the airway diameters remain constant during the process. The airway diameters were calculated only once at the beginning of expiration where the lung volume is equal to the total lung capacity (TLC). This means that the airway narrowing, which takes place during expiration due to the variation of the transmural pressure as described by *Lambert et al.* (Lambert, Wilson, Hyatt, Rodarte, 1982), was not taken under consideration. This is a simplified approximation which only helps us understand the qualitive and not the quantitive variation of the airflow during the process. The main result of our calculation, which can be directly compared to spirometry test results is the Maximum Expiratory Flow Volume Curve (MEFV). MEFV is the airflow versus expired air volume curve which is produced during a Forced Expiration Maneuver.

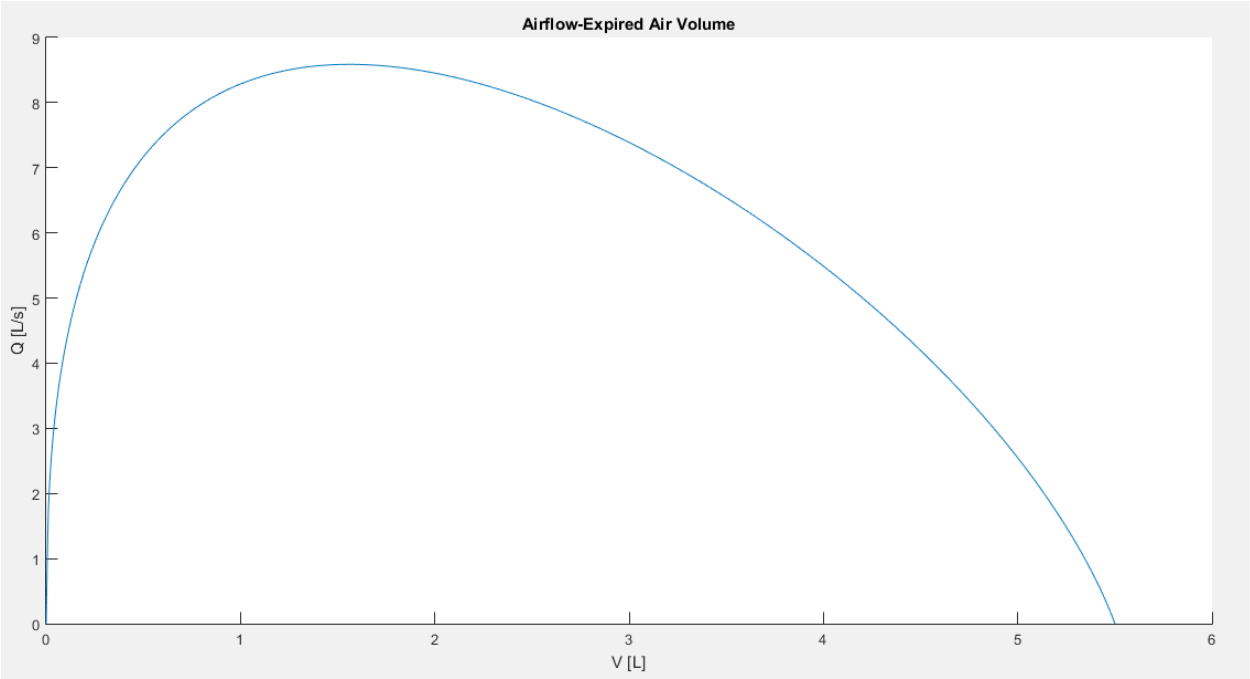

Figure 5.1.1: The MEFV curve for a subject with Pm=24kPa and τ=0.2s, using airways of constant diameter during forced expiration.

Airflow (Q) is calculated during a full vital capacity (VC) volume exchange. Maximum airflow is reached relatively soon after the beginning of expiration, at around 30% VC.

In addition to the MEFV curve an airflow versus time curve was created and is cited below. According to this graph maximal airflow is reached approximately 0.3s after the beginning, while the whole expiration process is approximately 1.5s long, since there's no airflow after that time.

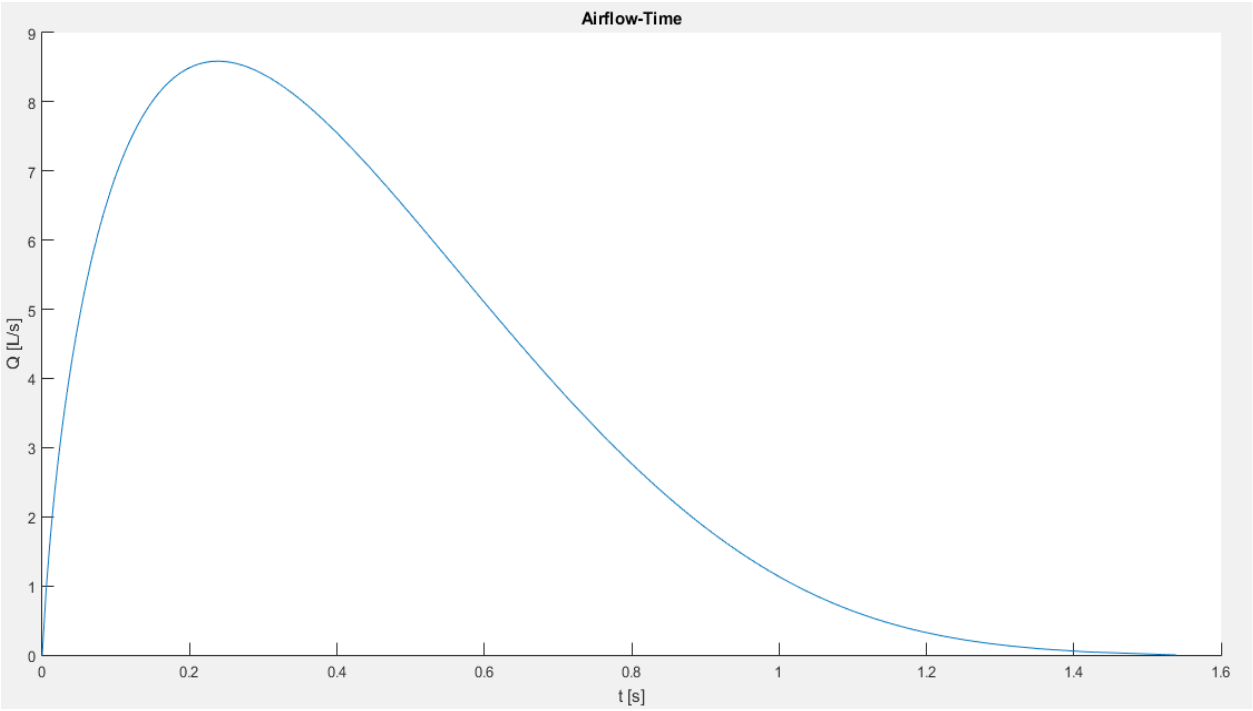

Figure 5.1.2: Airflow-time curve for a subject with Pm=24kPa and τ=0.2s.

The lung volume (VL) and the expired air volume (V) versus time curves show the variation of these two volumes. Expired air volume and lung volume are connected according to the formula: VL=VC+RV-V or VL=TLC-V since TLC=VC+RV. This means that when one of these volumes is maximal the other is minimal. Thus at the beginning of expiration we have: VL=TLC and V=0, while at the end: VL=RV and V=VC.

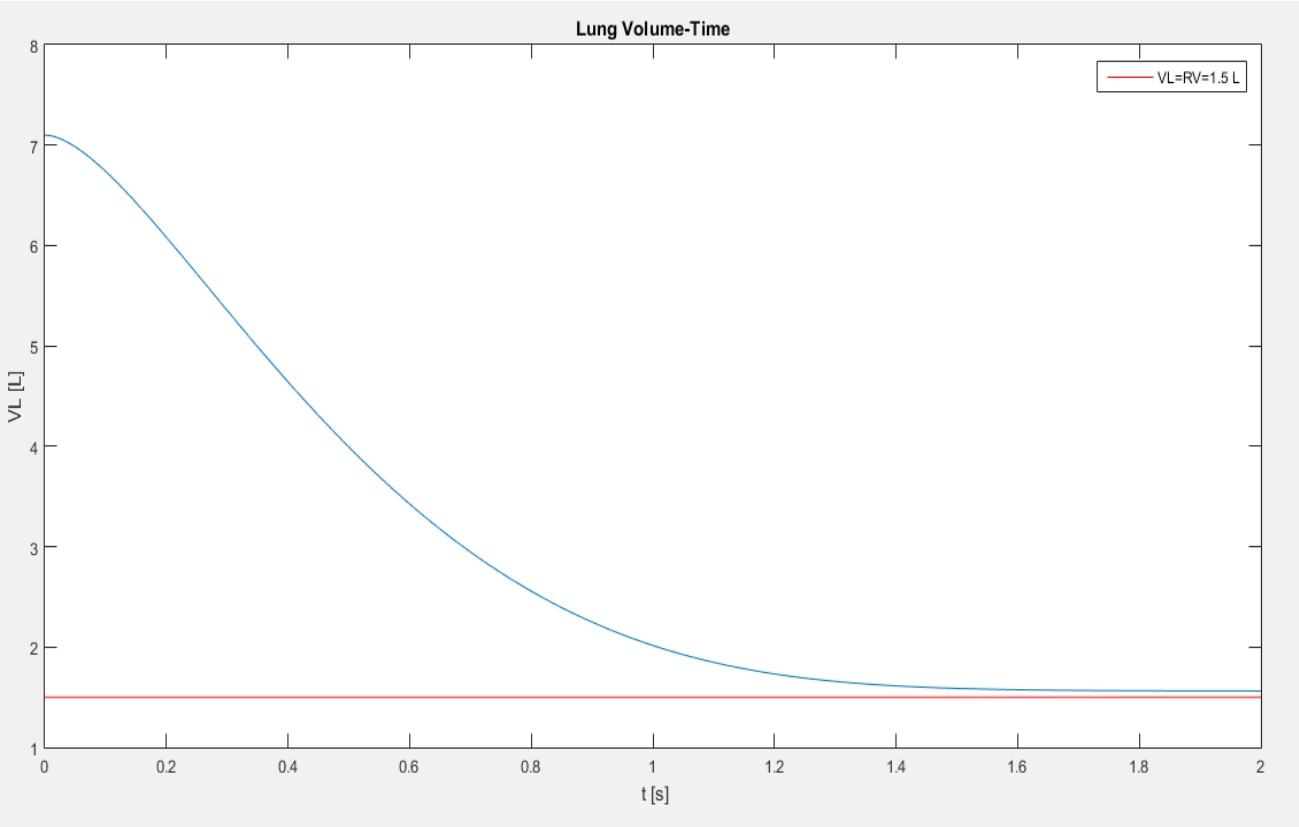

Figure 5.1.3: The change in lung volume with time during a forced expiration.

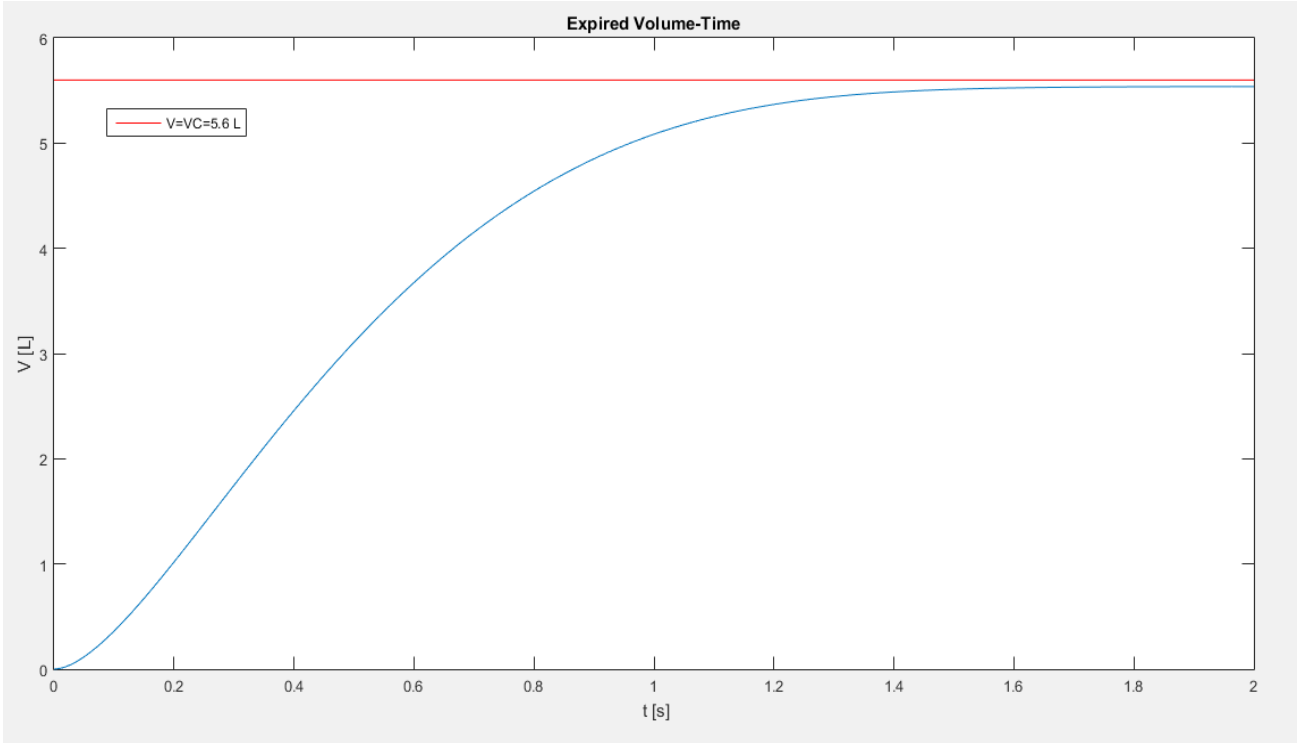

Figure 5.1.4: The amount of expired air volume versus time curve during a forced expiration.

5.2 Variable Diameters

A significant improvement of the above model is the consideration of the airway diameters' variability during expiration. This can be done by calculating the pleural and transmural pressures at each time step and then calculating the respective airway diameters using the *Lambert et al* (Lambert, Wilson, Hyatt, Rodarte, 1982) equations, which were cited in a previous chapter.

However, all airways are still considered to maintain the same diameter along their length at each time step, which is not accurate since the pressure inside each airway continually drops from its inlet to its outlet. This means that transural pressure varies across the airway's length and so does its cross-sectional area. Our simplified approach was to calculate an average transmural prassure for each airway as the difference beteween the average internal pressure and the uniform external or pleural pressure. The accurate solution for the problem designed by *Filoche and Florens (*Filoche, Florens, 2011) was presented in *chapter 4.8*.

This approach inevitably ignores convective pressure drops inside each airway due to the variation of its diameter across its length and thus convective pressure losses are only present at the junctions between generations as described in our mathematical model analysis. This makes our model unable to predict the exact flow limitation site according to the wave speed mechanism.

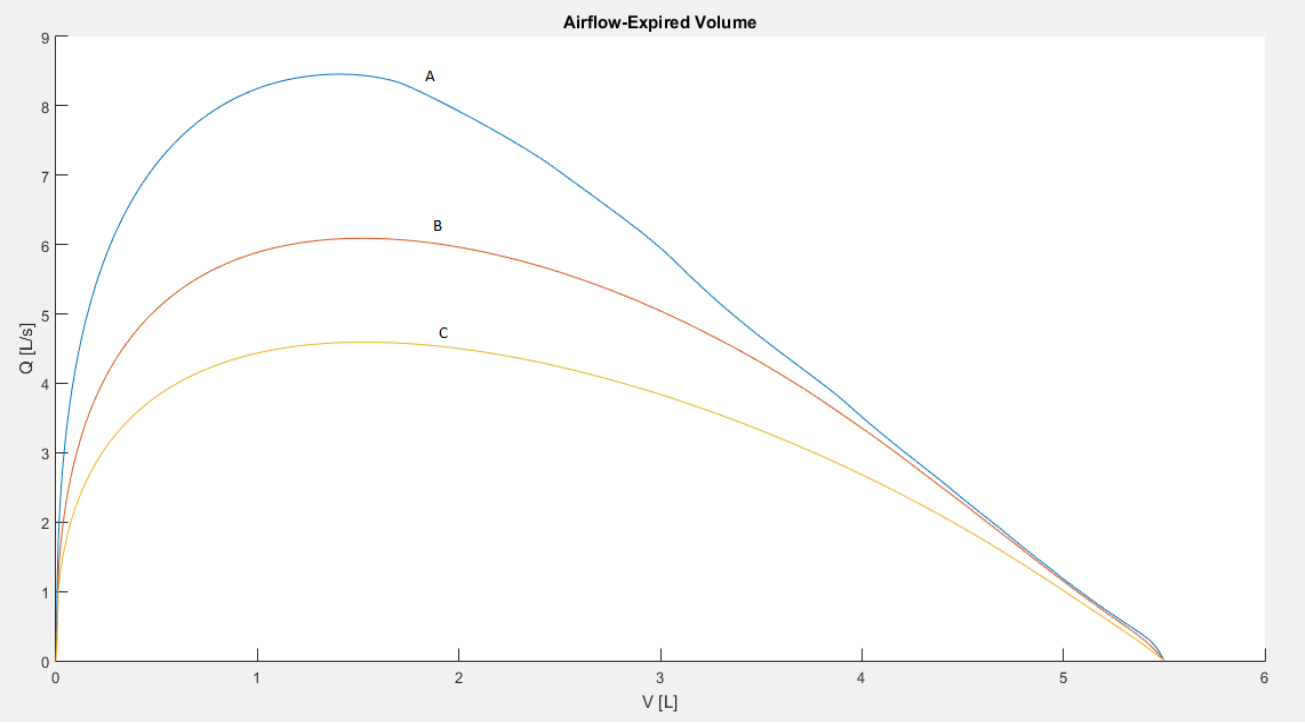

Figure 5.2.1: MEFV curves for three different subjects : (A) Pm=24kPa. τ=0.2s, (B) Pm=15kPa, τ=0.3s, (C) Pm=24Pa, τ=0.4s.

Focusing on subject A who has the same characteristics, which were used in our analysis for the steady diameters, we can see that maximal airflow is slightly lower than that of the previous model. Moreover the drop after the peak is more rapid, as a result of flow limitation. We can see that the curves of the three different subjects tend to merge into a rapid dropping straight line as we approach vital capacity. This part of the airflow-volume graph is known as effort-independence and is a common phenomenon in spirometric tests.

The respective airflow- time curve is created for subject (A):

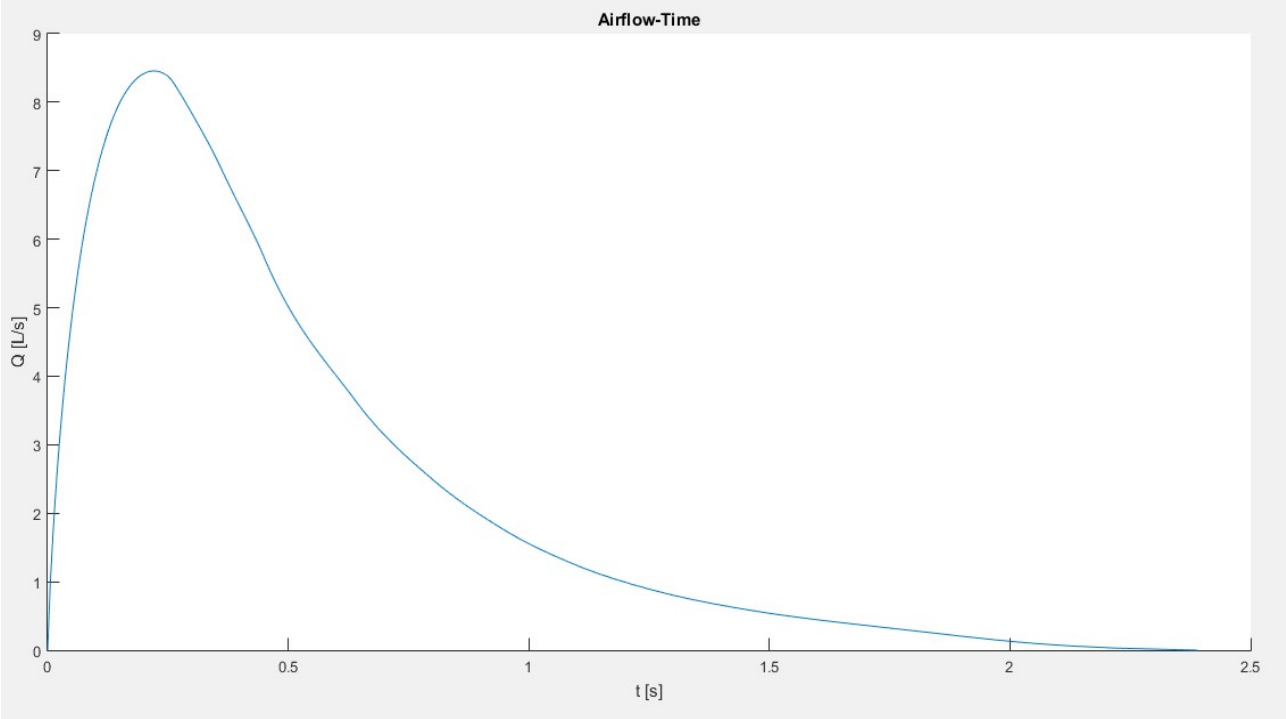

Figure 5.2.2: Airflow-time curve for a subject with Pm=24kPa and τ=0.2s.

We can see that the whole expiration process lasts around 2.5s, which is greater than the respective time calculated with the previous model. This means that airway narrowing slows down the process of forced expiration.

Slightly different results are produced with the use of the modified model for the expiratory driving pressure, which was constructed in order to include the elastic forces of the respiratory system in our calculation, as described in *chapter 4.2*. In this case the effort independent part of the curves is greater.

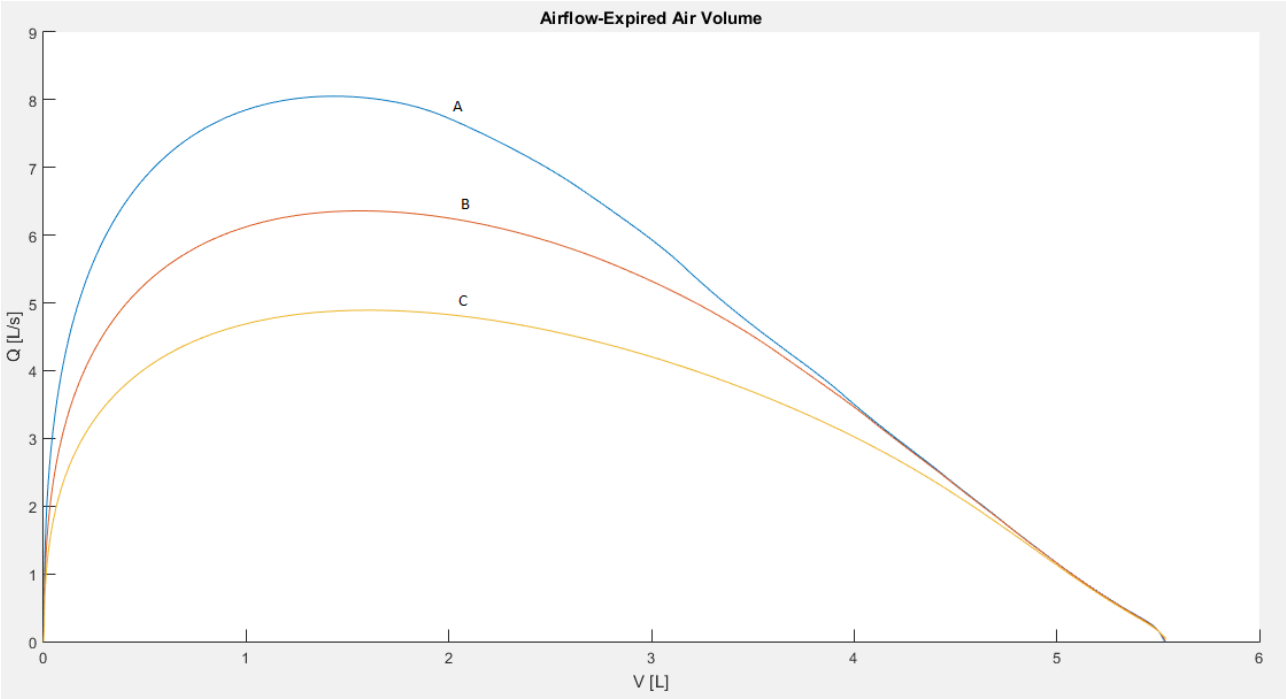

Figure 5.2.3: MEFV curves for three different patients : (A) Pm=20kPa. τ=0.2s, (B) Pm=15kPa, τ=0.3s, (C) Pm=10kPa, τ=0.4s

5.3 Inspiration

Using the algorithm found in A*ppendix B* we've been able to constract and demonstrate different graphs concerning the airflow- volume behavior during inspiration. Maximum Inspiratory Pressure (MIP) exerted by muscles was an important parameter of our calculation. There are many data found in bibliography determining MIP as a variable depending on many factors. Indicatively we present the following table:

	Men		Women	
Age group, years	Studies, n/sample size, n	MIP, cmH_2O, mean (95% CI)	Studies, n/sample size, n	MIP, cmH_2O, mean (95% CI)
18–29	6/96	128.0 (116.3–139.5)	6/92	97.0 (88.6–105.4)
30–39	6/69	128.5 (118.3–138.7)	6/66	89.0 (84.5–93.5)
40–49	6/72	117.1 (104.9–129.2)	6/71	92.9 (78.4–107.4)
50–59	5/61	108.1 (98.7–117.6)	5/60	79.7 (74.9–84.9)
60–69	5/65	92.7 (84.6–100.8)	5/66	75.1 (67.3–82.9)
70–83	5/63	76.2 (66.1–86.4)	5/59	65.3 (57.8–72.7)

Table 7: Maximal inspiratory pressure (MIP) for men and women in different age groups (Pessoa et al., 2014).

Thus selecting a subject with a MIP of 11kPa (Pm=11kPa or 112 cmH_2O) and an inspiratory muscle time contant of 0.2s (τ=0.2s), the following graphs was created:

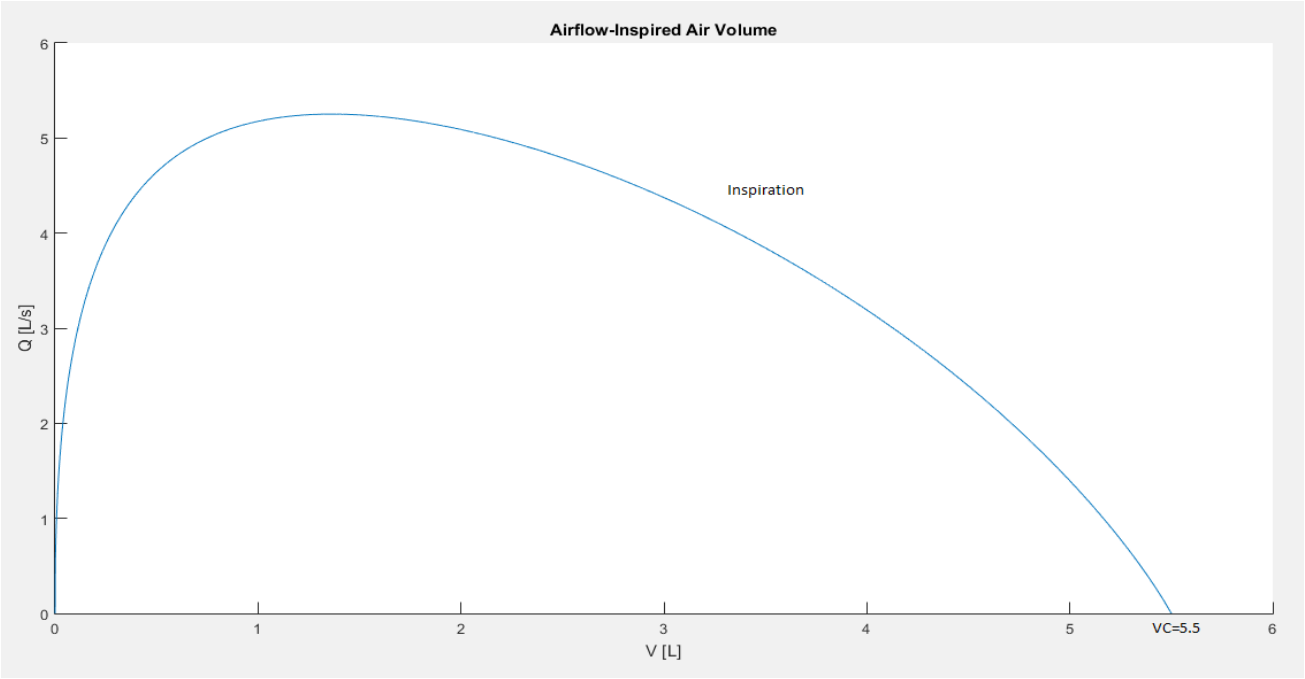

Figure 5.3.1: Airflow- inspired volume curve for subject with Pm=11kPa and τ=0.2s

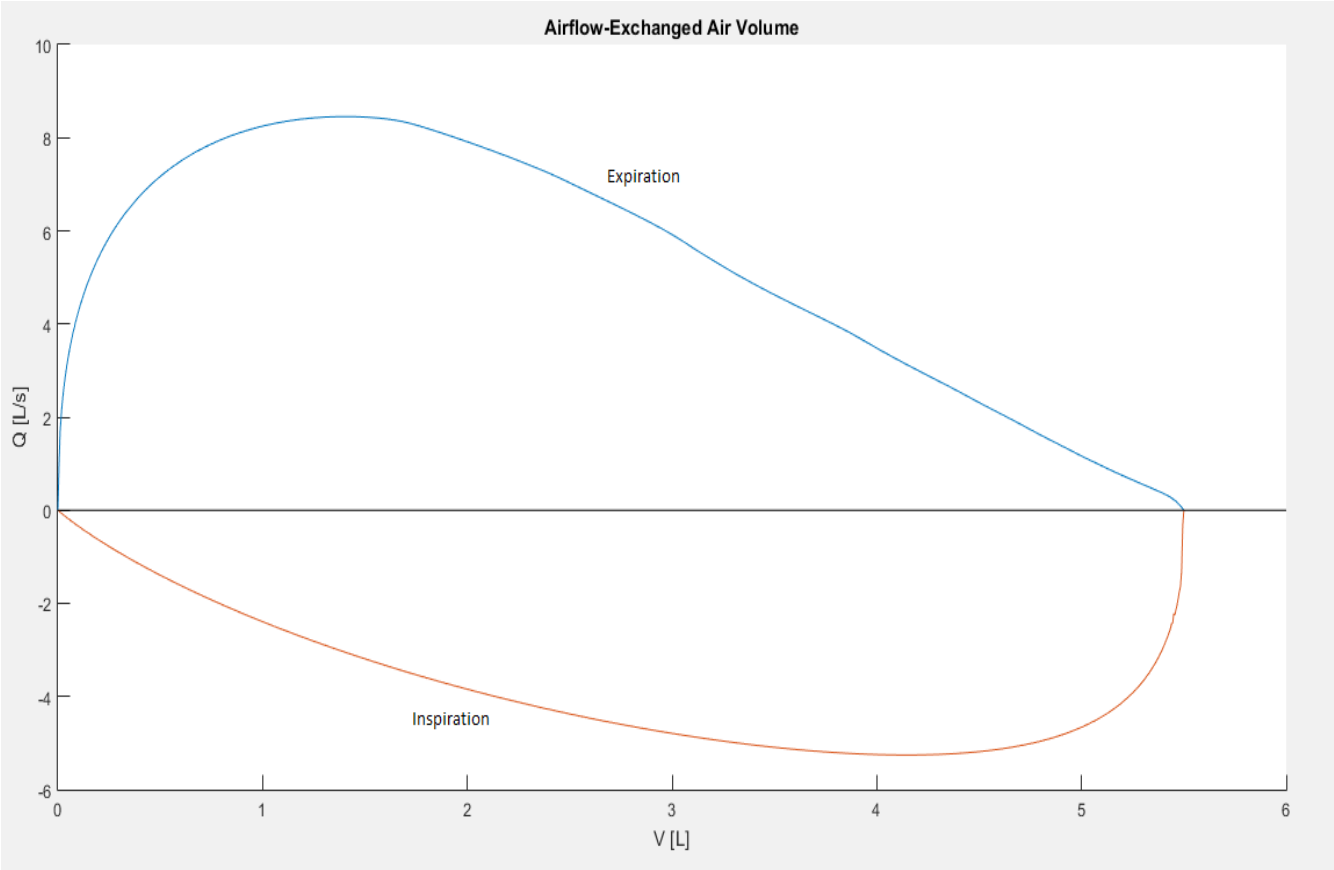

Figure 5.3.2: Inspiration-expiration airflow curves comparison for subject with Pm,exp=24kPa , Pm,insp=11 kPa and τ=0.2s.

A comparison between expiration and inspiration airflow curves was also created with the above graph of the two. Inspiration begins right at the end of expiration which is the reserve volume (RV) and it ends at total lung capacity (TLC) where expiration begins. Both processes happen during a

full vital capacity (VC) volume exchange (5.5L).

Plotting resulting airflow curves for different subjects both for expiration and inspiration in a combined graph helps us understand the basic differences between the two respiration processes, as far as our simulation is able to highlight them:

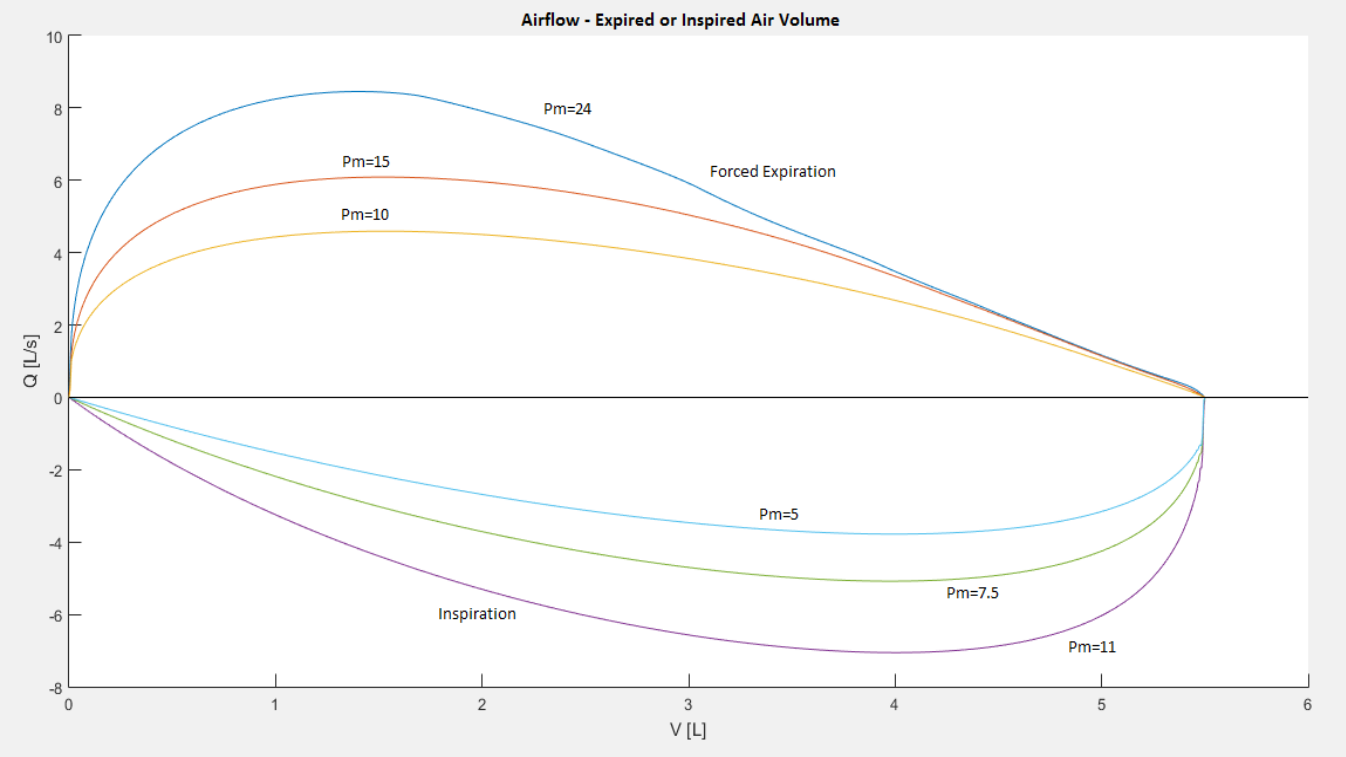

Figure 5.3.3: Forced expiration and inspiration airflow curves for subjects with different maximal muscle pressure capacities. Inspiratory muscle pressures were chosen to be half of the respective expiratory for the same subject. Maximal muscle pressure (Pm) is given in [Pa].

Maximum airflow of forced expiration is higher than that of inspiration since the expiratory muscles are more than twice as powerful as the inspiratory muscles. Moreover, according to spirometry test results the peak of inspiratory airflow should appear somewhere in the middle of vital capacity for normal healthy subjects. This is not verified in our model, since maximal inspiratory airflow appears too soon after the beginning of inspiration. This is a problem which is probably derived from the insufficient description of the inspiratory muscle force variation.

Another difference between the two breathing processes is the effect of flow limitation. Flow limitation is only present during forced expiration. This results to an effort indepented part in the expiratory curves which is non existant in the respective inspiratory curves.

5.4 Single Compliant Tube Behavior

Using the accurate analysis of *Filoche and Florens (*Filoche, Florens, 2011), we've been able to demonstrate the airflow-pressure drop behavior for a single compliant tube and explain the emergence of flow limitation. Flow limitation is present for compliant tubes of higher generations, when they are subjected in significant narrowing due to great drops of the transmural pressure at some point along their length.

In general, airflow through a pipe of steady diameter is proportional to the square root of the pressure drop between its inlet and its outlet ($Q \sim \sqrt{\Delta P}$). As demonstrated in *Figure 5.4.1* below, this relation is verified for the airways of the bronchial tree, which are non-compliant and have rigid walls i.e. the trachea and the first bronchi. The diameters of these airways don't significantly change along their length and they are insensitive in variations of the transmural pressure during expiration.

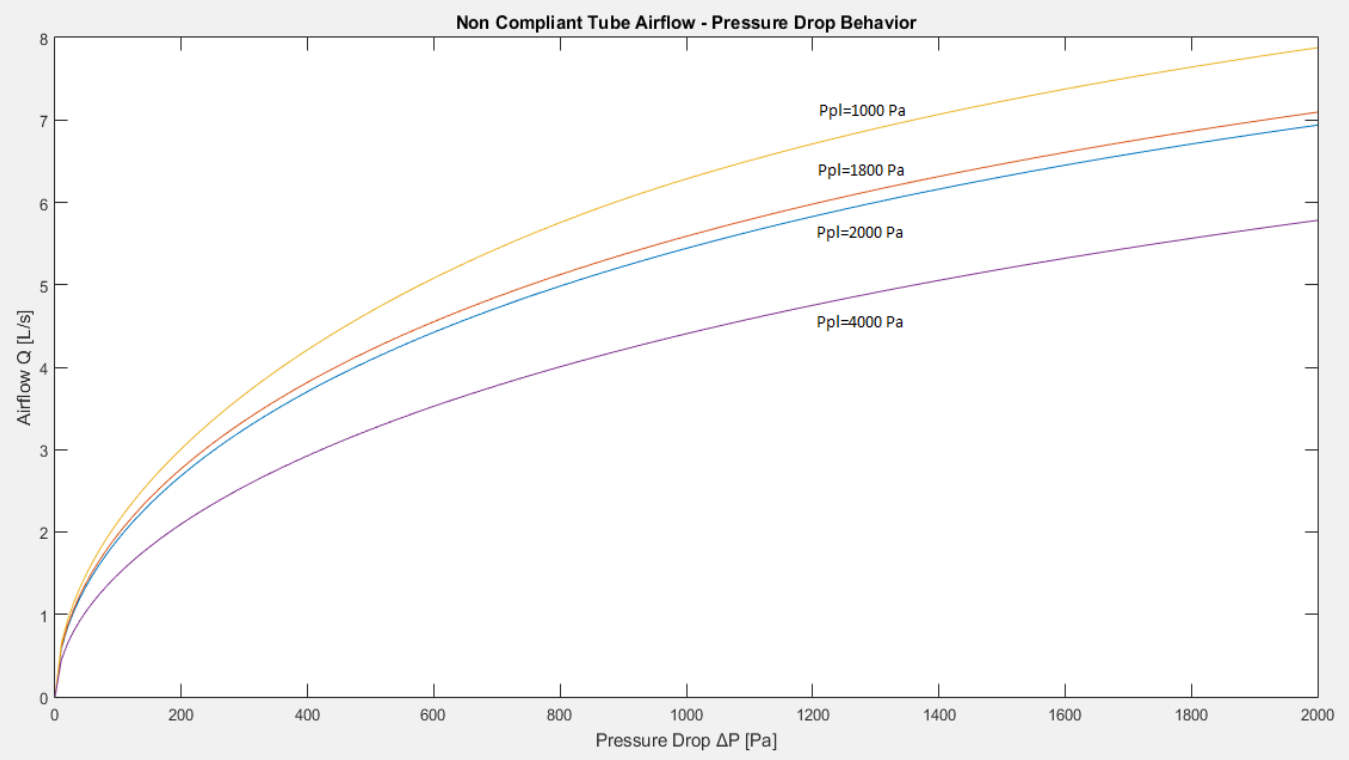

Figure 5.4.1: Airflow-Pressure Drop behavior of a non compliant tube (specifically the trachea) for different pleural pressures. The pressure at the inlet of the airway is 2000 (Pa).

The increase of pleural pressure slightly narrows the pipe. This leads to smaller airflows for the same pressure drop. However, this narrowing is not enough to produce flow limitation at any point of the airway and thus the proportionality between the airflow and the square root of the pressure drop is maintained.

In contrast to non-compliant tubes, compliant tubes are sensitive in the variation of the transmural pressure along their length. As pressure inside the airway continually drops as we move to its outlet, transmural pressure also decreases. This leads to a decrease of the airway's cross-sectional area as described by *Lambert et al.* (Lambert, Wilson, Hyatt, Rodarte, 1982). At some point the airway collapses limiting the flow. This behavior is demonstrated in *Figure 5.4.2,* below:

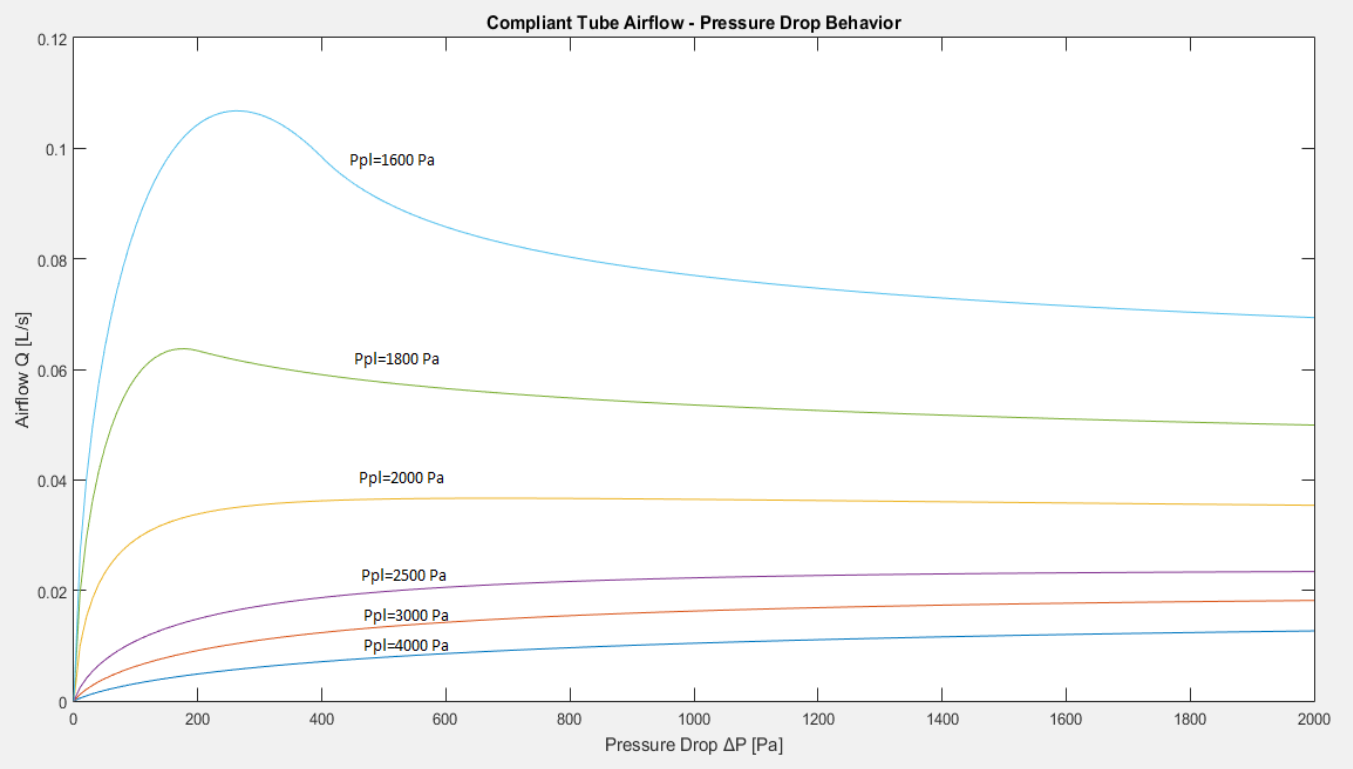

Figure 5.4.2: Airflow-Pressure Drop behavior of a compliant tube of 6th generation for different pleural pressures. The pressure at the inlet of the airway is 2000 (Pa).

Airflow-pressure drop behavior is normal for high values of the pleural pressure. This can be explained considering that internal pressure is considerably smaller than pleural pressure which leads to very narrow airways, with pressure drop along their length making no significant difference. Airflow reaches a plateau for intermediate values of the pleural pressure, where pleural pressure is comparable to internal pressure.

Flow limitation emerges when transmural pressure varies significantly from point to point along the pipe's length, which happens at lower pleural pressures. In this case, the sudden drop in airflow, as pressure drop increases, is obvious.

5.5 General Remarks - Conclusions - Suggestions

The results of our model for forced expiration are quite satisfactory when compared to the results of previous models or with experimentally determined results produced by spirometric tests. Two such results are demonstrated below. The spirometry test resulting airflow curves :

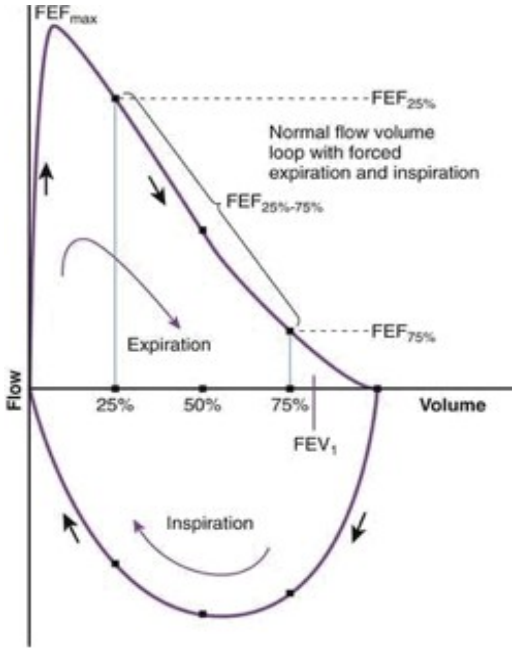

Figure 5.5.1: Flow Volume Loops generated by spirometry results (http://respiratory.guide/spirometry/spirometry-lecture?courseid=451&seq=11)

The resulting curves of the *Filoche and Florens* (Filoche, Florens, 2011) model are:

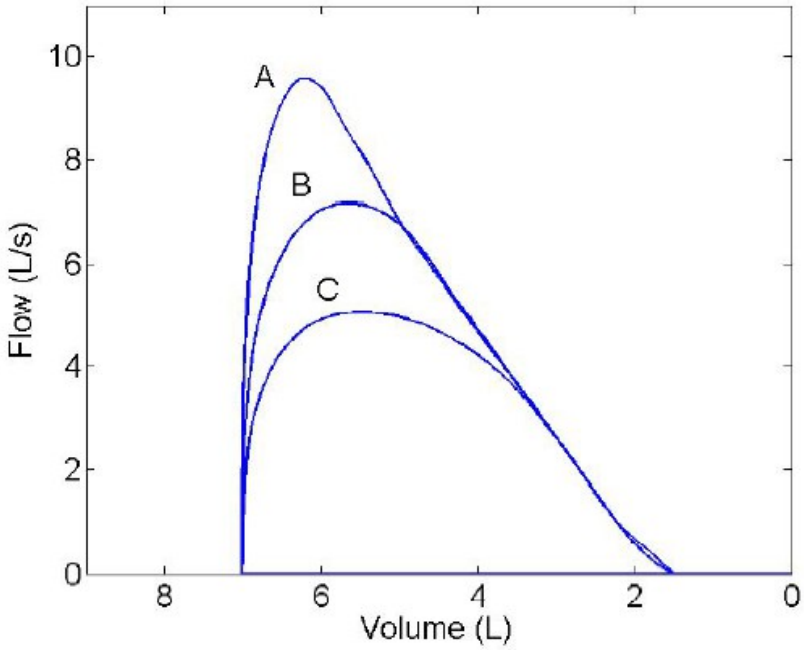

Figure 5.5.2: Flow-volume loops computated using a quasi-static computation of flow in the lung airway system. A: Pm=24 kPa and τ=0.2 s, B: Pm=12 kPa and τ=0.2 s, C: Pm=6 kPa and τ=0.4 s (Filoche,Florens, 2011)

Flow limitation is predicted more efficiently by this model, due to the exact integration of pressure drop which was described in *chapter 4.8*. However, there is no remarkable difference between *Figure 5.5.2* and *Figure 5.2.3*, neither qualitatively nor quantitatively.

Conclusions:

This paper achieved some of its primary goals. More specifically :

- the description of the elastic behavior of the repiratory system using analytical equations
- the development of an equation for the calculation of driving pressure, which includes the elastic forces of the respiratory system, something that previous models neglected
- we managed to calculate dissipative, convective and mouth pressure drops along the bronchial tree, using mean values for the transmural pressure
- the diameter variation during the two breathing processes was a key element to our calculation and therefore it was taken under consideration, increasing the accuracy of our results
- we produced resulting curves of the airflow over full vital capacity volume, which resemble at a great extent results of previous models and spirometric tests
- we've been able to expand the problem of airflow calculation, to include inspiration process, producing satisfactory, yet not completely accurate results.
- we have also been able to apply a more accurate model for the calculation of airflow through a single compliant tube and clearly demonstrate the emergence of flow limitation

Suggestions:

Some suggestions for future research topics are made here. More specifically :

- airflow calculation for the whole trancheobronchial tree using compliant airways and analytically integrating transmural pressure along their lengths.
- the inspiration airflow calculation results of this paper can be used for future research, concerning the deposition of aerosolized air particles in human lungs during the use of different inspiratory medicines.
- lung static behavior (no airflow), especially when the lungs are exposed to extreme conditions such as big sea depths or high mountain altitudes is another interesting research subject.

References

Agostoni E., Fenn W. O., Velocity of muscle shortening as a limiting factor in respiratory air flow, American Physiological Society (1960), https://doi.org/10.1152/jappl.1960.15.3.349

Appelberg, J., Pavlenko, T., Bergman, H., Rothen, H. U., Hedenstierna, G., (2007), Lung aeration during sleep, Chest 131, 122–129.

Barbini P., Bringhenti C., Cevenini G., Gnudi G., A Dynamic Morphometric Model of the Normal Lung for Studying Expiratory Flow Limitation in Mechanical Ventilation, Annals of Biomedical Engineering, Vol. 33, No. 4, May (2005), 518–530, doi: 10.1007/s10439-005-2511-6

Barrow A., Pandit J. J., Lung ventilation and the physiology of breathing, Surgery (2017), http://dx.doi.org/10.1016/j.mpsur.2017.02.004

Burger, E. J., Macklem, P., (1968). Airway closure: Demonstration by breathing 100% O2 at low lung volumes and by N2 washout. Journal of Applied Physiology 25, 139–148.

Çengel Y. A., Cimbala J. M., Fluid Mechanics: Fundamentals and Applications, 1st edition (2006), ISBN 0–07–247236–7

Cheesman K., Burdett E., Anatomy of the nose and pharynx, Anaesthesia & Intensive Care Medicine, Volume 12, Issue 7, July (2011), Pages 283-286

Cheng W., DeLong D. S., Franz G. N., Petsonk E. L., Frazer D. G., Contribution of opening and closing of lung units to lung hysteresis, Respiration Physiology 102 (1995), 205-215

Cotes J. E., Chinn D. J., Miller M. R., Lung function. Physiology, measurement and application in medicine, Oxford: Blackwell Publishing (2006)

D'Angelo E., Calderini E., Torri G., et al., Respiratory mechanics in anaesthetised paralysed humans: effects of flow, volume and time, J Appl Physiol. (1989) 67, 2556-2564.

D'Angelo E., Tavola M., Milic-Emili J., Volume and time dependence of respiratory system mechanics in normal anaesthetised paralysed humans. Eur Respir J. (2000) 16, 665-672.

Dawson S. V., Elliott E. A., Wave-speed limitation on expiratory flow-a unifying concept. J. Appl. Physiol.: Respirat. Environ. Exercise Physiol. 43: 198-515, (1977)

Espinosa, F. F., Kamm, R. D., (1998). Meniscus formation during tracheal instillation of surfactant, Journal of Applied Physiology 85, 266–272.

Feher J., Quantitative Human Physiology: An Introduction - 2nd edition (2016), ISBN: 978-0-12-800883-6

Filoche M., Florens M., The stationary flow in a heterogeneous compliant vessel network, Journal of Physics:Conference Series 319 (2011) 012008, doi:10.1088/1742-6596/319/1/01/012008

Gauthier A. P., Verbanck S., Estenne M., et al., Three-dimensional reconstruction of the in vivo human diaphragm shape at different lung volumes, J Appl. Physiol. (1994), 76, 495-506.

Guyton A. C., Hall, J. H. (1956). Textbook of Medical Physioloy. Jackson, Mississippi: Elsevier

Hammersley J. R., Olson D. E., Physical model of the smaller pulmonary airways, J. Appl. Physiol. 72 (1992) 2402-2414

Heil M., Hazel A. L., Smith J. A., The mechanics of airway closure, Respiratory Physiology & Neurobiology, Volume 163, Issues 1–3, 30 November (2008), Pages 214-221

Hughes J. M. B., Hoppin F. G. Jr., Mead J., Effect of lung inflation on bronchial length and diameter in excised lungs. J. AppL Physiol. 32 (1972), 25-35.

Hughes, J. M. B., Rosenzweig, D. Y., Kivitz, P. B., (1970). Site of airway closure in excised dog lungs: Histologic demonstration. Journal of Applied Physiology 29, 340–344.

Hyatt R. E., The interrelationships of pressure-flow and volume during various respiratory maneuvers in normal and emphysematous subjects. Am. Rev. Diseases 83: 676-683, (1961)

Isabey D., Steady and Pulsatile Flow Distribution in a Multiple Branching Network with Physiological Applications, J. Biomechanics, Vol. 15 (1982). No. 5, 395-404

Jaeger M. J., Matthys H., The pattern of flow in the upper human airways, Resp. Physiol. 6 (1968)

113-127

Johnson W. L., Packing, freedivingsolutions.com, 12 April (2015).

Jordanoglou J., Koursouba E., Lalenis C., Gotsis T., Kontos J., Gardikas C., Effective time of the forced expiratory spirogram in health and airways obstruction, Thorax, (1979), 34, 187-193

Kaminsky D., Introduction to airway resistance measurements, Department of Medicine, The University of Vermont

Koeppen B. M., Stanton B. A., Berne and Levy Physiology, 6th edition (2008)

Kundu P. K., Cohen I. M., Dowling D. R., Fluid Mechanics (Fifth Edition), (2012), ISBN: 978-0-12-382100-3

Lai S. K., Wang Y. Y., Wirtz D., Hanes J., Micro- and macrorheology of mucus, Advanced Drug Delivery Reviews 61 (2009) 86–100

Lambert R. K., Wilson T. A, Hyatt R. E., Rodarte J. R, A computational model for expiratory flow, J. Appl. Physiol. Resp. Environ. Exerc. Physiol. 52 (1982) 44-56

Lumb A. B., Nunn's Applied Respiratory Phsyiology, Eighth Edition, (2017)

Mahadevan V., Anatomy of the oesophagus, Surgery (Oxford), Volume 35, Issue 11, November (2017), Pages 603-607

Marshall R., Holden W. S.,Changes in calibre of the smaller airways in man.Thorax 18(1963),54-58

Mehran J. R., Fundamental and Practical Aspects of Airway Anatomy From Glottis to Segmental Bronchus, Thorac Surg Clin 28 (2018) 117–125

Mount L. E., The ventilation flow–resistance and compliance of rat lungs, J Physiol (1955) 127, 157-167

Pedley T. J., Schroter R. C., Sudlow M. F., The prediction of pressure drop and variation of resistance within the human bronchial airways. Respir. Physiol. 9 (1970), 387-495.

Pessoa I. M.B. Sclauser, Parreira V. F., Fregonezi G. A. F., Sheel A. W., Chung F., Reid W. D.. Reference values for maximal inspiratory pressure: A systematic review. Can Respir J (2014); 21(1):43-50.

Polak A. G., Computers in Biology and Medicine 28 (1998) 614-625

Quanjer, P. H., Tammeling, G. J., Cotes, J. E., Pedersen, O. F., Peslin, R., Yernault, J. C., (1993), April). Lung volumes and forced ventilatory flows. The European respiratory journal, Vol5: 5-40

Reynolds D. B., Steady Expiratory Flow-Pressure Relationship in a Model of the Human Bronchial Tree , J Biomech Eng 104 (2), 153-158 May 01, (1982), doi:10.1115/1.3138330

Rubenstein D., Yin W., Frame M. D., Biofluid Mechanics (Second Edition): An Introduction to Fluid Mechanics, Macrocirculation, and Microcirculation A volume in Biomedical Engineering, (2015) ISBN: 978-0-12-800944-4

Sinaga N., http://slideplayer.com/slide/7781501/#, INTERNAL INCOMPRESSIBLE VISCOUS FLOW Nazaruddin Sinaga Laboratorium Efisiensi dan Konservasi Energi Universitas Diponegoro 1., Slide 8/109

Soong T. T., Nicolaides P., Yu C. P., Soong S. C, A statistical description of the human tracheobronchial tree geometry, Respiration Physiology (1979) 37, 161-172

Weibel E. R., Morphometry of the Human Lung, Academic Press, New York, (1963).

Weibel E. R., Gomez D. M., A principle for counting tissue structures on random sections. J. Appl. Physiol. 17 (1962), 343-345.

West J. B., Respiratory Physiology:The Essentials -9th edition (2012), ISBN 978-1-60913-640-6

Wheatley J. R., Amis T. C., Engel L. A., Nasal and oral airway pressure-flow relationships, J. Appl. Physiol. 71 (1991) 2317-2324

Wilson A.G., Massarella G. R.,Pride N. B., Elastic properties of airways in human lung post mortem, (1974) Am. Rev. Respir. Dis. 110~ 716-729.

Παπαϊωάννου Α. Θ., Μηχανική των Ρευστών, Τόμος Ι, Β' Έκδοση (2002)

Παπανίκας Δ., Εφαρμοσμένη Ρευστομηχανική, 4η Έκδοση (2010)

[1] https://chemengineering.wikispaces.com/Gas+constant

[2] https://chemistry.tutorvista.com/physical-chemistry/boyles-law.html

[3] https://www.engineeringtoolbox.com/entrance-length-flow-d_615.html

[4] https://en.wikipedia.org/wiki/Entrance_length

[5] https://en.wikipedia.org/wiki/Lung_volumes

[6] https://en.wikipedia.org/wiki/Moody_chart

[7] https://en.wikipedia.org/wiki/Pulmonary_alveolus

[8] http://www.innerbody.com/image_digeov/dige02-new2.html

[9]https://www.tandfonline.com/doi/full/10.1080/10255842.2017.1307343?scroll=top&needAccess=true&

[10] http://www.therespiratorysystem.com/nasal-conchae-nasal-turbinates/

[11] http://respiratory.guide/spirometry/spirometry-lecture?courseid=451&seq=11

Appendix A: Algorithm for the calculation of airflow during forced expiration

The algorithm consists of three parts: the main algorithm and the two functions (Initials.m and Flow_Limitation.m). The main algorithm is given below:

```
%--------------------------------------------------------------------------
% Computational Simulation of Forced Expiratory Maneuver
%--------------------------------------------------------------------------

%{

The following algorithm calculates the airflow at each time or expired
volume step during a forced expiration. There are two alternatives A and B.

The first alternative A is the use of a constant expired volume step and a
variable time step calculated after the determination of the airflow of
every next step. In this muscle pressure is calculated according to the
equation used by A.G.Polak.

The second alternative B is the use of a constant time step and a variable
volume step. In this case an approximation of the maximum expiratory time
tmax is needed. The muscle pressure is calculated according to a modified
equation in order to include the respiratory system's elastic forces or
static recoil pressure.

%--------------------------------------------------------------------------
Alternative A :

A constant step for the expired volume dV is used, with imax being the
number of nodes. From V(1)=0 to V(imax)=FVC.

The time step dt is calculated according to the airflow of the next step as
dt=dV/Q(i).Thus the time of each step is t(i)=t(i-1)+dV/Q(i).
This means that the algorithm uses a forward scheme and thus an
initial approximation for the value of the airflow at the second node Q(2)
is needed in order for the calculation to begin.

Alternative B :

A constant time step dt is used. An approximation, which can be corrected
afterwards, for the tmax is made. From t(1)=0 to t(imax)=tmax. The volume
step is calculated as dV(i)=dt*Q(i).


%}
%--------------------------------------------------------------------------
%Parameter Values

FVC=5.5 ;      % (L) Forced Vital Capacity
RV=1.5 ;       % (L) Residual Volume
VC=5.6 ;       % (L) Vital Capacity
TLC=RV+VC;     % (L) Total Lung Capacity
FRC=2.6;       % (L) Functional Residual Capacity

V0=0.19*TLC;   % (L)     (Polak pg. 621)
Vm=1.06*TLC;   % (L)     (Polak pg. 621)
CL=0.0057;     % (L/Pa)  (Polak pg. 621)

Pm=24*1000 ;    % [Pa](Polak page 621) (Maximum Expiratory Muscle Pressure)
tc=0.2 ;        % [s] (Polak page 621)

m=0.0000189;   % (kg/m/s) T_air=20°C
r=1.205;       % (kg/m^3) T_air=20°C
al=1.5 ;       % (Filoche,Florens)
b=0.0035;      % (Filoche,Florens)
Rt=500000 ;    % [Pa*s/m^3) %Polak page 621
RU=1.2E7;      % Mouth Flow Resistance
ro=1.68;       % Mouth Pressure Drop Airflow Exponent

```

```
pi=3.14;

%-----------------------------------------------------------------
%Bronchial Tree Geometry

%Initial airway diameters calculation with the help of function : Initials.m

VLin=TLC;                              %Initial Lung Volume

[D,S,Spipe]=Initials(VLin,V0,Vm,CL);   %Airway diameters : D (m)
                                       %Total generation cross-sectional areas : S (m^2)
                                       %Airways cross-sectional areas : Spipe (m^2)

L=[12.000; 4.760; 1.900; 0.760; 1.270; 1.070;
    0.900; 0.760; 0.640; 0.540; 0.460; 0.390;
    0.330; 0.270; 0.230; 0.200; 0.165;]*10^-2 ; % Airway Lenghts (m) Weibel

g=0:1:16 ;   %Generation Number
n=2.^g   ;   %Number of Branches for each Generation


%-------------------------------------------------------------------------
%A :Constant Expired Volume Step

imax=1000;         %Number of values for the arrays t,V,VL,Q
k=imax-1  ;        %Number of intervals

dV=FVC/k;          %Expired volume step
V=0:dV:FVC;        %Expired volume array
VL=TLC-V;          %Lung volume array

%-------------------------------------------------------------------------
%B :Constant Time Step
%imax=1000;         %Number of values for the arrays t,V,VL,Q
%k=imax-1  ;        %Number of intervals

%tmax=3;            %Maximum expiratory time
%dt=tmax/k;         %Time step
%t=[0:dt:tmax];     %Time array

%-------------------------------------------------------------------------
%Static Recoil Pressure Parameters

Cth=-CL* log((FRC-V0)/(0.75*Vm-V0))/log((Vm-V0)/(Vm-FRC)); %(L/Pa)
Pmax=((Vm-V0)/Cth)*log((Vm-V0)/(0.75*Vm-V0)); % (Pa)
DPLTLC=((Vm-V0)/CL)*log((Vm-V0)/(Vm-TLC));
DPthTLC=(Pmax-((Vm-V0)/Cth)*log((Vm-V0)/(TLC-V0)));
DPtotalTLC=DPLTLC+DPthTLC;
DPthRV=(Pmax-((Vm-V0)/Cth)*log((Vm-V0)/(RV-V0)));

%-------------------------------------------------------------------------
%Lung Volume- Static Recoil Pressure curve production

%{
%DPL=((Vm-V0)./CL).*log((Vm-V0)./(Vm-VL));  %(Pa)
%DPth=(Pmax-((Vm-V0)/Cth).*log((Vm-V0)./(VL-V0)));  %(Pa)
%DPtotal=DPL+DPth; %(Pa)

DPL=DPL*0.010197;                  %Conversion Pa - cmH2O
DPth=DPth*0.010197;
DPtotal=DPtotal*0.010197;
```

```
127
128     plot(DPtotal,VL)
129     hold on
130     plot(DPL,VL)
131     hold on
132     plot(DPth,VL)
133
134     legend('Respiratory','Lung','Chest')
135     hline = refline([0 RV]);
136     hline.Color = 'black';
137     set(hline,'LineStyle','--');
138     hline = refline([0 FRC]);
139     hline.Color = 'black';
140     set(hline,'LineStyle','--');
141     hline = refline([0 TLC]);
142     hline.Color = 'black';
143     set(hline,'LineStyle','--');
144     title('Lung Volume - Static Recoil Pressure')
145     xlabel(' Static Recoil Pressure, Pst[cmH2O] ')
146     ylabel(' Lung Volume, VL[L] ')
147     hold on
148
149     %}
150
151     %-------------------------------------------------------------------------
152     %A : Initial Values of Q,t at V(1)=0
153
154 -   Q(1)=0;
155 -   t(1)=0;
156
157     %-------------------------------------------------------------------------
158     %B : Initial Values of Q,V,VL at t(1)=0
159
160     %Q(1)=0;
161     %V(1)=0;
162     %VL(1)=TLC;
163
164     %-------------------------------------------------------------------------
165     %Main calculation
166
167     %An initial approximation for the airflow in the node i=2 is required
168     %in order for the calculation to begin. The approximation Q_approx is
169     %corrected with a trial and error method until its sufficiently close to
170     %the calculated Q(2).
171
172
173 -   Q_approx= 0.001;     %Approximation assigned to Q(2)
174                          %Gia imax=10 Q_approx=0.0065 dinei tmax=0.9281s
175                          %Gia imax=100 Q_approx=0.0028 dinei tmax=1.2564s
176                          %Gia imax=1000 Q_approx=0.001 dinei tmax=1.5389s
177                          %Gia imax=10000 Q_approx=0.00034 dinei tmax=1.8132s
178                          %Gia imax=100000 Q_approx=0.0001 dinei tmax=2.0857s
179
180 -   for i=2:imax         %Iteration
181
182         %Initial approximations of Q(i)
183         %At i=2 Q(2)=Q_approx
184         %For i>2 the airflow of the previous step Q(i)=Q(i-1) is given as
185         %initial guess for the Newton-Raphson method that follows.
186
187 -       if (i==2)
188 -          Q(i)=Q_approx;
189 -       else
190 -          Q(i)=Q(i-1);
```

```
    end

    %-------------------------------------------------------------------
    %A :Variable time step
    dt(i)=dV/(Q(i)*1000); %Time step calculation
    t(i)=t(i-1)+dt(i);    %Time calculation

    %-------------------------------------------------------------------
    %B :Variable volume step

    %dV(i)=dt*Q(i)*1000;
    %V(i)=V(i-1)+dV(i);   %Expired air volume
    %VL(i)=TLC-V(i);      %Lung volume

    %-------------------------------------------------------------------
    %B :Static Recoil Pressures

    %DPL(i)=((Vm-V0)/CL)*log((Vm-V0)/(Vm-VL(i)));  %(Pa)  %Lung
    %DPth(i)=(Pmax-((Vm-V0)/Cth)*log((Vm-V0)/(VL(i)-V0)));  %(Pa) %Chest
    %DPtotal(i)=DPL(i)+DPth(i); %(Pa) %Total

    %-------------------------------------------------------------------
    %Expiratory muscle pressure at V(i),t(i)
    %A :Pmuscle used by Polak
    Pe(i)=(Pm/FVC)*(1-exp(-t(i)/tc))*(FVC-V(i)) ; %[Pa]

    %-------------------------------------------------------------------
    %B :Modified Pmuscle
    %Pe(i)=-DPtotalTLC+(1-exp(-t(i)/tc))*(Pm*(FVC-V(i))/FVC+DPtotalTLC-DPthRV); %[Pa] %Nea Pmuscle

    %-------------------------------------------------------------------
    %Different pressure drop calculations : Dissipative (A and B) and
    %Convective (E)

    A=0;  % Q friction multiplier
    B=0;  % Q^2 friction multiplier
    E=0;  % Q^2 convection multiplier

    for j=1:17
        A=A+(128*m*L(j)*a1)/(pi*D(j)^4*2^g(j)) ;     %Friction term
        B=B+(512*r*L(j)*b)/(pi^2*D(j)^5*2^(2*g(j))); %Friction term
      if (j<17)
         E=E+abs((r/(2^(2*g(j)+1)))*(-1/(4*S(j+1)^2)+1/S(j)^2)); %Convection term
      end
    end

%-------------------------------------------------------------------
%Newton-Raphson algorithm for correct Q(i) calculation

    F=1;
    index(i)=0; %Index counting the iterations of Newton-Raphson method
                %until convergance at each step (3-4 iterations).


    while (abs(F)>10^-6)
       %-----------------------------------------------------------
       %Driving pressure and Total pressure drop equation
       %A :Pdriving=Pmuscle-Rt*Q
       F=A*Q(i)+B*Q(i)^2+E*Q(i)^2+Q(i)^ro*(RU)+Rt*Q(i)-Pe(i);
       %-----------------------------------------------------------
       %B :%Pdriving=Pmuscle+DPtotal-Rt*Q
       %F=(A*Q(i)+B*Q(i)^2)+E*Q(i)^2+Q(i)^ro*(RU)+Rt*Q(i)-DPtotal(i)-Pe(i);
       %-----------------------------------------------------------
       dF=A+2*B*Q(i)+2*E*Q(i)+ro*RU*Q(i)^(ro-1)+Rt;%+Pm*((FVC-V(i))/FVC)*(dV/(1000*tc*Q(i)^2))*exp(-t(i)/tc);
```

```
255 -           Q(i)=Q(i)-F/dF;
256 -           index(i)=index(i)+1;
257 -       end
258
259     %-------------------------------------------------------------------------
260     %ATTENTION : The function has alternative A or B choice inside it.
261
262 -   [S,D,Spipe]=Flow_Limitation(V(i),Q(i),Pe(i),D,S); %New Diameters calculation
263 -   D;
264     %-------------------------------------------------------------------------
265 -   end
266
267 -   t(imax);  %Total expiration process time
268 -   index;
269 -   athroisma=sum(index);
270
271
272 -   Q(2) ;    %Helps correct the Q_approx value
273 -   Q=Q*1000; %Airflow conversion to (L/s)
274     %-------------------------------------------------------------------------
275     %Plotting Results
276
277
278     %Airflow-Expired Air Volume Curve
279 -   hold on
280 -   plot(V,Q)
281 -   title('Airflow-Expired Air Volume')
282 -   xlabel(' V [L] ')
283 -   ylabel(' Q [L/s] ')
284 -   legend('Pm=24kPa,τ=0.2')
285
286     %Airflow-Time Curve
287     %plot(t,Q)
288     %title('Airflow-Time')
289     %xlabel(' t [s] ')
290     %ylabel(' Q [L/s] ')
291     %legend('Pm=24kPa,τ=0.2')
292
293     %Time-Expired Air Volume Curve
294     %plot(t,V)
295     %hline = refline([0 VC]);
296     %legend(hline,'V=VC=5.6 L')
297     %hline.Color = 'r';
298     %xlabel(' t [s]')
299     %ylabel(' V [L] ')
300     %title('Expired Volume-Time')
301
302     %Time-Lung Volume Curve
303     %plot(t,VL)
304     %hline = refline([0 RV]);
305     %legend(hline,'VL=RV=1.5 L')
306     %hline.Color = 'r';
307     %xlabel(' t [s]')
308     %ylabel(' VL [L] ')
309     %title('Lung Volume-Time')
310
311     %hold on
312     %plot(V,Pe)
```

Function Initials.m which calculates the initial airway diameters is:

```
function [D,S,Spipe]=Initials(VLin,V0,Vm,CL)

%-------------------------------------------------------------------------
%The function Initials calculates the initial airway diameters for
%generations from 0 to 16.Using as input data the initial lung volume (VLin)
%it calculates the transmural pressure at that volume, which is uniform and
%equal to the static recoil pressure of the lung, since there is no airflow.
%Then diameters are calculated according to the Lambert equations.

VL=VLin;

DPL=((Vm-V0)/CL)*log((Vm-V0)/(Vm-VL));  %(Pa)

Ptm=DPL;                                %Transmural pressure(Pa)

Ptm=Ptm*0.010197162129779282;           % Metatroph Ptm   ! (cmH2O) !

%-------------------------------------------------------------------------
% Model parameters of bronchial mechanical properties (Lambert page 46)

g=[0:1:16];  %Generation Number
n=2.^g;      %Number of Branches for each Generation

a0= [0.882; 0.882; 0.686; 0.546; 0.450; 0.370; 0.310; 0.255; 0.213; 0.184;
     0.153; 0.125; 0.100; 0.075; 0.057; 0.045; 0.030;] ;

a0t= [0.011; 0.011; 0.051; 0.08; 0.1; 0.125; 0.142; 0.159; 0.174; 0.184;
      0.194; 0.206; 0.218; 0.226; 0.233; 0.239; 0.243;] ;

n1= [0.5; 0.50; 0.6; 0.6; 0.7; 0.8; 0.9; 1; 1; 1; 1; 1; 1; 1; 1; 1; 1;];

n2= [10; 10; 10; 10; 10; 10; 10; 10; 10; 10; 10; 9; 8; 8; 8; 7; 7;];

Am= [2.37; 2.37; 2.80; 3.50; 4.50; 5.30; 6.50; 8; 10.20; 12.70; 15.94;
     20.70; 28.80; 44.50; 69.40; 113; 180;]*10^(-4); %(m^2)

L= [12.000; 4.760; 1.900; 0.760; 1.270; 1.070; 0.900; 0.760; 0.640; 0.540;
    0.460; 0.390; 0.330; 0.270; 0.230; 0.200; 0.17;]*10^(-2); % (m)

P1= a0.*n1./a0t ;      %vertical asymptote

P2= -n2.*(1-a0)./a0t ; %vertical asymptote


    for j=1:17

        if (Ptm<0)
          a= a0(j)*(1-Ptm/P1(j))^(-n1(j));       %Lambert pg. 46
        else
          a=1-(1-a0(j))*(1-Ptm/P2(j))^(-n2(j));  %Lambert pg. 46
        end

        S(j)=a*Am(j);
        D(j)=sqrt((S(j)*4)/(pi*n(j)));
        Spipe(j)=pi*D(j)^2/4;

    end
end
```

Function Flow_Limitation.m which the change in the airway diameters as described, is:

```
function [S,D,Spipe]=Flow_Limitation(V,Q,Pe,D,S)

%-------------------------------------------------------------------------
%The function Flow_Limitation is called at each step of the iteration after
%the calculation of the airflow in order to compute the change in the
%airway diameters.The input data are the expired volume,the airflow,
%the muscle pressure at the current step, as well as the current diameters.
%At first pleural and driving or alveolar pressures are calculated.Then an
%average internal pressure is calculated for each airway from 0 to 16
%generation.Pressures at the inlet and the outlet of each airway are calculated,
%beginning from the known pressure at the trachea's outlet,using pressure
%drop and bernoullis calculations and reaching until the inlet of the
%sixteenth generation equations Transmural pressure is determined as
%the pressure difference between the average internal pressure and the
%external pressure, which is the pleural pressure.Thus the applying
%Lambert's formulas the calculation of the new diameters is possible.

%-------------------------------------------------------------------------
%Calculation Parameters
m=0.0000189;  % (kg/m/s) T_air=20°C
r=1.205;      % (kg/m^3) T_air=20°C
al=1.5 ;      % (Filoche,Florens)
b=0.0035;     % (Filoche,Florens)
pi=3.14159265358979323846;

%-------------------------------------------------------------------------
%Static Recoil Pressures
RV=1.5 ;      % (L) Residual Volume
VC=5.6 ;      % (L) Vital Capacity
FRC=2.6;      % (L) Functional Residual Capacity
TLC=RV+VC ;   % (L) Total Lung Capacity
V0=0.19*TLC;  % (L)    (Polak pg. 621)
Vm=1.06*TLC;  % (L)    (Polak pg. 621)
CL=0.0057;    % (L/Pa) (Polak pg. 621)
VL=TLC-V;     % (L) VLung=TLC-VExpired
DPL=((Vm-V0)/CL)*log((Vm-V0)/(Vm-VL));  % (Pa)
Cth=-CL* log((FRC-V0)/(0.75*Vm-V0))/log((Vm-V0)/(Vm-FRC)); %(L/Pa)
Pmax=((Vm-V0)/Cth)*log((Vm-V0)/(0.75*Vm-V0)); % (Pa)
DPth=(Pmax-((Vm-V0)/Cth)*log((Vm-V0)/(VL-V0)));  %(Pa)
DPtotal=DPL+DPth; %(Pa)

%-------------------------------------------------------------------------
%Driving and Alveolar Pressures
Rt=500000 ;   % [Pa*s/m^3) %Polak page 621

%-------------------------------------------------------------------------
%A
Pd=Pe-Rt*Q;
%-------------------------------------------------------------------------
%B
%Pd=Pe+DPtotal-Rt*Q;

%-------------------------------------------------------------------------
%Alveolar Pressure
Palv=Pd;
%Pleural Pressure
Ppl=Palv-DPL; % !(Pa)!

%-------------------------------------------------------------------------
%Lambert Parameters

g=[0:1:16];  %Generation Number
n=2.^g;      %Number of Branches for each Generation

```

```
a0= [0.882; 0.882; 0.686; 0.546; 0.450; 0.370; 0.310; 0.255; 0.213; 0.184;
     0.153; 0.125; 0.100; 0.075; 0.057; 0.045; 0.030;] ;

a0t= [0.011; 0.011; 0.051; 0.08; 0.1; 0.125; 0.142; 0.159; 0.174; 0.184;
      0.194; 0.206; 0.218; 0.226; 0.233; 0.239; 0.243;] ;

n1= [0.5; 0.50; 0.6; 0.6; 0.7; 0.8; 0.9; 1; 1; 1; 1; 1; 1; 1; 1; 1; 1;];

n2= [10; 10; 10; 10; 10; 10; 10; 10; 10; 10; 10; 9; 8; 8; 8; 7; 7;];

Am= [2.37; 2.37; 2.80; 3.50; 4.50; 5.30; 6.50; 8; 10.20; 12.70; 15.94;
     20.70; 28.80; 44.50; 69.40; 113; 180;]*10^(-4); %(m^2)

L= [12.000; 4.760; 1.900; 0.760; 1.270; 1.070; 0.900; 0.760; 0.640; 0.540;
    0.460; 0.390; 0.330; 0.270; 0.230; 0.200; 0.17;]*10^(-2); % (m)

P1= a0.*n1./a0t ;      %vertical asymptote

P2= -n2.*(1-a0)./a0t ; %vertical asymptote

%-------------------------------------------------------------------------
%Calculation of Pin,Pout,Pav and Ptm for each of the 17 generations (g=[0:16])
%j=1:17

RU=1.2E7;          % Mouth Flow Resistance
ro=1.68;           % Mouth Pressure Drop Airflow Exponent
Pout(1)=0+RU*Q^ro; %Pressure at the exit of trachea (generation 0 (j=1)) is
                   %bigger than atmospheric (0 Pa) by the mouth pressure drop


for j=1:17

   fA(j)=(128*m*L(j)*a1)/(pi*D(j)^4*2^g(j)) ;      %Friction factor j generation
   fB(j)=(512*r*L(j)*b)/(pi^2*D(j)^5*2^(2*g(j))) ; %Friction factor j generation
   DP(j)=(fA(j)*Q+fB(j)*(Q^2)) ;
   Pin(j)=Pout(j)+DP(j);                          %Pressure at the inlet of j generation's airways
   Pav(j)=(Pin(j)+Pout(j))/2 ;                    %Average j generation airways' pressure

   %-----------------------------------------------------------------
   %Transmural pressure. The first two generations g=0 kai g=1 or j=1 kai j=2
   %are considered to be outside the pleural liquid and thus the
   %transmural pressure is equal to the internal pressure (Pav)
   %of these airways, since the pressure outside them is atmospheric (0Pa)

   if(j<3)
       Ptm(j)=Pav(j); % (Pa) Transmural pressure of trachea and first bronchus airways
   else
       Ptm(j)=Pav(j)-Ppl; % (Pa) Transmural pressure of j generation airways
   end

   Ptm(j)=Ptm(j)*0.010197162129779282; % Conversion in ! (cmH2O) !

   if (Ptm(j)<0)
       a=a0(j)*(1-Ptm(j)/P1(j))^(-n1(j));         %Lambert pg. 46
   else
       a=1-(1-a0(j))*(1-Ptm(j)/P2(j))^(-n2(j));   %Lambert pg. 46
   end
```

```
122
123 -       S(j)=a*Am(j);
124 -       D(j)=sqrt(4*S(j)/(n(j)*pi));
125 -       Spipe(j)=(pi*D(j)^2)/4;
126
127         %Next generation (j+1) outlet pressure calculation with Bernoulli's equation
128 -       if (j<17)
129 -            Pout(j+1)=Pin(j)+Q^2*abs((r/(2^(2*g(j)+1)))*(-1/(4*S(j+1)^2)+1/S(j)^2));
130 -       end
131
132 -     end
133 -     Ptm;
134 -   end
```

Note: The above algorithm also contains a part for the production of the static recoil pressure- volume graphs (line 115 to 151).

Appendix B: Inspiration Process

The Matlab code used for the production of the inspiration curves is:

```
%-------------------------------------------------------------------------
%Airflow during Inspiration calculation VL(1)=RV kai VL(imax)=TLC

%-------------------------------------------------------------------------
%Parameters

m=0.0000189;  % (kg/m/s) T_air=20°C
r=1.205;      % (kg/m^3) T_air=20°C
al=1.5 ;      % (Filoche,Florens)
b=0.0035;     % (Filoche,Florens)
Rt=500000 ;   % [Pa*s/m^3) %Polak page 621
pi=3.14;
RU=1.2E7;     % Mouth Flow Resistance
ro=1.68;      % Mouth Pressure Drop Airflow Exponent

RV=1.5 ;      % (L) Residual Volume
VC=5.5 ;      % (L) Vital Capacity
TLC=RV+VC;    % (L) Total Lung Capacity
FRC=2.6;      % (L) Functional Residual Capacity

V0=0.19*TLC;  % (L)     (Polak pg. 621)
Vm=1.06*TLC;  % (L)     (Polak pg. 621)
CL=0.0057;    % (L/Pa)  (Polak pg. 621)

Pm=11*1000;   %Maximum Inspiratory Muscle Pressure
tc=0.2;       %Inspiratory Muscle time constant

%-------------------------------------------------------------------------
%Geometry

%Initial airway diameters calculation with the help of function : Initials.m

VLarx=RV;
[D,S,Spipe]=Initials(VLarx,V0,Vm,CL);   %Calculates D,S,Spipe (m,m^2,m^2)

L=[12.000; 4.760; 1.900; 0.760; 1.270; 1.070;
    0.900; 0.760; 0.640; 0.540; 0.460; 0.390;
    0.330; 0.270; 0.230; 0.200; 0.165;]*10^-2 ; % Airway Lenghts (m) Weibel

g=0:1:16 ;   %Generation Number
n=2.^g   ;   %Number of Branches for each Generation

%-------------------------------------------------------------------------
%Expired air volume step

imax=10000;          %Number of values for the arrays t,V,VL,Q
k=imax-1  ;          %Number of intervals

dV=VC/k;           %Expired volume step
V=0:dV:VC;         %Expired volume array
VL=RV+V;           %Lung volume array

%-------------------------------------------------------------------------

Q(1)=0;
t(1)=0;

%-------------------------------------------------------------------------

Q_approx= 0.00034; %Approximation for the calculation to begin, assigned at Q(2)


for i=2:imax

```

```
    if (i==2)
        Q(i)=Q_approx;
     else
        Q(i)=Q(i-1);
    end

    dt(i)=dV/(Q(i)*1000); %Time step calculation
    t(i)=t(i-1)+dt(i);    %Time calculation

    Pe(i)=(Pm/VC)*(1-exp(-t(i)/tc))*(VC-V(i)) ; %[Pa]

    A=0;  % Q friction multiplier
    B=0;  % Q^2 friction multiplier
    E=0;  % Q^2 convection multiplier

    for j=1:17
         A=A+(128*m*L(j)*al)/(pi*D(j)^4*2^g(j)) ;     %Friction term
         B=B+(512*r*L(j)*b)/(pi^2*D(j)^5*2^(2*g(j))); %Friction term
        if (j<17)
        if (S(j+1)>S(j))
         E=E+abs((r/(2^(2*g(j)+1)))*(1/(4*S(j+1)^2)-1/S(j)^2)); %Convection term
        end
        end
    end


  %-------------------------------------------------------------------------
  %Newton-Raphson

    F=1;
    index(i)=0;

    while (abs(F)>10^-6)
      F=(B-E)*Q(i)^2+(A+Rt)*Q(i)+Q(i)^ro*(RU)-Pe(i);
      dF=2*(B-E)*Q(i)+(A+Rt);
      Q(i)=Q(i)-F/dF;
      index(i)=index(i)+1;
    end


[S,D,Spipe]=Diameters(V(i),Q(i),Pe(i),D,S);

end

Q(2);  % Check for calculated Q(2) to agree with approxomation Q_approx
Q=Q.*1000;

%V=VC-V;
%Q=-Q.*1000;

hold on
plot(V,Q) %,'LineWidth',2)
title('Airflow-Inspired Air Volume')
xlabel(' V [L] ')
ylabel(' Q [L/s] ')
%hline = refline([0 0]);
%hline.Color = 'black';
```

where, Diamteters.m function used above is:

```
function [S,D,Spipe]=Diameters(V,Q,Pe,D,S)
%-------------------------------------------------------------------------
%Part of Inspiration_New script.This function helps to calculate the
%diameter variation during inspiration.

%-------------------------------------------------------------------------
%Calculation Parameters
m=0.0000189;  % (kg/m/s) T_air=20°C
r=1.205;      % (kg/m^3) T_air=20°C
al=1.5 ;      % (Filoche,Florens)
b=0.0035;     % (Filoche,Florens)
pi=3.14;

%-------------------------------------------------------------------------
%Static Recoil Pressures
RV=1.5 ;      % (L) Residual Volume
VC=5.5 ;      % (L) Vital Capacity
FRC=2.6;      % (L) Functional Residual Capacity
TLC=RV+VC ;   % (L) Total Lung Capacity
V0=0.19*TLC;  % (L)     (Polak pg. 621)
Vm=1.06*TLC;  % (L)     (Polak pg. 621)
CL=0.0057;    % (L/Pa) (Polak pg. 621)
VL=RV+V;     % (L) VLung=TLC-VExpired
DPL=((Vm-V0)/CL)*log((Vm-V0)/(Vm-VL));  % (Pa)
Cth=-CL* log((FRC-V0)/(0.75*Vm-V0))/log((Vm-V0)/(Vm-FRC)); %(L/Pa)
Pmax=((Vm-V0)/Cth)*log((Vm-V0)/(0.75*Vm-V0)); % (Pa)
DPth=(Pmax-((Vm-V0)/Cth)*log((Vm-V0)/(VL-V0)));  %(Pa)
DPtotal=DPL+DPth; %(Pa)

%-------------------------------------------------------------------------
%Driving and Alveolar Pressures

Rt=500000 ;   % [Pa*s/m^3) %Polak page 621
Pd=Pe-Rt*Q;
Palv=-Pd;
Ppl=Palv-DPL; % !(Pa)!

%-------------------------------------------------------------------------
%Lambert Parameters

g=[0:1:16];  %Generation Number
n=2.^g;      %Number of Branches for each Generation

a0= [0.882; 0.882; 0.686; 0.546; 0.450; 0.370; 0.310; 0.255; 0.213; 0.184;
     0.153; 0.125; 0.100; 0.075; 0.057; 0.045; 0.030;] ;

a0t= [0.011; 0.011; 0.051; 0.08; 0.1; 0.125; 0.142; 0.159; 0.174; 0.184;
      0.194; 0.206; 0.218; 0.226; 0.233; 0.239; 0.243;] ;

n1= [0.5; 0.50; 0.6; 0.6; 0.7; 0.8; 0.9; 1; 1; 1; 1; 1; 1; 1; 1; 1; 1;];

n2= [10; 10; 10; 10; 10; 10; 10; 10; 10; 10; 10; 9; 8; 8; 8; 7; 7;];

Am= [2.37; 2.37; 2.80; 3.50; 4.50; 5.30; 6.50; 8; 10.20; 12.70; 15.94;
     20.70; 28.80; 44.50; 69.40; 113; 180;]*10^(-4); %(m^2)

L= [12.000; 4.760; 1.900; 0.760; 1.270; 1.070; 0.900; 0.760; 0.640; 0.540;
    0.460; 0.390; 0.330; 0.270; 0.230; 0.200; 0.17;]*10^(-2); % (m)

Pl= a0.*n1./a0t ;      %vertical asymptote

P2= -n2.*(1-a0)./a0t ; %vertical asymptote

```

```
%-------------------------------------------------------------------------
RU=1.2E7;          % Mouth Flow Resistance
ro=1.68;           % Mouth Pressure Drop Airflow Exponent

Pin(1)=0-RU*Q^ro; %Pressure at the entrance of trachea (generation 0 (j=1)) is zero

for j=1:17

  fA(j)=(128*m*L(j)*a1)/(pi*D(j)^4*2^g(j)) ;      %Friction factor j generation
  fB(j)=(512*r*L(j)*b)/(pi^2*D(j)^5*2^(2*g(j))) ; %Friction factor j generation
  DP(j)=fA(j)*Q+fB(j)*(Q^2);
  Pout(j)=Pin(j)-DP(j);
  Pav(j)=(Pin(j)+Pout(j))/2 ;

  if(j<3)
      Ptm(j)=Pav(j); % (Pa) Transmural pressure of trachea and first bronchus airways
   else
      Ptm(j)=Pav(j)-Ppl; % (Pa) Transmural pressure of j generation airways
   end

   Ptm(j)=Ptm(j)*0.010197; % Conversion in ! (cmH2O) !

   if (Ptm(j)<0)
      a=a0(j)*(1-Ptm(j)/P1(j))^(-n1(j));          %Lambert pg. 46
   else
      a=1-(1-a0(j))*(1-Ptm(j)/P2(j))^(-n2(j));    %Lambert pg. 46
   end

   S(j)=a*Am(j);
   D(j)=sqrt(4*S(j)/(n(j)*pi));
   Spipe(j)=(pi*D(j)^2)/4;

   %Next generation (j+1) outlet pressure calculation using Bernoulli's equation
   if (j<17)
     if (S(j+1)>S(j))
        Pin(j+1)=Pout(j)+Q^2*abs((r/(2^(2*g(j)+1)))*(-1/(4*S(j+1)^2)+1/S(j)^2));
     else
        Pin(j+1)=Pout(j);
     end
   end

end
end
```

Note: The function Initials.m used to calculate the initial diameters of the inspiration process, is same as the one used in Appendix B, during forced expiration.

Appendix C: Airflow-Pressure graph for a single compliant airway

```
function [Qflow Qflow0]=Lambert_DP(i,Ppl,PA,PB)

%This function calculates the airflow (Q_flow) through a compliant airway
%of generation i for known pleural pressure (Ppl) and inlet (PA) and outlet
%pressures (PB). Thus the airflow- pressure drop graph can be produced.

% Lung geometry
NG = 17;    %Number of generations (0,1,...,23)
gen = (0:1:16)';

%Soong et al model scaled to FRC = 3.2 liters
d_k = [1.574; 1.067; 0.726; 0.490; 0.394; 0.306;...
     0.245; 0.201; 0.163; 0.135; 0.114; 0.095; 0.083;...
     0.072; 0.065; 0.058; 0.052]*10^-2; %Airways diameter
l_k = [10.494; 4.163; 1.662; 0.665; 1.111; 0.936; 0.787;...
     0.665; 0.560; 0.472; 0.402; 0.341; 0.289; 0.236; 0.201;...
     0.175; 0.144]*10^-2;

% Parameters of Lambert model
a_0=[0.882; 0.882; 0.686; 0.546; 0.450; 0.370; 0.310; 0.255; ...
    0.213; 0.184; 0.153; 0.125; 0.100; 0.075; 0.057; 0.045; 0.039];
ap_0=[1.1; 1.1; 5.1; 8.0; 10.0; 12.5; 14.2; 15.9; 17.4; ...
    18.4; 19.4; 20.6; 21.8; 22.6; 23.3; 23.9; 24.3]*10^-4;  %Pa^-1
n_1=[0.52; 0.52; 0.6; 0.6; 0.7; 0.8; 0.9; 1.0; 1.0; 1.0; ...
    1.0; 1.0; 1.0; 1.0; 1.0; 1.0; 1.0];
n_2=[10.0; 10.0; 10.0; 10.0; 10.0; 10.0; 10.0; 10.0; 10.0; ...
    10.0; 10.0; 9.0; 8.0; 8.0; 8.0; 7.0; 7.0];
P_1=a_0.*n_1./ap_0;
P_2=-n_2.*(1-a_0)./ap_0;

%Calculation of d_max for the specific model
P_frc = 500;    % Pa
d_max=d_k./sqrt(1-(1-a_0).*(1-P_frc./P_2).^(-n_2));
d_0=d_max.*sqrt(a_0);

a0=a_0(i);
n1=n_1(i);
n2=n_2(i);
P1=P_1(i);
P2=P_2(i);
dmax=d_max(i);
lk=l_k(i);
dk=d_0(i);

dens=1.14;   % kg/m^3
visc=1.84*10^-5;  % kg/m/s
a=1.5;
b=0.0035;

nit=numel(PB);
Qflow=zeros(nit,1);
Qflow0=zeros(nit,1);

Pi = PA - Ppl;
if Pi<0
   dA=dmax*sqrt(a0*(1-Pi/P1)^(-n1));
   vali=(a0^2)*(dmax^4)*P1*(1-(1-Pi/P1)^(1-2*n1))/(1-2*n1);
else
   dA=dmax*sqrt(1-(1-a0)*(1-Pi/P2)^(-n2));
   vali=(dmax^4)*(Pi+2*P2*(1-a0)*((1-Pi/P2)^(-n2+1)-1)/(1-n2)- ...
       ((1-a0)^2)*P2*((1-Pi/P2)^(-2*n2+1)-1)/(1-2*n2));
end
```

```
63
64 -  for i=1:nit
65 -  Pe = PB(i) - Ppl;
66
67 -    if Pe<0
68 -     dB=dmax*sqrt(a0*(1-Pe/P1)^(-n1));
69 -     vale=(a0^2)*(dmax^4)*P1*(1-(1-Pe/P1)^(1-2*n1))/(1-2*n1);
70 -    else
71 -     dB=dmax*sqrt(1-(1-a0)*(1-Pe/P2)^(-n2));
72 -     vale=(dmax^4)*(Pe+2*P2*(1-a0)*((1-Pe/P2)^(-n2+1)-1)/(1-n2)- ...
73           ((1-a0)^2)*P2*((1-Pe/P2)^(-2*n2+1)-1)/(1-2*n2));
74 -    end
75
76 -  a_tr=1024*lk*b*dens/(dA+dB)/pi^2 - 32*dens*log(dB/dA)/pi^2;
77 -  b_tr=128*visc*lk*a/pi;
78 -  g_tr=vale-vali;
79 -  Qflow(i)=(-b_tr+sqrt(b_tr^2-4*a_tr*g_tr))/2/a_tr;
80
81 -  a_tr0=512*lk*b*dens/dk/pi^2;
82 -  b_tr0=128*visc*lk*a/pi;
83 -  g_tr0=(dk^4)*(Pe-Pi);
84 -  Qflow0(i)=(-b_tr0+sqrt(b_tr0^2-4*a_tr0*g_tr0))/2/a_tr0;
85
86 -  end
```

Appendix D: Fractional airway cross-sectional area against transmural pressure plot

The Matlab code used to generate the fractional airway cross-sectional area (α) against transmural pressure (Ptm) plot, for each generation from the trachea (z=0) to the 16th generation, is given below:

```
imax=10000 ;
k=imax-1 ;
Ptmmax=24 ;  %Maximum transmural pressure (cmH20)
Ptmmin=-14 ; %Minimum trasmural pressure (cmH20)
dPtm=(Ptmmax-Ptmmin)/k ;
Ptm=[Ptmmin:dPtm:Ptmmax] ; % (cm H2O)

g=0:16; %number of generations

for j=1:17
   n(j)=2^g(j); %number of branches per generation
end

% Model parameters of bronchial mechanical properties (Lambert page 46)

a0= [0.882; 0.882; 0.686; 0.546; 0.450; 0.370; 0.310; 0.255; 0.213; 0.184;
     0.153; 0.125; 0.100; 0.075; 0.057; 0.045; 0.030;] ;

a0t= [0.011; 0.011; 0.051; 0.08; 0.1; 0.125; 0.142; 0.159; 0.174; 0.184;
      0.194; 0.206; 0.218; 0.226; 0.233; 0.239; 0.243;] ;

n1= [0.5; 0.50; 0.6; 0.6; 0.7; 0.8; 0.9; 1; 1; 1; 1; 1; 1; 1; 1; 1; 1;];

n2= [10; 10; 10; 10; 10; 10; 10; 10; 10; 10; 10; 9; 8; 8; 8; 7; 7;];

Am= [2.37; 2.37; 2.80; 3.50; 4.50; 5.30; 6.50; 8; 10.20; 12.70; 15.94;
     20.70; 28.80; 44.50; 69.40; 113; 180;]*10^(-4); %(m^2)

L= [12.000; 4.760; 1.900; 0.760; 1.270; 1.070; 0.900; 0.760; 0.640; 0.540;
    0.460; 0.390; 0.330; 0.270; 0.230; 0.200; 0.17;]*10^(-2); % (m)

P1= a0.*n1./a0t ;      %vertical asymptote

P2= -n2.*(1-a0)./a0t ; %vertical asymptote

for j=1:17 %step for each generation

    for i=1:imax %step for each pressure

        if (Ptm(i)<0)

        a(i)= a0(j)*(1-Ptm(i)/P1(j))^(-n1(j));      %(Lambert page 46)

        else

        a(i)=1-(1-a0(j))*(1-Ptm(i)/P2(j))^(-n2(j)); %(Lambert page 46)

        end
    end

 plot(Ptm,a)

 %legend(strcat('Generation', num2str(j-1)))
 if (j>1)
 legendInfo{j} = ['Generation ' num2str(j-1)];
 end
 hold on
 title('Airway mechanical properties utilized in model (Lambert,Wilson,Hyatt,Rodarte)')
 xlabel(' Ptm (cmH20) ')
 ylabel('Fractional Airway Area (α)')

end

 legend(legendInfo)
```